The metabolic profile of phenylbutyric acid and its antioxidant capacity in vervet monkeys

Wilhelmina Johanna van der Linde

(B.Pharm.)

Dissertation submitted in the partial fulfillment of the requirements for the degree

MAGISTER SCIENTIAE

in the

Faculty of Health Sciences, School of Pharmacy (Pharmaceutical Chemistry)

at the

North-West University, Potchefstroom Campus

Supervisor: Dr. G. Terre'Blanche

Co-supervisors: Dr. L. du Plessis

Prof. L.J. Mienie

Potchefstroom

2010

INDEX

LIST OF ABBREVIATIONS

Aβ	β-amyloid
ABC transporters	ATP-binding cassette transporters
ACOX	Acyl-CoA oxidases
ADLP	Adrenoleukodystrophy protein
AGT	Alanine glyoxylate aminotransferase
ALDRP	Adrenoleukodystrophy related protein
AMN	Adrenomyeloneuropathy
AO	Addison only
APOP	Apoptosis
Arbit. Units	Arbitary units
BCFAs	Branched-chain fatty acids
BMT	Bone marrow transplantation
cALD	Cerebral adrenoleukodystrophy
CF	Clofibrate / Clofibric acid
CFTR	Cystic fibrosis transmembrane conductance regulator
CO_2	Carbon dioxide
CoASHs	Acyl-CoA synthetases

DBP	D-bifunctional protein
DCAs	Dicarboxylic acids
DCF	Dichlorofluorescein
DCFH-DA	2',7'-dichlorodihydrofluorescein diacetate
DHCA	Dihydroxycholestanoic acids
DMEM	Dulbecco's modified eagle's medium
DMSO	Dimethyl sulphoxide
DN	Diabetic nephropathy
ER	Endoplasmic reticulum
FACS	Fluorescence activated cell sorter
FAs	Fatty acids
FBS	Foetal bovine serum
FPP	Farnesyl diphosphate
FSC	Forward scatter
GC/MS	Gas chromatography-mass spectrometry
GSIS	Glucose-stimulated insulin secretion
GTE	Glyceryl trierucate
GTO	Glyceryl trioleate
H_2O	Water

H_2O_2	Hydrogen peroxide
HATs	Histone acetyltransferase
HbF	Fetal hemoglobin
HbS	Sickle hemoglobin
HD	Huntington's disease
HDACs	Histone deacetylase
HDACI	Histone deacetylase inhibitor
HMG-CoA	3-hydroxy-3-methylglutaryl-CoA
IL	Interleukin
IRD	Infantile Refsum disease
LDLR	Low-density lipoprotein response
LECs	Lens epithelial cells
LO	Lorenzo's oil
LP	Lipid peroxidation
MCFAs	Medium-chain fatty acids
MFI	Mean fluorescence Intensity
MS	Mass spectrometer
NALD	Neonatal adrenoleukodystrophy
NBD	Nucleotide-binding domain
NIST	National Institute of Standards and Technology

O_2^-	Superoxide
·OH	Hydroxyl radical
OTC	Ornithine transcarbamylase
P70R	PMP70-related protein
PA	Phenylacetate
PAGN	Phenylacetylglutamine
PBA / 4-PBA	Phenylbutyrate / 4-phenylbutyric acid
PBGM	Phenylbutyrylglutamine
PBDs	Peroxisomal biogenesis disorders
PBMC	Peripheral blood mononuclear cells
PC-plasmalogens	Choline plasmalogens
PDs	Peroxisomal disorders
PEDs	Peroxisomal enzyme/transporter deficiencies
PE-plasmalogens	Ethanolamine plasmalogens
PEX	Peroxins
PFIC2	Progressive familial intrahepatic cholestasis type 2
PI	Propidium iodide
PMPs	Peroxisomal membrane proteins
PMP69	69 kDa peroxisomal membrane protein
PMP70	70 kDa peroxisomal membrane protein
PPARα	Peroxisome proliferator-activated receptor α
PPRE	Peroxisome proliferator response element

PPs	Peroxisome proliferators
PTS	Peroxisome-targeting signal
RBCs	Red blood cells
RCDP	Rhizomelic chondrodysplasia punctata
Rf	Response factor
ROS	Reactive oxygen species
RxR	9-cis-retinoic acid receptor
SCC	Side scatter
SCFAs	Short-chain fatty acids
SE	Standard error
SRE	Sterol regulatory element
SREBP	Sterol regulatory element binding protein
T_3	3,5,3'-tri-iodothyronine
THCA	Trihydroxycholestanoic acids
UCDs	Urea cycle disorders
UPR	Unfolded protein response
VLCFAs	Very-long-chain fatty acids
VPA	Valproic acid

X-ALD	X-linked adrenoleukodystrophy
ZS	Zellweger syndrome
ZSDs	Zellweger spectrum disorders

LIST OF FIGURES

LIST OF TABLES

LIST OF EQUATIONS

ACKNOWLEDGEMENTS

I would like to thank and glorify my Heavenly Father for the blessings, opportunities and the talent He provided me to fulfil my dream and be an instrument in His hands.

A special thanks to my supervisor, Dr Gisella Terre'Blanche, for all your time, your effort and support. I cannot thank you enough for everything you have done and meant to me in this past two years. I deeply appreciate you.

To Dr Lissinda du Plessis, my co-supervisor, thank you very much for your input, assistance and valuable time regarding the cell experiments. I am so grateful for all you've done for me and everything I've learnt. Without all of your input and contributions, this project would never have been accomplished.

To Professor Mienie and his staff at Biochemistry, thank you for all the precious time you all spent analysing my samples. Professor Mienie, thank you for your guidance and support.

I would like to extend my gratitude towards the faculty members of Pharmaceutical Chemistry, especially Professor Bergh for his valuable assistance.

I am also grateful to all the staff at the Animal Research Centre. Thank you very much for your assistance and hard work.

To Chrizaan Slabbert, thank you for helping me with the cultivation of the HeLa cells and your well appreciated advice.

I would like to express a long distance thank you for my parents living in Namibia. Although you are living far away, you always remain close to my heart. Thank you for your prayers, love, support and believing in me. Also to my brothers, Leinard and Casper, thanks for being there for me and looking after me.

To my deeply treasured hostel parents, Aunty Karin and Uncle Willie, thank you for your indispensable support, guidance and friendship through the past six years. You have meant so much to me.

To all my dear (older) friends: Suné, Monique, Alsonette, Corinne, Michelle, Anell, Anneke and Soretha; thank you for your support and friendship through the years. To my dear (younger) friends: Susan, Anmaré, Genevieve, Bianca (Awesome Foursome), Jané and Ilka; thank you for all the cherished moments filled with laughter. To all the girls in Eikenhof, thanks for being part of my life and my dream. Be who you are: live, love and inspire!

OPSOMMING

X-gekoppelde adrenoleukodistrofië (X-ALD) is die mees algemene enkelperoksisomale ensiemsiekte wat gekenmerk word deur foutiewe mutasies in die ABCD1 geen, ‘n ATP-bindende kassette (ABC) halwe-transporter. Die ABCD1 geen kodeer die andrenoleukodistrofieprotein (ALDP), wat verantwoordelik is vir die vervoer van baie-lang-ketting vetsure (BLKV, C >22:0) vanaf die sitosol na die peroksisoom om sodoende die peroksimale β-oksidasieweg te betree. Verhoogde vlakke van BLKV, wat ophoop in verskillende weefsels en vloeistowwe, is die diagnostiese merker van X-ALD en lei tot inflammatoriese demiëlinering, neurodegenerasie en adrenale ontoereikendheid. Tot hede is daar geen effektiewe behandeling vir X-ALD nie. Tog is daar ‘n ander ABC halwe-transporter, ALDRP wat kompenseer vir die verlore funksie ALDP en wat gekodeer word deur die ABCD2 geen. Bogenoemde bevinding het gelei tot ‘n nuwe benadering om X-ALD te behandel. Fenielbottersuur (PBA) verhoog die uitdrukking van die ABCD2 geen wat lei tot ‘n verhoging in ALDRP en PBA verlaag BLKV vlakke deur verhoogde aktiwiteit in die peroksimale β-oksidasieweg. In hierdie studie het ons die antioksidatiewe kapasiteit van PBA bepaal en bekende sowel as nuwe metaboliete van PBA in die uriene geïdentifiseer.

HeLa selle is *in vitro* gekweek en vir 48 uur behandel met 0.5 mM, 1 mM, 2 mM en 5 mM PBA. Die reaktiewe suurstof spesies (RSS), lipiedperoksidasie, apoptose en lewensvatbaarheid van die selle is bepaal deur fluoresensie-gebaseerde vloeisitometrie en foto’s is geneem om die peroksisoomproliferasie waar te neem. *In vivo*, is ‘n blou-aap met ‘n enkel orale dosering van 130 mg/kg PBA behandel. Bloed is getrek voor behandeling en daarna op 15 minute, 30 minute, 1, 2 en 3 ure na behandeling. RSS, apoptose en lipiedperoksidasie is deur middel van fluoresensie-gebaseerde vloeisitometrie bepaal. Uriene is versamel voor behandeling en daarna op 15 minute, 30 minute, 1, 2, 3, 7 en 24 uur na behandeling met PBA. Die organiese sure in die uriene en die vetsure in die bloed is met behulp van gaschromatografie-massa-spektrometrie (GC/MS) bepaal.

Die *in vitro* resultate het verlaagde vlakke van RSS en lipiedperoksidasie by toenemende konsentrasies van PBA getoon. PBA het ‘n beskermende effek teenoor die HeLa selle vertoon deur ‘n verlaging apoptose asook asook die groot aantal selle wat oorleef het. *In vivo* het die vlakke van RSS en lipiedperoksidasie oor tyd verlaag tydens behandeling met PBA. Die fluoresensiefoto’s bevestig ‘n toename in die aantal peroksisome na PBA behandeling. Die korttermyn effek van PBA toon ‘n aanvanklike, maar klein verlaging in die

vlakke van baie-lang-ketting vetsure, wat ‘n aanduiding is dat die peroksimale β-oksadieweg oor ‘n laner periode geïnduseer word in plaas van aktivering wat plaasvind.

In dié studie het ons nuwe metaboliete in die uriene van die blou-aap geïdentifiseer. Die metaboliete vind hul oorsprong via mono-oksigenase, N-fenielasetiel-glutamien sintetase en as β-oksidasie byprodukte. Van die metaboliete wat onlangs in die mens en die rot geïdentifiseer is, is ook in die uriene van die blou-aap aangetoon.

In die lig van bogenoemde stel ons voor dat PBA, in die lig van dié verbinding se vermoë om BLKV-bloedvlakke te herstel en oksidatiewe stres te verminder, oorweeg word as ‘n nuwe benadering in die behandeling van X-ALD.

***Kern woorde**: X-ALD, 4-PB, BLKV, ROS, LP, peroksisoom proliferasie*

ABSTRACT

X-linked adrenoleukodystrophy (X-ALD) is the most common peroxisomal enzyme deficiency disorder, characterized by inborn mutations in the ABCD1 gene, an ATP-binding cassette (ABC) half-transporter. The ABCD1 gene encodes the adrenoleukodystrophy protein (ALDP), the transporter for the very-long-chain fatty acids (VLCFA; C > 22:0) from the cytosol into the peroxisomes to enter the peroxisomal β-oxidation pathway. The diagnostic disease marker is the elevated levels of VLCFAs which accumulate in different tissues and body fluids, leading to inflammatory demyelination, neuro-deterioration and adrenocortical insufficiency. At present, there is no satisfactory therapy for X-ALD available. However, another peroxisomal ABC half-transporter, ALDRP can compensate for the functional loss of ALDP and is encoded by the ABCD2 gene. This prompted a new approach to treatment strategies. Phenylbutyric acid (PBA) over-expresses the ABCD2 gene, leading to an increased expression of ALDRP and PBA decreases VLCFA levels by increasing peroxisomal β-oxidation. This study had a dual aim: to determine the antioxidant capacity of PBA and to verify known and identify new metabolites of PBA.

In vitro, HeLa cells were cultivated and treated with 0.5 mM, 1 mM, 2 mM and 5 mM PBA for 48 hours. The ROS, lipid peroxidation, apoptosis and cell viability were determined using fluorescein-based flow cytometry. Images were taken to visualize the peroxisome proliferation. *In vivo,* a vervet monkey was given a single dose of 130 mg/kg PBA. Blood was collected before treatment and 15 minutes, 30 minutes, 1, 2 and 3 hours after treatment. ROS, apoptosis and lipid peroxidation were determined by fluorescein-based flow cytometry. Urine was collected before treatment and 15 minutes, 30 minutes, 1, 2, 3, 7 and 24 hours after PBA treatment. A standardised method, employing gas chromatography-mass spectrometry (GC/MS), was used to analyse the organic acids in the urine and fatty acids in the blood.

In vitro results showed decreased levels of ROS and lipid peroxidation with increased concentrations of PBA. PBA showed a protective effect towards the HeLa cells with reduced apoptosis and a high number of viable cells. *In vivo* levels of ROS en lipid peroxidation decreased over time of treatment with PBA. The fluorescence microscope images confirmed an increased number of peroxisomes after PBA treatment. The short term effect of PBA showed an initial, but small decrease in the levels of the fatty acids, suggesting induction over a longer period rather than activation of peroxisomal β-oxidation.

New metabolites of phenylbutyrate were identified in the urine of a vervet monkey. These new metabolites originated from monooxygenase, N-phenylacetyl-glutamine synthases and β-oxidation byproducts. Recently discovered metabolites in humans and rats were also verified and confirmed in the vervet monkey.

We therefore propose that treatment with PBA, on account of its beneficial effects of restoring VLCFA levels and reducing oxidative stress, could be considered a novel approach for the treatment of X-ALD.

***Keywords**: X-ALD, 4-PB, VLCFA, ROS, LP, peroxisome proliferation*

CHAPTER 1

PEROXISOMES

1.1 INTRODUCTION

Peroxisomes are small, single membrane organelles found in every eukaryotic cell except matured erythrocytes (Fidaleo, 2009). Rhodin (1954) discovered peroxisomes in mouse renal cells and described them as membrane-limited, round cytoplasmic particles that did not compare to any traditional cell organelles. He named them microbodies (Fawcett, 1981). In 1966, DeDuve and Baudhuin renamed it to peroxisomes, after discovering two enzymes, generating hydrogen peroxide that was associated with catalase.

Peroxisomes participate in diverse metabolic pathways such as the β-oxidation of fatty acids, leukotrienes and prostaglandins. Other biochemical functions include the biosynthesis of ether lipid (plasmalogens), cholesterol, dolichol and bile acids in the liver. Peroxisomes are versatile organelles that also take part in purine degradation and the detoxification of hydrogen peroxide (Islinger *et al*., 2010; Fidaleo, 2009; Thoms *et al*., 2009).

Peroxisomes attain all their proteins, called peroxins, by selective import from the cytosol (Heberle *et al*., 2001). The peroxins are encoded by PEX genes that are required for the formation of the peroxisomal membrane, the imports of proteins into the peroxisomal matrix and are involved in peroxisome proliferation (Thoms *et al*., 2009)

In order for peroxisomes to meet the exact metabolic needs of a particular organism, they adjust their protein composition. They adapt their physiological role according to the cell type, tissue and developmental and metabolic state of the organism (Fidaleo, 2009).

Peroxisomes with their peroxisomal activities are vital to human growth. Many diseases result from peroxisomal defects. Defects in peroxisomal enzymes can cause X-linked adrenoleukodystrophy (X-ALD) and Acyl-CoA oxidase deficiency. Defects in peroxisome biogenesis can cause Zellweger syndrome and Neonatal adrenoleukodystrophy (NALD). Most of these diseases are fatal (Wanders, 2004).

Peroxisomes are equipped with several enzymes, including oxidative enzymes, such as catalase and urate oxidase that play an important role in hydrogen peroxide catabolism,

defence against oxidative stress and controlling reactive oxygen species (ROS) metabolism (Fidaleo, 2009; Thoms *et al*., 2009).

1.2 PEROXISOMAL BIOGENESIS

Peroxisomal biogenesis includes different processes such as the incorporation of proteins into the organelle's membrane, known as peroxisomal membrane proteins (PMP), the fusion of the organelle, the import of peroxisomal matrix proteins and the addition of lipids to form the membrane. There are 31 proteins, the peroxins (PEX), involved in these processes (Galland & Michels, 2010; Thoms *et al.*, 2009, Voorn-Brouwer *et al*., 2001).

1.2.1 Assembly of peroxisomal membrane proteins (PMP)

The peroxisome membrane is the barrier between the cell and the peroxisome. There are highly permeable porines in the membrane to allow small metabolites to diffuse into the matrix (Pinto *et al*., 2006; Johnson & Olsen, 2001).

The PMPs are synthesized on free ribosomes in the cytosol. Type II PMPs are inserted directly from the cytoplasm into the peroxisome. Type I peroxisome assembly starts in the rough endoplasmic reticululm (ER). The transmembrane protein peroxin 3 (PEX3) attracts PEX19 to the ER membrane. They interact with each other and cause the vesicle to bud off the ER. These vesicles can fuse either with pre-peroxisomes or one another to form new peroxisomes (Figure 1.1).

PEX3 and PEX19 act as receptors for the import of the other peroxins, like PEX13 and PEX14, into the peroxisomal membrane (Galland & Michels, 2010; Thoms *et al.*, 2009; Voorn-Brouwer *et al*., 2001).

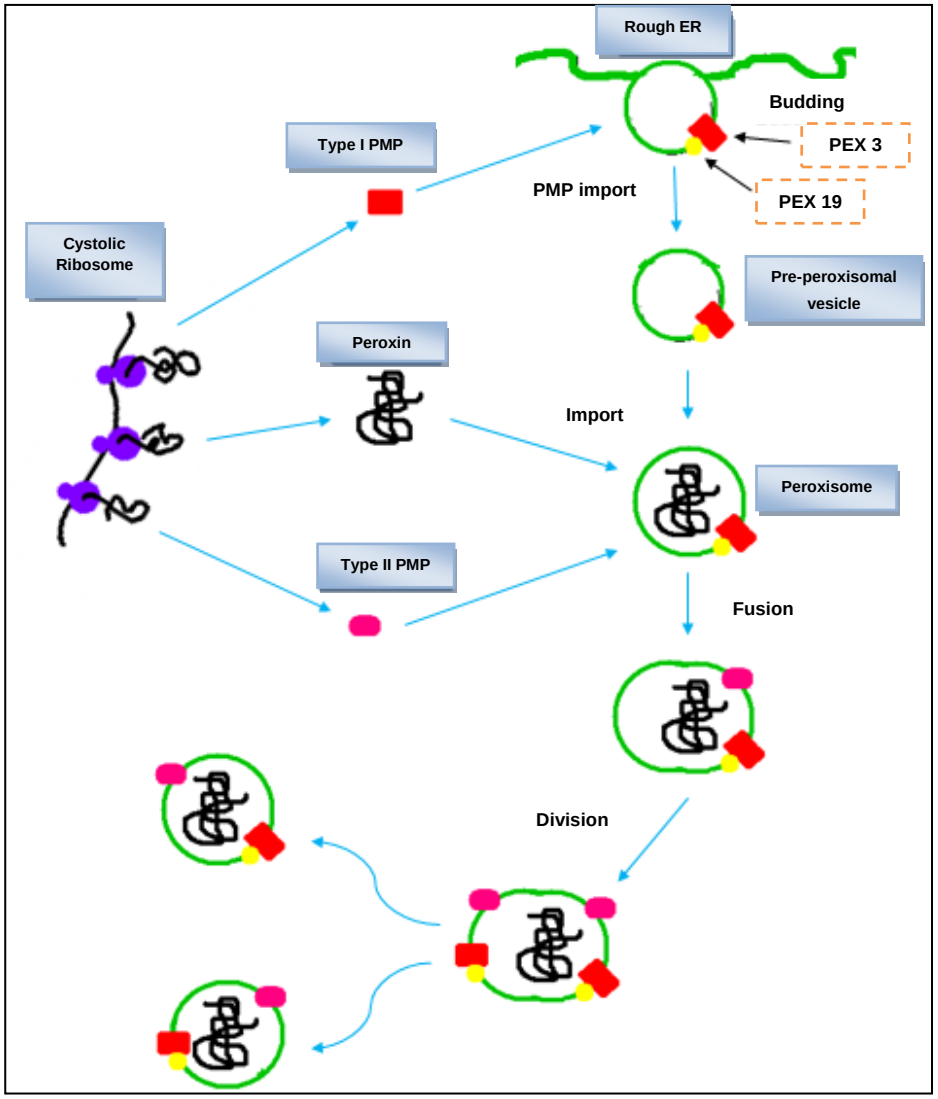

Figure 1.1: *Summary of the assembly of Peroxisomal membrane proteins (PMPs) (adapted from Fidaleo, 2009; Johnson & Olsen, 2001).*

1.2.2 Peroxisomal matrix protein import

After the proteins are imported into the peroxisomal membrane, the matrix proteins are imported from the cytosol. These proteins have one of two peroxisome-targeting signals (PTSs), each needed to direct proteins from the cytosol into the peroxisomes. They are classified as PTS1 and PTS2 (Galland & Michels, 2010; Johnson & Olsen, 2001).

The PTS matrix proteins are recognized by two cystolic receptors, PEX5 and PEX7 that interacts with PTS1 and PTS2, respectively. The PEX5-PTS1-protein-complex interacts with PEX13 and PEX7-PTS2-protein-complex binds to PEX14 and translocates across the membrane, where PEX5 and PEX7 release their proteins in the peroxisomal matrix. PEX5 and PEX7 are recycled back to the cytoplasma (Figure 1.2) (Johnson & Olsen, 2001).

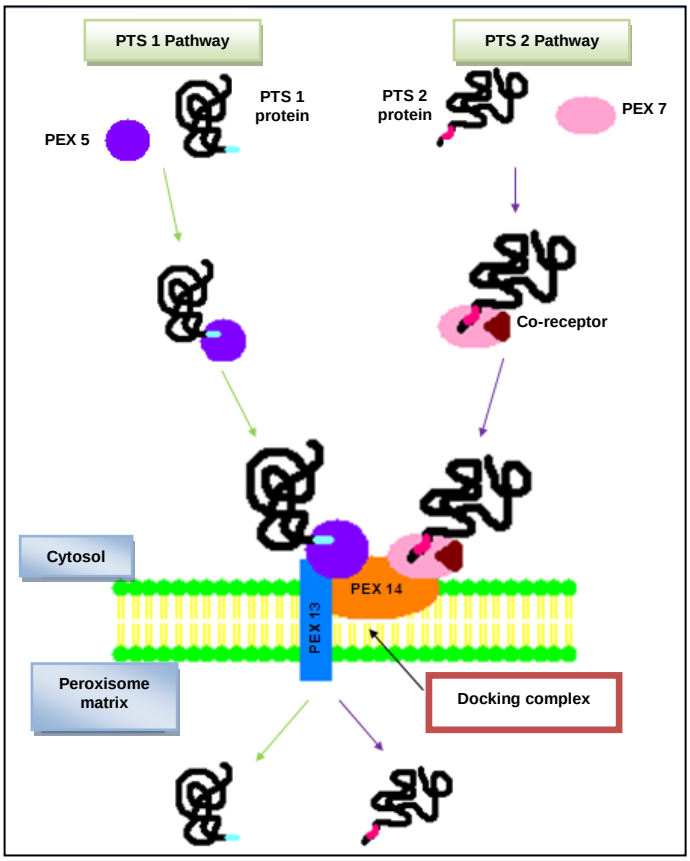

Figure 1.2: *Peroxisomal matrix protein import. PEX5 binds directly to PTS1 protein, forming a PEX5-PTS1-protein-complex and PEX7 to PTS2. These complexes dock on the peroxisome and bind to PEX13 and PEX14. After docking, these receptor-protein-complexes translocate across the membrane. In the peroxisomal matrix the complexes dissociate from the receptors. PEX5 and PEX7 release their proteins in the matrix and are recycled back to the cytoplasma (adapted from Fidaleo, 2009; Heberle et al., 2001; Johnson & Olsen, 2001).*

Peroxisomes grow by importing proteins and recruiting lipids from the rough ER. Peroxisomes mature through a complex process. They import diverse classes of proteins from the cytosol at different times, as a result leading to an alteration in the enzymes and metabolic activities as they mature (Johnson & Olsen, 2001).

1.2.3 ABC transporters

Ions, sugars, amino acids and other molecules can be moved across all cellular and organelle membranes using ion channels, transporters, aquaporins or ATP-powered pumps (Vasiliou *et al*., 2009).

ATP-binding cassette (ABC) transporters are ATP-dependent pumps located in the plasma membrane and other intracellular membranes. The transporters use energy released by

ATP hydrolysis for uphill transport of the substrates across the membranes, into (influx) or out of (efflux) of cells (Vasiliou *et al*., 2009).

The full ABC transporters have two hydrophobic transmembrane domains and two hydrophilic domains, each containing a nucleotide-binding domain (NBD) (Couture *et al*., 2006; Netik *et al.*, 1999). An ABC half-transporter only has one hydrophobic transmembrane domain and one hydrophilic domain (Lin *et al*., 2006) (Figure 1.3).

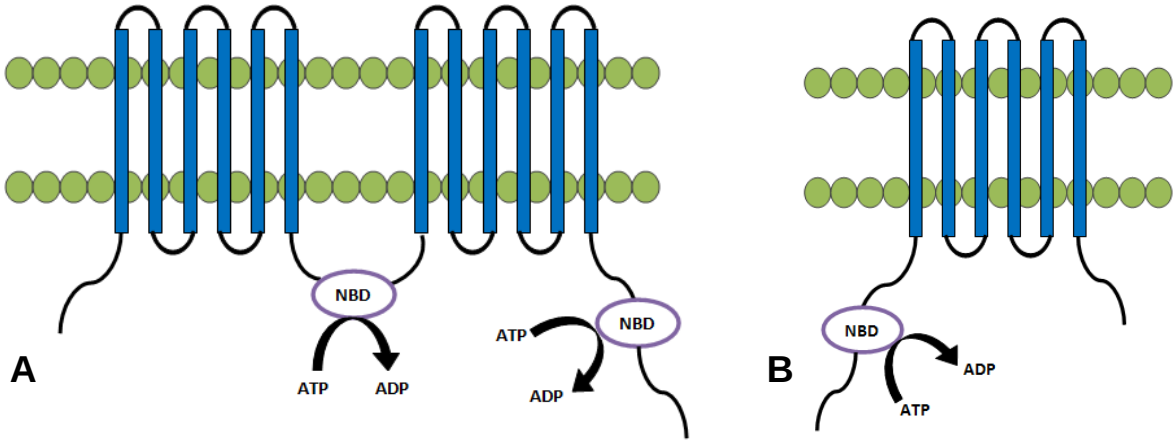

Figure 1.3: *(A) An illustration of full ABC transporters that consist of two transmembrane domains and two nucleotide binding domains (NBD) where ATP is used for uphill transport. (B) An ABC half-transporter, like ALDP, that consists of one transmembrane domain and one nucleotide binding domain.(adapted Couture et al., 2006; Lin et al., 2006; Scotto, 2003)*

ABC transporters are found primarily in the liver, intestine, blood-brain barrier, blood-testis barrier, placenta and kidneys. These transporters contribute also to the movement of drugs across the cell membranes (Vasiliou *et al*., 2009; Scotto, 2003).

The human genome contains 49 ABC genes divided into eight subfamilies. Mutations in at least 11 of these genes cause severe inherited diseases e.g. cystic fibrosis and X-linked adrenoleukodystrophy (Vasiliou *et al*., 2009).

The subfamily D of the ABC family (ABCD) is known as the peroxisomal or ALD transporters. There are four types of the ABC half-transporters, encoded by four different genes: adrenoleukodystrophy protein (ALDP), adrenoleukodystrophy related protein (ALDRP), 70 kDa peroxisomal membrane protein (PMP70) and PMP70-related protein (P70R) or also known as 69 kDa peroxisomal membrane protein (PMP69) (Table 1.1). These proteins are encoded by ABCD1, ABCD2, ABCD3 and ABCD4 genes, respectively (Vasiliou *et al.*, 2009; Wanders, 2004).

Table 1.1: *ABC half-transporters (Vasiliou et al., 2009; Eichler & Aubourg, 2008).*

Gene	Protein		Chromosome
ABCD1	ALDP	adrenoleukodystrophy protein	Xq28
ABCD2	ALDR	adrenoleukodystrophy related protein	12q11-q12
ABCD3	PMP70	70 kDa peroxisomal membrane protein	1p22-p21
ABCD4	P70R PMP69	PMP70-related protein (P70R) or 69 kDa peroxisomal membrane protein	14q24

1.3 PEROXISOME PROLIFERATION

The abundance of peroxisomes present in a cell, reflects the peroxisomal death rate and the forming of new peroxisomes. The different processes can be divided into: a) peroxisome proliferation by division, b) peroxisome biogenesis, c) peroxisome inheritance and d) peroxisome degradation by a specialized version of autophagy, breaking down the cell's damaged internal components (Fidaleo, 2009; Holden & Tugwood, 1999).

Peroxisome proliferators (PPs) are various chemicals that are able to stimulate peroxisome proliferation. This process leads to an increase in amount and/or size of peroxisomes (Kliewer *et al*., 2001; Pineau *et al*., 1996).

The initial observations of peroxisome proliferation were obtained from research on fibrate drugs while experimenting on rodents. Fibrates such as clofibrate are amphipathic carboxylic acids which are used in therapy for hypercholesterolemia and are also used as hypolipidemic agents to reduce triglyceride levels (Figure 1.4). The rats and mice exposed to these agents showed a significant increase in peroxisomes; mostly in the liver, and also exhibited an increased expression of numerous peroxisomal enzymes which are involved in the fatty acid oxidation pathway. Fibrates bind to the peroxisome proliferator-activated receptor α (PPARα) (Kliewer *et al*., 2001; Holden & Tugwood, 1999).

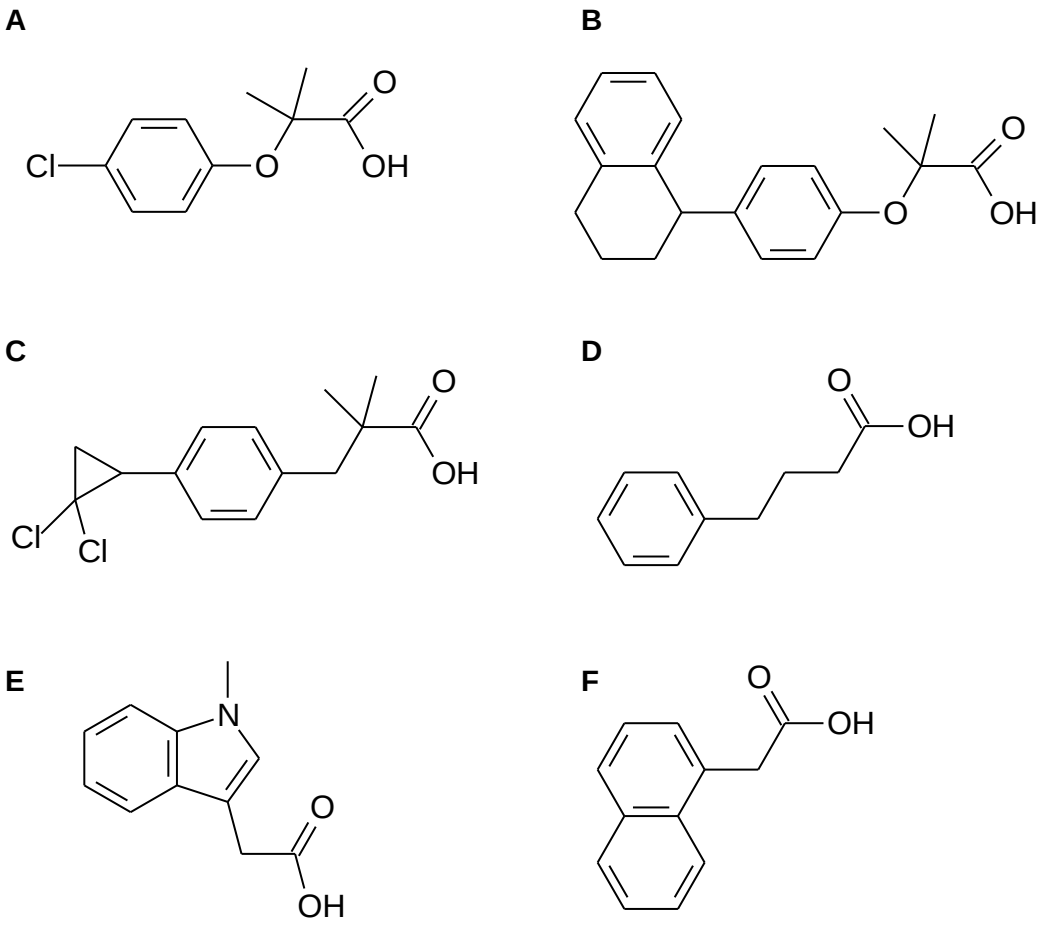

Figure 1.4: *Various peroxisome proliferator compounds. (A) clofibrate, (B) nafenopin, (C) ciprofibrate, (D) phenylbutyric acid, (E) Indole acetic acid and (F) naphthylacetic acid (Reddy, 2004; Pineau et al., 1996)*

PPARα binds to a DNA sequence called PPRE (peroxisome proliferation response element) as heterodimers with the 9-cis-retinoic acid receptor (RxR). When PPARα/RxR is activated, there are up-regulating expressions of lipid-metabolizing enzymes, causing an increase in the fatty acid β-oxidation pathway in the peroxisomes and also an increase in the expression of PEX11 genes. The increased expression of either PEX11α or PEX11β is adequate to stimulate peroxisomal division in cultured cells (Islinger *et al*., 2010; Thoms *et al*., 2009; Holden & Tugwood, 1999).

Fidaleo (2009), observed that PPARα induced peroxisomal enzymes can lead to hepatomegaly, hypertrophy, and hyperplasia. Continued administration of PPs causes hepatocarcinogenesis.

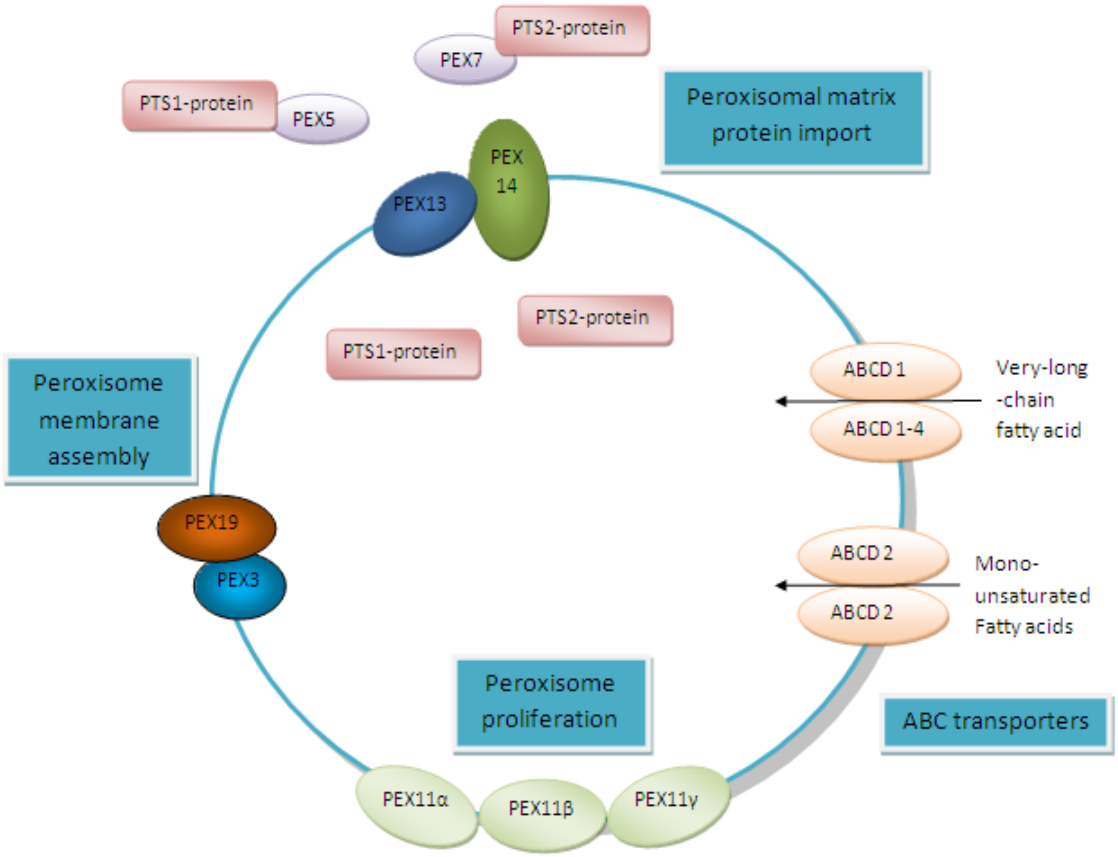

Figure 1.5: *A brief summary of the different proteins in peroxisomes. PEX19 and PEX3 forms part of the peroxisome membrane proteins (PMP's); the import of PTS1- and PTS2-proteins are directed by the cystolic protein receptors, PEX5 and PEX7, and docked with PEX13 and PEX14, to be transported into the peroxisome matrix; PEX11α, PEX11β and PEX11γ are needed for peroxisome proliferation and the ABC transporters transports fatty acids into the peroxisome for β-oxidation (adapted from Islinger et al., 2010; Fidaleo, 2009; Heberle et al., 2001; Johnson & Olsen, 2001).*

1.4 METABOLIC FUNCTIONS OF PEROXISOMES

The different enzymes in peroxisomes are involved in a variety of biochemical pathways. They produce oxidation reactions leading to the production of hydrogen peroxide (H_2O_2) which is destructive to the cell. Peroxisomes also contain the enzyme catalase, which converts hydrogen peroxide into water or by using it to oxidize another organic compound. A number of substrates, including uric acid, amino acids, purines, methanol and fatty acids are decomposed by peroxisomes. The oxidation of fatty acid provides a major source of metabolic energy.

Except for oxidative reactions, peroxisomes are also involved in the biosynthesis of lipids and the synthesis of cholesterol and dolichol that also occurs in the ER. In the liver, peroxisomes are involved in the synthesis of bile acids, which are derived from cholesterol. Peroxisomes contain enzymes necessary for the synthesis of plasmalogens – a family of phospholipids in which one of the hydrocarbon chains is attached to glycerol by an ether bond rather than an ester bond (Wanders & Waterham, 2006).

1.4.1 Peroxisomal β-oxidation

Wanders (2004) recognized that the peroxisomal β-oxidation of fatty acids (FAs) are formed through an identical pathway as in the mitochondria.

There is a significant difference in mitochondrial and peroxisomal β-oxidation systems, each with a distinct role to play in the whole cell's β-oxidation. One of these differences is their substrate specificity. Mitochondria primarily oxidize short, medium and most long-chain fatty (C<20) acids, while peroxisomes oxidize very-long-chain fatty acids (VLCFAs) (C>20) and branched-chain fatty acids (BCFAs) (Wanders, 2004).

Peroxisomal β-oxidation is only able to shorten fatty acids chains and is not able to degrade the fatty acid completely. The enzymes involved in the β-oxidation of these FAs include two acyl-CoA oxidases, two multifunctional proteins with enoyl-CoA hydratase and 3-hydroxyacyl-CoA dehydrogenase activities and two different peroxisomal thiolases (Wanders & Waterham, 2006).

The mechanism of peroxisomal β-oxidation implies four successive steps: (1) dehydrogenation, (2) hydration, (3) oxidation and (4) thiolytic cleavage (Wanders & Waterham, 2006; Wanders, 2004). After each cycle, fatty acids are reduced by two carbon atoms a time, converting the fatty acids to acetyl-CoA. The acetyl-CoA is released from the peroxisomes to the cytosol for reuse in other metabolic reactions. After the peroxisomes reduce the fatty acid chains in length, they are conjugated to carnitine and transported to mitochondria as acetylcarnitine, to be completely oxidised to CO_2 and H_2O (Wanders *et al*., 2001).

1.4.1.1 Peroxisomal β-oxidation substrate specificities

In the mitochondria, the bulk dietary short- and medium-chain fatty acid (SCFAs and MCFAs), including palmitic (C16:0), oleic (C18:1), linoleic (C18:2) and linolenic (C18:3) acid are solely oxidized (Fidaleo, 2009).

Peroxisomes oxidize three different types of fatty acids: (i) VLCFA, such as hexacosanoic acid (C26:0), tetracosanoic acid (C24:0), tertracosa-hexaenoic acid (C24:6ω-3) and long-chain dicarboxylic acids (DCAs) (Ferdinandusse *et al*, 2004), (ii) 2-methyl branched-chain fatty acids (BCFAs) such as pristanic acid and (iii) bile acids intermediates, di- and trihydroxycholestanoic acid (DHCA and THCA). VLCFAs originate from the diet and are also produced by chain-elongation of long-chain fatty acids (Wanders *et al*. 2010; Wanders, 2004). Peroxisomal β-oxidation is partial and produces medium-chain acyl-CoA (octanoyl-CoA) and acetyl-CoA. These products can be exported to the mitochondria via carnitine, where the β-oxidation allows a total degradation of the fatty acids (Fidaleo, 2009; Wanders *et al*., 2001).

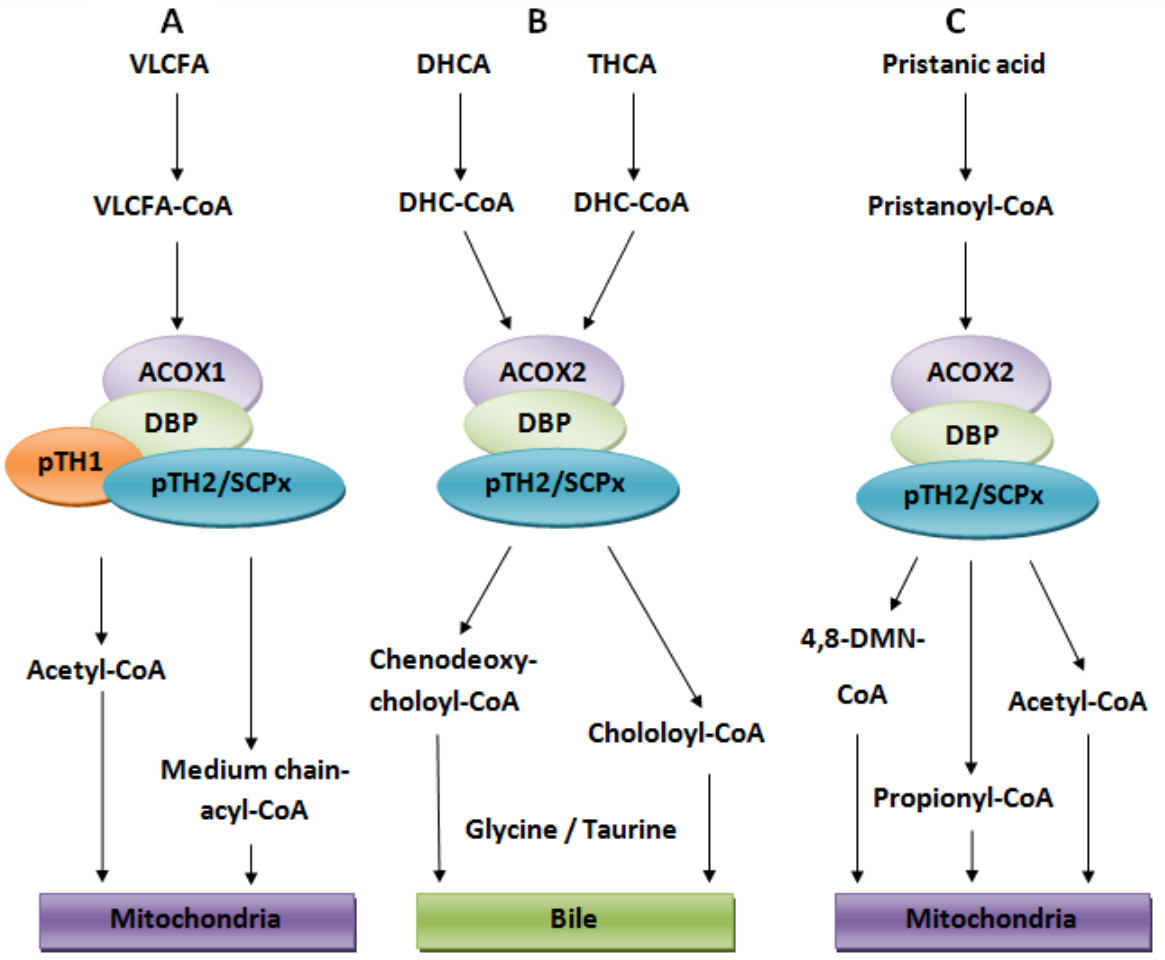

Figure 1.6: *Peroxisomal β-oxidation. (A) The β-oxidation of VLCFA consists of different enzymes: ACOX1 is an Acyl-CoA oxidases, specific for straight-chain fatty acids, DBP is the D-bifunctional protein and two tiolase, pTH1 and pTH2/SCPx. (B) Enzymes part of the β-oxidation of DHCA and THCA: ACOX2 is an Acyl-CoA oxidases specific for branched-chain fatty acids, DBP is the D-bifunctional protein and only one tiolase, pTH2/SCPx. (C) The enzymes forming β-oxidation of pristanic acid the same as for DHCA/THCA (adapted from Wanders et al. 2010; Wanders, 2004).*

1.4.1.2 Activation and transport of fatty acids

Fatty acids (FAs) come from dietary sources, stored FAs in adipocytes and from the synthesis or degradation of lipid complexes within lysosomes (Fidaleo, 2009).

FAs are esterified to CoA in the cytosol by the acyl-CoA synthetases (CoASHs). These enzymes are specific for all type of fatty acids (Wanders, 2004).

ALDP is the peroxisomal ABC half-transporter that imports the activated fatty acids into the peroxisomes (see 1.2.3). The additional ABC half-transporter ALDRP, can also form homo- and heterodimers within the peroxisomal membrane and import very-long-chain fatty acids. This functional similarity, discovered by Pujol *et al*. (2004), demonstrated that ALDRP can compensate for the loss of the ALDP during X-ALD. This route of transport is further discussed in chapter 2.

1.4.2 Fatty acid α-oxidation

FAs, with a β-positioned methyl group or branched-chain fatty acids, like phytanic acid, cannot be β-oxidized because the methyl group at the β-position blocks the β-oxidation. Phytanic acid is first converted to its CoA-ester and then phytanoyl-CoA serves as a substrate in an α-oxidation process. The α-oxidation reaction (as well as the remainder of the reactions of phytanic acid oxidation) occur within the peroxisomes and require phytanoyl-CoA hydroxylase (phytanoyl-CoA-dioxygenase), which adds a hydroxyl group to the α-carbon of phytanic acid, generating the 19-carbon homologue, pristanic acid. Pristanic acid and other 2-methyl fatty acid can subsequently be degraded by β-oxidation (Figure 1.7). Human peroxisomes are the only organelle to perform α-oxidation (Jansen *et al*., 2001; Wanders *et al*., 2001; Jansen *et al*., 1999).

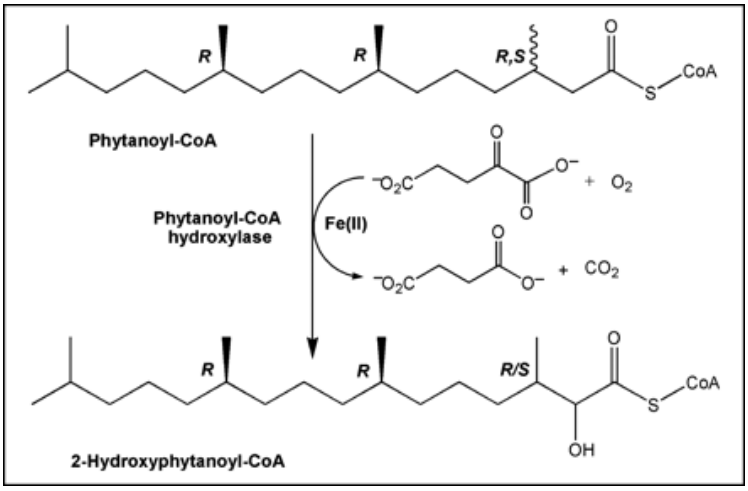

Figure 1.7: *The catalyzed conversion of phytanoyl-CoA to 2-hydroxyphkytanoyl-CoA with co-evolution of carbondioxide and succinic acid (adapted from McDonough et al., 2005).*

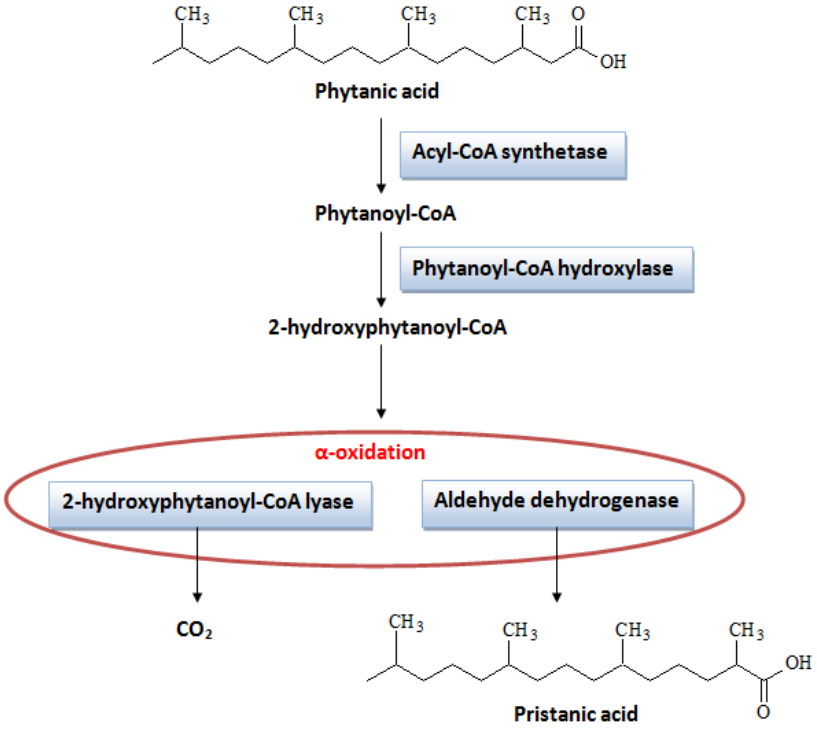

Figure 1.8: *Phytanic acid forms pristanic acid and CO_2 after peroxisomal α-oxidation. The enzymes required for fatty acid α-oxidation includes: acyl-CoA synthetase, phytanoyl-CoA hydroxylase, 2-hydroxyphytanoyl-CoA lyase and aldehyde dehydrogenase (adapted from Wanders & Waterham, 2006; Jansen et al., 2001; Jansen et al., 1999).*

Refsum disease is an example of a deficiency of the dioxygenase catalysing the conversion of phytanoyl-CoA into 2-hydroxyphytanoyl-CoA leading to the accumulation of phytanic acid in the plasma (McDonough *et al.,* 2005).

1.4.3 Cholesterol biosynthesis

The organelles involved in the synthesis of cholesterol are peroxisomes, mitochondria and the endoplasmic reticulum (ER). The first conversion occurs in peroxisomes, ER and mitochondria. Acetyl-CoA is converted to 3-hydroxy-3-methylglutaryl-CoA (HMG-CoA), catalyzed by HMG-CoA synthase. The following conversion of HMG-CoA to mevalonate can take place in the ER and peroxisomes, both containg HMG-CoA reductases. The next conversion occurs mainly in the peroxisomes when mevalonate is converted to farnesyl diphosphate (FPP) by Farnesyl PP-synthase. The metabolism of FPP to squalene catalyzed by squalene synthase proceeds solely in the ER. The final conversion of lanosterol to cholesterol occurs in the ER and may be localized to the peroxisomes (Fidaleo, 2009).

1.4.4 Metabolism of bile acids

Bile acids are metabolites of cholesterol. The enzymes involved in the degradation of cholesterol are situated in peroxisomes (Wanders *et al*., 2010).

Firstly, cholesterol is converted to the precursors of bile acid: 3α, 7α, 12α-trihydroxy-5β-cholestanoic acid (THCA) and 3α, 7α-dihydroxy-5β-cholestanoic acid (DHCA) (Wanders *et al*., 2001).

THCA and DHCA are activated and transported to the peroxisomes, and imported by the ATP-binding cassette (ABC) transporters. Their methyl-branched side chain is shortened by β-oxidation (Wanders, 2004).

In the hepatocyte, the bile acids are conjugated to the amino acid glycine or taurine catalysed by bile acyl-CoA amino-acid N-acyltransferase and then stored in the gallbladder (Wanders *et al*., 2010).

1.4.5 Role of peroxisomes in biosynthesis of polyunsaturated fatty acids

Ferdinandusse *et al*., (2004), revealed the vital role of peroxisomes in the production of very long-chain fatty acids, such as docosahexaenoic acid (C22:6n-3, DHA).

DHA is obtained after a chain of alternating desaturation and elongation steps from the dietary essential fatty acid linolenic acid (C18:3n-3). The final step of synthesis of DHA occurs in peroxisomes (Ferdinandusse *et al*., 2004).

1.4.6 Synthesis of plasmalogens

Peroxisomes contain enzymes required for the synthesis of plasmalogens, a class of etherphospholipids. In mammals, high levels of ethanolamine plasmalogens (PE-plasmalogens) are located in the brain myelin while choline plasmalogens (PC-plasmalogens) are found in the heart muscle. Moderate levels of plasmalogens are present in the kidney, spleen, skeletal muscles and blood cells whereas liver has lower amounts of plasmalogens. Absence of plasmalogens causes profound abnormalities in the myelination of nerve cells, which is one of the reasons why many peroxisomal disorders lead to neurological disease (Brites *et al*., 2009; Wanders & Waterham, 2006, Wanders, 2004).

1.4.7 Oxidative stress

Oxidative stress occurs when the production of reactive oxygen species (ROS) exceeds the biological system's ability to detoxify the ROS or repair the damage caused by ROS. De Duve and Baudhuin (1966), described a respiratory pathway in the peroxisomes where the electrons, removed from different metabolites, converted O_2 to H_2O_2 (Fidaleo, 2009).

ROS are radical species containing free or unpaired electrons. An example is the superoxide anion (O_2^-), formed during the reduction of O_2: $O_2 + e^- \rightarrow O_2^-$. Hydrogen

peroxide (H_2O_2) is also a ROS, even though it has no unpaired electrons and therefore it is not a radical. The most reactive and toxic form of oxygen is the hydroxyl radical (·OH) (Santos *et al*., 2005)

Elevated levels of ROS produce a toxic effect on biomolecules such as DNA, proteins and lipids. It leads to oxidative damage in assorted cellular compartments, apoptosis (cell death), ischemic injury, the activation of metabolic and signalling pathways and deadly effects (Thoms *et al*., 2009).

In peroxisomes, electrons from the dehydrogenation process during β-oxidation, are transferred directly to oxygen, generating hydrogen peroxide. In addition to the production of ROS, peroxisomes contain ROS-metabolizing enzymes: peroxisomal catalase and glutathione peroxidase. Thoms *et al* (2009) emphasized the important role in reactive oxygen species (ROS) metabolism. Peroxisomes play an important role both in the production and scavenging of ROS in the cell.

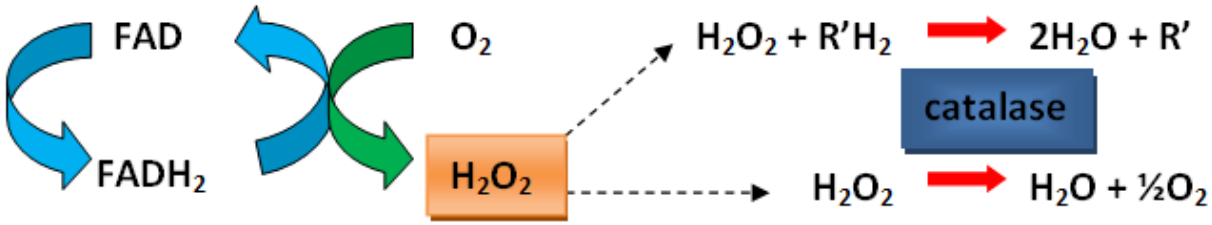

Figure 1.9: *Peroxisomal catalase uses the H_2O_2 generated, that is harmful to cell to oxidize different substrates (R). This oxidative reaction is important in liver and kidney cells where peroxisomes can detoxify different molecules that enter the bloodstream. When H_2O_2 accumulates in the cell, catalase converts it to H_2O (adapted from Fidaleo, 2009; Thoms et al., 2009; Santos et al., 2005).*

1.5 PEROXISOMAL DISORDERS

Peroxisomal disorders (PDs) are recently discovered diseases because peroxisomes where the last subcellular organelle to be discovered. Wanders (2004) explained the essence of peroxisomes in humans after the disturbing consequences in patients with Zellweger syndrome caused by the absence of peroxisomes. The peroxisomal disorders can be divided into two main groups: (1) peroxisome biogenesis disorders (PBDs) and (2) peroxisomal enzyme/transporter deficiencies (PEDs) (Wanders & Waterham, 2006; Raas-Rothschild, 2002).

Peroxisomal disorders affect different biological processes such as endochondral ossification, neuronal migration and myelination (Raas-Rothschild, 2002).

1.5.1 Peroxisome biogenesis disorder

PBDs are caused by mutations of some peroxins (PEX genes), which are responsible for the import of peroxisomal proteins from the cytosol to the peroxisome matrix (Gould *et al*., 2008; Thieringer *et al*., 2003).

The biochemical manifestations associated with these diseases (Table 1.2) present an increased level of VLCFAs (C24:0, C25:0, C26:0), THCA and DHCA (from bile acid synthesis), branched-chain fatty acid (pristanic and phytanic acid) and a decline in synthesis of plasmalogens and DHA (Wanders *et al*., 2010; Wanders, 2004).

Table 1.2: *List of peroxisome biogenesis disorders (PBDs) (Adapted from Wanders et al., 2010; Wanders, 2004; Thieringer et al., 2003)*

Peroxisome biogenesis disorders (PBDs)
Zellweger spectrum disorders (ZSDs)
Zellweger syndrome (ZS)
Neonatal adrenoleukodystrophy (NALD)
Infantile Refsum disease (IRD)
Rhizomelic chondrodysplasia punctata (RCDP) type 1

1.5.2 Peroxisomal enzyme / transporter deficiencies

PEDs are disorders where the peroxisomes are present and still functional, but a deficiency in a single enzyme causes the main biochemical irregularity (Wanders *et al.,* 2008; Wanders & Waterham, 2006).

Wanders *et al*., (2010) demonstrated that the mutant gene affects proteins involved in the different peroxisomal pathways: (1) plasmalogen biosynthesis, (2) fatty acid β-oxidation, (3) peroxisomal α-oxidation, (4) glyoxylate detoxification and (5) H_2O_2 metabolism.

X-linked adrenoleukodystrophy (X-ALD) is an example of a defect in the peroxisomal β-oxidation system which causes an accumulation in VLCFAs in the blood. X-ALD is discussed in detail in Chapter 2. Except for X-ALD, all of the other PEDs are autosomal

recessive, meaning that two copies of the mutant gene must be present in order for the disease to develop (Wanders & Waterham, 2006; Hemming *et al*., 1999).

Even though PEDs involve only a single peroxisome deficiency, they are severe and imitate the PBDs closely (Fidaleo, 2009; Wanders *et al.,* 2008).

Table 1.3: *The peroxisomal enzyme/transporter deficiencies (PEDs) (Wanders et al. 2010; Wanders & Waterham, 2006).*

Pathway affected	**Peroxisomal enzyme/transporter deficiencies (PEDs)**	**Enzyme defect**
Plasmalogen biosynthesis	Rhizomelic chonodrodysplasia punctata Type 2 (RCDP)	DHAPAT
	Rhizomelic chonodrodysplasia punctata Type 3 (RCDP)	AlkylDHAP synthase
Peroxisomal β-oxidation	X-linked adrenoleukodystrophy	ALDP
	ACOX1-deficiency	Acyl-CoA oxidase
	DBP-deficiency	D-bifunctional protein
	2-Methyl-acylCoA racemase (AMACR) deficiency	2-Methyl-acylCoA racemase
	SCPx-deficiency	Sterol carrier protein X
Peroxisomal α-oxidation	Refsum disease	phytanoyl-CoA hydroxylase
Glyoxylate detoxification	Hyperoxaluria Type 1	Alanine glyoxylate aminotransferase (AGT)
H_2O_2 metabolism	Acatalasaemia	Carnitine acetyl transferase

1.6 CONCLUSION

Peroxisomes are virtually ubiquitous organelles involved in numerous catabolic and anabolic pathways. About 50 peroxisomal enzymes have so far been identified, which contribute to several crucial metabolic processes such as β-oxidation and α-oxidation of fatty acids, biosynthesis of ether phospholipids and metabolism of reactive oxygen species, thus making peroxisomes indispensable for human health and development.

CHAPTER 2

X-LINKED ADRENOLEUKODYSTROPHY

2.1 INTRODUCTION

Adrenoleukodystrophy is the most frequent peroxisomal enzyme deficiency disorder, occurring approximately 1 in 20 000 individuals (Fidaleo, 2009). It is a severe inherited X chromosome linked disease (Fourcade *et al.*, 2008) and a progressive neurodegenerative disorder with various clinical expressions (Moser, 2006; Guimarãea *et al*., 2002; Weinhofer *et al*., 2002).

X-ALD is characterized by inborn mutations in the ABCD1 gene (Moser, 2006; Guimarães *et al*., 2002). This gene is located on the Xq28 chromosome (Eichler & Aubourg, 2008; Fourcade *et al.,* 2008). As previously explained in chapter 1, the ABCD1 gene belongs to the ATP-binding cassette (ABC) transporters which transport substrates across the peroxisomal membrane. More exclusively, the ABCD1 gene encodes the adrenoleukodystrophy protein (ALDP), the transporter for the very-long-chain fatty acids (VLCFA) (Kemp & Wanders, 2007).

X-ALD is a heterogeneous disease that manifests with diverse clinical phenotypes. Seven phenotypes in males have been identified: childhood cerebral form (CCER), adolescent cerebral ALD, adrenomyeloneuropathy (AMN), adult cerebral ALD, olivo-ponto-cerebelar, Addison disease only (AO) and asymptomatic (Guimarães *et al*., 2002; Kemp *et al*., 1998). Five phenotypes in female carriers have been identified: asymptomatic, mild myelopathy, moderate to severe myeloneuropathy, cerebral involvement and clinically evident adrenal insufficiency.

The dysfunctional ABCD1 gene leads to the impaired transport of VLCFAs. The VLCFAs accumulate in different tissues and body fluids (Pujol *et al.*, 2004). These elevated levels of VLCFAs are the diagnostic disease markers, providing reliable criteria for prenatal and postnatal disease identification in males and in the female carriers (Moser, 2006).

In X-ALD there is an increase in reactive oxygen species (ROS) and lipid peroxidation, leading to defective oxidative stress homeostasis (Deon *et al*., 2008; Fourcade *et al*., 2008; Pujol *et al*., 2004)

There are limited therapeutic options for X-ALD with no curative outcome. None of the current treatments can stop the neurological progression of X-ALD.

2.2 GENETICS OF X-ALD

The ABCD1 gene is mapped to the Xq28. The genetic abnormality of X-ALD occurs on the X chromosome (Eichler & Aubourg, 2008; Fourcade *et al.*, 2008).

Females have two X chromosomes (XX). During the embryonic stage, females undergo X-inactivation, where one of the two X chromosomes becomes condensed and permanently inactive. This inactivation prevents women from producing double the number of normal X chromosome proteins (Engelen & Kemp 2009*;* Rosebusch *et al*., 1999).

If the faulty allele of X-ALD is on the inactive chromosome, there will be no manifestation of the disease, but if the faulty allele is on the active X chromosome, the disease progresses (Engelen & Kemp 2009; Rosebusch *et al*., 1999) (Figure 2.1).

.

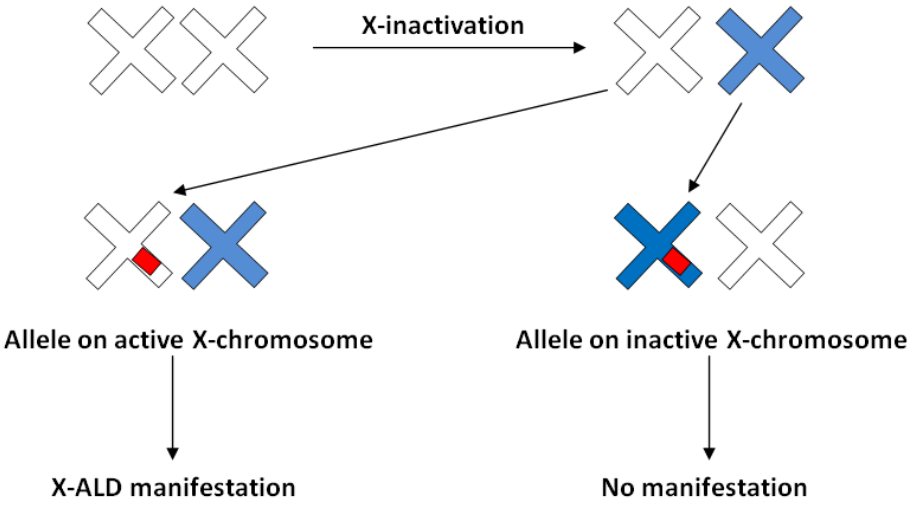

Figure 2.1: *Schematic illustration of genetics of X-ALD. The female chromosomes are inactivated. The defective allele can be on the active X-chromosome leading to X-ALD disease (adapted from Rosebusch et al., 1999).*

There are also genetic implications in families with an X-linked inherited disorder like X-ALD. In case of a female carrier of the X-ALD X chromosome there is a chance that the daughter will be a carrier and the son will have X-ALD. Males with the X-ALD X chromosome can pass it on to their daughters but not to their sons (Engelen & Kemp 2009; Rosebusch *et al*., 1999). Males have an X chromosome and a Y chromosome (XY). They pass the Y chromosome along to their sons (Figure 2.2).

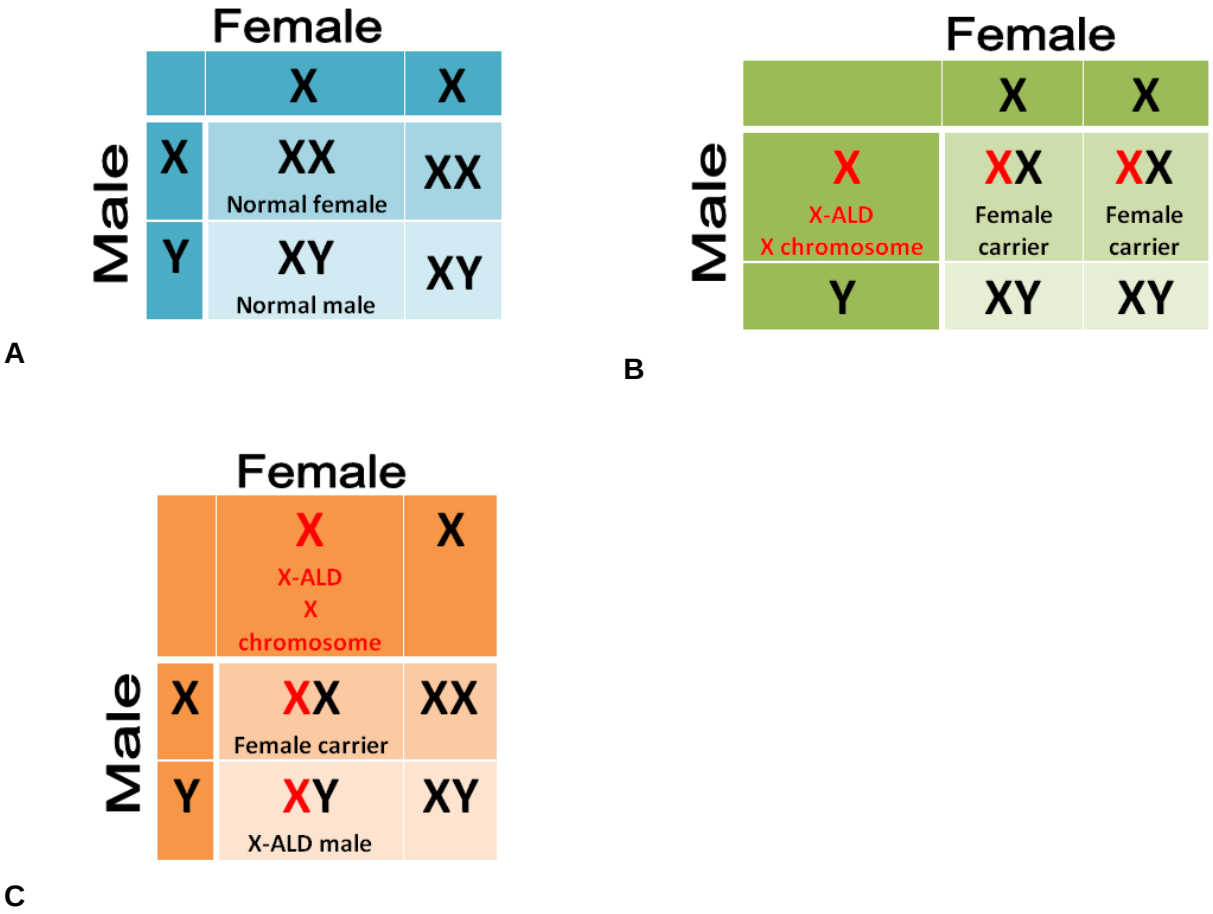

Figure 2.2: *(A) Both the female and male have normal genes with no defective X-chromosome. (B) The female has normal genes, but the male has X-ALD with the defective X chromosome, resulting that his daughters will be carriers of X-ALD. (C) The male has normal genes, but the female is a X-ALD carrier resulting that there is a chance the daughter will be a carrier and the son will have X-ALD (adapted from Engelen & Kemp 2009; Rosebusch et al., 1999).*

2.3 THE CLINICAL PICTURE OF X-ALD

The wide variety in phenotypes led to a classification according to the age the disease began, the affected organs and the neurological progression rate (Berger & Gärtner, 2006; Guimarães *et al*., 2002; Pujol *et al.,* 2002).

2.3.1 Phenotypes in male X-ALD

Table 2.1: *The different phenotypes diagnosed in males with X-ALD (Adapted from Moser et al. 2008; Moser, 1997).*

Phenotype	**Description**	**Estimated Relative Frequency**	**Age of onset**
Childhood cerebral	• Developing behavioural, cognitive and neurologic deficiency • Inflammatory brain demyelination. • Overall disability often within 3 years	31-35%	3-10 years
Adolescent	• Slower progression similar to childhood cerebral	4-7%	11-12 years
Adult cerebral	• Rapid progression resembling childhood cerebral • Dementia • behavioural disturbances	2-5%	After 21 years
Adrenomyelo neuropathy (AMN)	• Slowly progressive paraparesis • sphincter disturbances • mainly spinal cord involvement	40-46%	28 ± 9 years
Addison only	• Adrenal insufficiency without neurologic abnormalities • Ultimately developing AMN	Varies with age. Up to 50% in childhood	Before 7.5 years
Asymptomatic	• ALD gene abnormality with no neurologic or adrenal involvement.	reduce with age	Common before 4 years. Rare after 40 years.

2.3.2 Phenotypes in female carriers

Over 50% of female carriers show symptoms over the age of 40 years. They can be symptomatic resembling AMN but with milder clinical symptoms and a slow progression rate. There are rarely cerebral demyelination and adrenal insufficiency. They can by misdiagnosed as multiple sclerosis (Berger & Gärtner, 2006; Moser, 2006; Pujol *et al.,* 2002).

Table 2.2: *The different phenotypes diagnosed in female X-ALD carriers (Adapted from Deon et al., 2008; Moser et al., 2008).*

Phenotype	**Description**	**Estimated relative frequency**	**Age of onset**
Asymptomatic	• No neurological or adrenal involvement	Reduce with age. Majority of female carriers.	<30 years
Mild myelopathy	• Increasing changes in the deep tendon reflexes and distal sensory of the lower extremities • No or mild disability	Increases with age. ~ 50%	>40 years
Moderate to severe myeloneuropathy	• Similar to AMN, but milder and later onset	Increases with age. ~ 20%	>40 years
Cerebral involvement	• Rarely in childhood • More common in middle age and later	~ 1%	<30 years
Clinically evident adrenal insufficiency	• Rare at any age	~ 1%	<30 years

2.4 THE MUTATED ABCD1 GENE AND THE ADRENOLEUKODYSTROPHY PROTEIN (ALDP)

In 1997 Moser and co-workers identified the mutated gene that caused X-ALD by positional cloning and named it adrenoleukodystrophy gene. This gene encodes a 745 amino acid

peroxisomal transmembrane protein with a similar structure than an ATP-binding cassette (ABC) transporter. The gene was renamed as ATP-binding cassette transporter subfamily D member 1 (ABCD1) (Engelen & Kemp 2009; Berger & Gärtner, 2006).

The ABCD1 gene encodes the peroxisomal adrenoleukodystrophy protein (ALDP). The ALDP transports VLCFAs into the peroxisome to be β-oxidized. The ALDP is an ABC half-transporter (See chapter 1) that has to dimerize to be functional. The lack or defect of ALDP leads to impaired peroxisomal β-oxidation of VLCFA (Berger & Gärtner, 2006; McGuinness *et al.,* 2003).

The other three ABC peroxisomal membrane transporters are structurally similar to ALDP (refer to chapter 1). ALDR shares a 66% amino identity with ALDP, 33% with PMP70 and 25% with P70R (Figure 2.3).

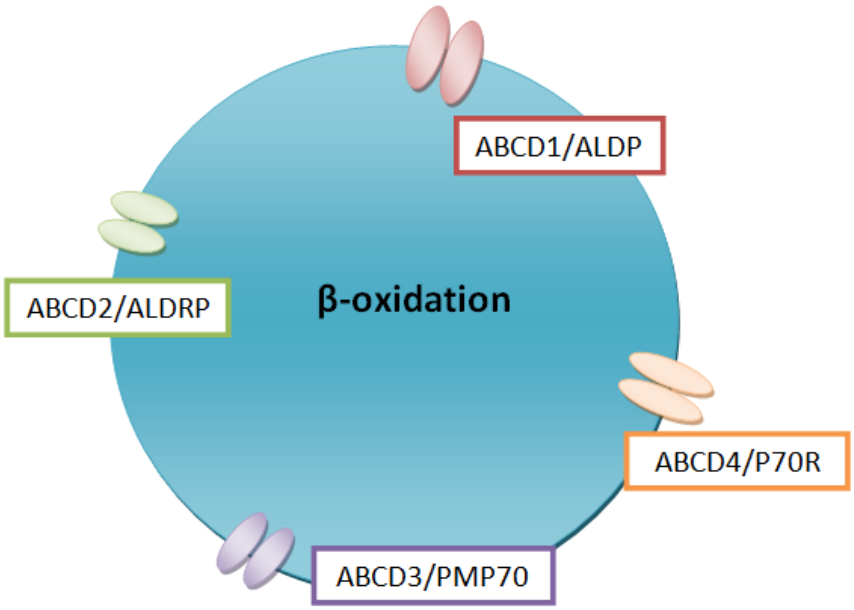

Figure 2.3: *The additional three peroxisomal ABC half-transporters. ALDP and ALDRP can transport VLCFA and VLCFA-CoA into the peroxisome (adapted from Fidaleo, 2009).*

With a high degree of similarity, ALDR is the closest relative to ALDP, suggesting functional similarity. Pujol *et al*. (2004) demonstrated that ALDRP can compensate for the loss of the defective ALDP under *in vivo* conditions. McGuinness and co-workers (2003) also demonstrated that ALDRP can facilitate the transport of the VLCFA in fibroblast with no ALDP. These findings suggested novel strategies for treating X-ALD (Kemp & Wanders, 2006). The therapy is based on pharmacological stimulation of the ABCD2 gene, elevating the amount of ALDRP to compensate for the loss of ALDP (Weinhofer *et al*., 2002; McGuinness *et al.,* 2003; Kemp *et al*., 1998).

2.5 BIOCHEMICAL ABNORMALITY IN X-ALD

X-ALD is a peroxisomal disorder. The inability of ALDP to transport the substrates, VLCFAs, from the cytoplasma to the peroxisomal lumen for β-oxidation, result in the increased intracellular levels of saturated, unbranched, VLCFAs mainly tetracosanoic (C24:0) and hexasanoic acid (C26:0). There is also a decrease in activity of peroxisomal VLCF-acyl CoA synthetase. The accumulation of the VLCFAs is the only biochemical abnormality that occurs in all the clinical phenotypes of X-ALD and is also present in pre-symptomatic patients (Fourcade *et al*., 2008; Berger & Gärtner, 2006; Pujol *et al*., 2004; Yamada *et al*., 2000).

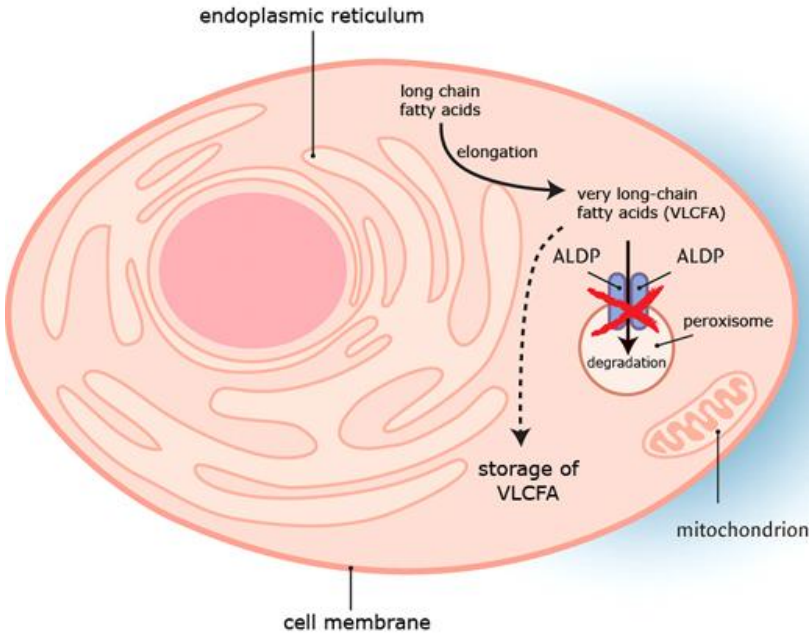

Figure 2.4: *The defective ADLP transporter lead to accumulation of VLCFA in all tissues (adapted from Engelen & Kemp 2009).*

The excess cytosolic VLCFAs accumulate in cultured cells, all tissues and body fluids leading to crystallization in the tissue. Initially the stored VLCFAs are incorporated in the lipids within the cell, then into the cell membrane phospholipid bilayer. This inclusion of VLCFA into the cell membrane of adrenal cortex cells result in a non-responsiveness to the adrenocorticotropic hormone (ACTH), leading to adrenal insufficiency (Fourcade *et al*., 2008; McGuinness *et al*., 2003; Rosebusch *et al*., 1999).

Rosebusch (1999) explained that a similar process affects the Schwann cells that produce myelin in the peripheral nervous system and in the central nervous system, the oligodendroglial cells. The phospholipid bilayers, enriched in VLCFA, destabilize and break

the myelin sheaths. The initial demyelination involves a macrophage response developing into a secondary phase of inflammatory demyelination (Pujol *et al*., 2002).

The biochemical impairment and the molecular basis are not well understood and call for further future investigation (Fourcade *et al*., 2008).

2.6 OXIDATIVE STRESS IN X-ALD

Oxidative stress occurs when the formation of free radicals, like reactive oxygen species (ROS) and lipid peroxidation, exceeds the antioxidant defences of the cell. This oxidative damage and stress are early events, leading to neuro-deterioration since the brain has lower levels of antioxidant defences with high substance of lipids, which are very vulnerable to reactive oxygen species assault. These oxidative damages are commonly observed in neurodegenerative diseases (Deon *et al*., 2008; Eichler & Aubourg, 2008; Fourcade *et al*., 2008; Deon *et al.,* 2006).

Cerebral X-ALD (cALD) is mainly a neuro-inflammatory disorder, where the inflammation stimulates the production of ROS and oxidative stress (Deon *et al*., 2008; Deon *et al.,* 2006). In the adrenal cortex and brain there is confirmation of oxidative damage, particularly from lipid peroxidation (Eichler & Aubourg, 2008; Khan *et al*., 2008).

Fourcade and co-workers (2008) investigated the toxic effect of hexasanoic acid (C26:0) and demonstrated that in the plasma and fibroblast of X-ALD patients there are indications of lipid peroxidation. They concluded that accumulated VLCFA generate ROS and cause oxidative injury in proteins.

Deon and colleagues (2008) also established that in female carriers and symptomatic X-ALD patients there are significant increase in lipid peroxidation and decrease of the tissues to handle free radical formation.

Eichler and Aubourg (2008) illustrated that antioxidants can reverse oxidative stress in X-ALD fibroblasts *in vitro*. Antioxidants could prevent neurological progression in X-ALD (Deon *et al*., 2008; Deon *et al.,* 2006)

2.7 THERAPIES IN X-ALD

Up to date, X-ALD is incurable. The present treatment is limited to (1) adrenal hormone replacement therapy for adrenal insufficiency, (2) Lorenzo's oil therapy, a dietary treatment, before the symptoms appear and (3) bone marrow or hematopoietic stem cell transplantation for boys and adolescents with early-stage cerebral involvement (Berger & Gärtner, 2006; Kemp & Wanders, 2006; Moser, 2006).

Nevertheless, the increasing interest in the molecular genetics and the unravelling of the pathogenesis of the disease and unknown mechanism promotes attempts to develop successful therapies. Novel therapies under evaluation include gene replacement and pharmacological gene therapy (Kemp & Wanders, 2006).

2.7.1 Symptomatic therapy

Symptomatic therapy can be used in the early-stage of the disease where there are a slight intellectual and behaviour changes. Patients need supportive assistance of parents, guardians and teacher. During the progression of the disease, changes occur in the sleep patterns, muscle tone and muscle dysfunction. Gastronomy feeding is used to ensure adequate intake of nutrition. Symptomatic therapy doesn't correct the genetic defect which is inevitably leading to a worsened status (Engelen & Kemp 2009; Berger & Gärtner, 2006; Moser, 2006).

2.7.2 Dietary therapy

Lorenzo's Oil (LO) is a 4:1 mixture of glyceryl trioleate (GTO) and glyceryl trierucate (GTE), the triglyceride froms of oleic and erucic acid. Oral administration of LO combined with a strict diet, low in VLCFA, reduced the VLCFA levels of asymptomatic boys with a normal brain MRI (Engelen & Kemp 2009; Deon *et al*., 2008; Berger & Gärtner, 2006; Van Geel *et al*., 1999).

LO with the diet restrictions disappointed in symptomatic patients. The therapy failed to alter the neurological progression nor did it improve the endocrine dysfunctions (Deon *et al*., 2008).

2.7.3 Bone marrow transplantation (BMT) / Hematopoietic stem cell transplantation (HSCT)

Bone marrow transplantation is able to alter the early-stage progression in cerebral X-ALD. This hematopoietic stem cell transplantation has a high mortality risk, but patients that survive do show improvement (Eichler & Aubourg, 2008; Kemp & Wander, 2006; Moser, 2006; Yamada *et al*., 2000).

Donor cells enter the central nervous system and gradually replace the perivascular microglia. They serve as a source of correction factors. Together with immunosuppressants and reconstitution of the immune system by the donor cell, this therapy can provide a permanent cure (Berger & Gärtner, 2006; Yamada *et al*., 2000).

This success story opened up a new research field. The often fruitless search for a matched donor can be overcome by somatic gene therapy (Deon *et al*., 2008; Berger & Gärtner, 2006; Singh *et al*., 1998).

2.7.4 Hormone replacement therapy

Adrenal hormone replacement therapy is mandatory because 70 % of male X-ALD patients persist with adrenocortical insufficiency. The ACTH levels must be monitored in all male patients.

Hormone therapy improves the general well-being and strength and endocrine status of these patients, but it has no significant effect on the neurological symptoms (Eichler & Aubourg, 2008; Deon *et al*., 2008; Kemp & Wander, 2006; Moser, 2006; Singh *et al*., 1998)

2.7.5 Hypolipidemic drugs

Treatment with a cholesterol-lowering drug, lovastatin, normalizes the accumulation of VLCFA in human X-ALD fibroblasts and plasma of X-ALD patients (Yamada *et al*., 2000; Singh *et al*., 1998). Lovastatin reduces cellular cholesterol by inhibiting 3-hydroxy-3-methylglutaryl-coenzyme A (HMGCoA) reductase in the cholesterol biosynthesis pathway. Weinhofer *et al*. (2002), suggested a molecular mechanism for lovastatin lowering the VLCFA levels. When the intracellular cholesterol is reduced, the sterol regulatory element binding protein (SREBP) transcription factors, that control the metabolism of cholesterol and fatty acids, interact with the sterol regulatory element (SRE) of the ABCD2 promoter, leading to overexpression of ABCD2 gene. This compensates for the impaired ABCD1 gene function, restoring the metabolism of VLCFAs.

It remains to be elucidated if lovastatin normalizes the levels of VLCFA in the nervous tissue, including the spinal cord and the brain (Berger & Gärtner, 2006).

2.7.6 Pharmacological gene therapy

Berger and co-workers (2005) described genes with overlapping functions. These suspected redundant genes form a complete or partial replacement for one another. The objective of the novel pharmacologic approach is to target the redundant genes for treatment of inherited diseases. The strategies are based on over-expressing the redundant gene so as to normalize the deficient function.

In X-ALD this approach is intended to induce the non-mutated, working ABCD2 gene to substitute the ABCD1 gene, compensating for its deficiency (Berger *et al*., 2005) (see 2.4).

Pujol and colleagues (2004), provided evidence that there is functional overlapping between ALDP and ALDRP. They demonstrated that the over-expression of ALDR in mouse tissue can completely correct the accumulation of VLCFAs. This overlapping function of ALDP and ALDR was also observed in cell cultures. These results revealed that ALDRP can compensate for the defective ALDP in vivo and in vitro (Kemp & Wanders, 2006; Berger *et al*., 2005; McGuinness *et al*., 2003; Kemp *et al*., 1998).

However, in humans the expression pattern of ABCD1 and ABCD2 genes in tissues are different. The diverse patterns of ABCD1 and ABCD2 genes in disease-associated tissues may clarify the failure of intrinsic ALDRP to compensate for ALDP deficiency in X-ALD patients. This observation leads to a new therapeutic strategy: stimulating pharmacologically the expression of the ABCD2 gene in tissues involved in X-ALD pathology. These tissues include peripheral nerve, brain white matter, testis and the adrenal cortex (Berger *et al*., 2005; Hemming *et al*., 1999).

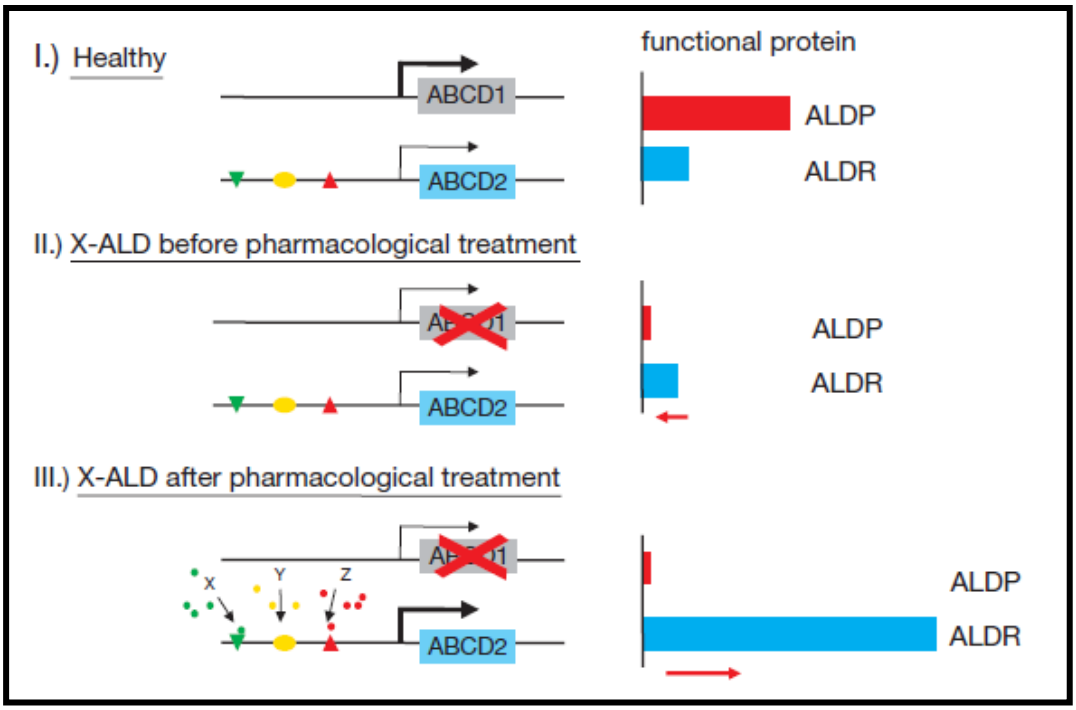

Figure 2.5: *The therapeutic approach in gene reduction. (I) In healthy humans, the ALDP is in abundance. (II) With a defective ALDP, the intrinsic ADRP cannot compensate for the ALDP loss. (III) Stimulating the ABCD2 pharmacologically results in an over-expressed ALDP (adapted from Berger et al., 2005).*

Examples of compounds regulating the expression of ABCD2 are: lovastatin (cholesterol-lowering drug); fenofibrate (peroxisome proliferators receptor α agonist,PPARα); 3,5,3'-tri-iodothyronine (T_3, a retinoid X receptor heterodimer, RXR) and phenylbutyrate, a nonclassical peroxisome proliferator.

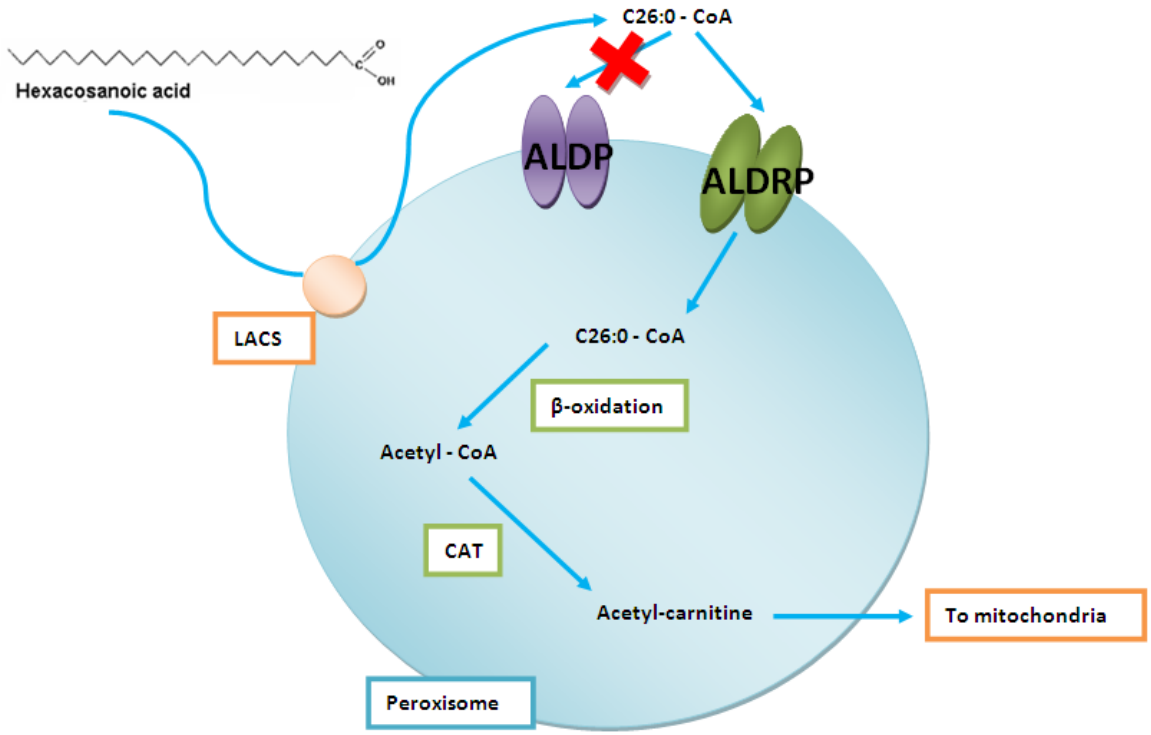

Figure 2.6: *Summary of the novel strategy to lower VLCFA levels. In X-ALD, the ALDP transporter is defective and cannot transport VLCFA into the peroxisome for β-oxidation. Alternatively, VLCFA can be transported through the over-expressed ALDRP (adapted from Kemp et al., 1998).*

Fourcade and co-workers (2010), demonstrated that valproic acid (VPA), a widely used anti-epileptic drug with histone deacetylase inhibitor properties, induced the expression of the functionally overlapping ABCD2 peroxisomal transporter. VPA corrected the oxidative damage and decreased the levels of monounsaturated VLCFA (C26:1 n-9), but not saturated VLCFA. Over-expression of ABCD2 alone prevented oxidative lesions to proteins in a mouse model of X-ALD. In a 6-month pilot trial of VPA in X-ALD patients they found reversion of the oxidative damage of proteins in peripheral blood mononuclear cells.

2.8 CONCLUSION

X-linked adrenoleukodystrophy (X-ALD) is a lethal un-curable peroxisomal disorder ranging from severe childhood cerebral phenotype to asymptomatic carriers, which is characterized by demyelination and adrenal insufficiency. X-ALD is caused by ABCD1 mutation, leading to a biochemical defect of the ALDP peroxisomal protein. This prohibits the transport of VLCFA into the peroxisome for β-oxidation, leading to the accumulation of VLCFA in tissue with a high content of lipids.

Currently, the most efficient therapeutic opportunity for patients with the cerebral form of X-ALD, is hematopoietic stem cell transplantation and possibly gene therapy of autologous hematopoietic stem cells. Both treatments, however, are only accessible to a subset of X-ALD patients, mainly because of the lack of markers that can predict the onset of cerebral demyelination. The use of Lorenzo's oil and lovastatin, to normalize very-long-chain fatty acids in clinical trials as well as currently experimental therapies, were reviewed. The latter include pharmacological gene therapy mediated by targeted upregulation of ABCD2, the closest homolog of ABCD1, using small molecule histone deacetylase inhibitors such as valproate and phenylbutyrate.

CHAPTER 3

PHENYLBUTYRIC ACID

3.1 INTRODUCTION

Phenylbutyrate (PBA; 4-phenylbutyric acid) is an orally, bio-available, aromatic, short-chain fatty acid with four carbon atoms in its side chain. It is a pro-drug that is converted to sodium phenylacetate by β-oxidation in the liver and kidney mitochondria. PBA was originally approved for treatment of urea cycle disorders (Zeitlin, 1999).

PBA has numerous biological activities: Because PBA inhibits histone deacetylase, (HDACI) (Daosukho *et al*., 2007; Goh *et al.,* 2001) it can be used as an anticancer drug (Burkitt & Ljungman, 2008). PBA also showed chemical chaperone activities to correct the cellular trafficking of several misfolded mutant proteins (Choi *et al*., 2008; Tveten *et al*., 2007). PBA has neuroprotective effects and reduces neuronal apoptosis (Gardian *et al*., 2005). These multiple mechanisms will be discussed further in this chapter.

The two most important activities of PBA is to induce peroxisome proliferation and provide protection against different stimuli, including oxidative stress (Qi *et al*., 2004; Kemp *et al*., 1998).

Phenylbutyrate is structurally related to peroxisome proliferators (PP) (discussed in chapter 1), e.g. clofibric acid (CF). These compounds share an aromatic nucleus and a carboxylic acid group (Figure 3.1). The difference between classical PPs (CF) and nonclassical PP (PBA) will be discussed later.

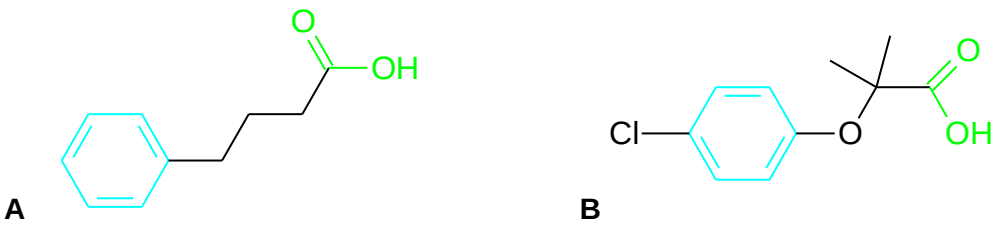

Figure 3.1: *(A) phenylbutyric acid and (B) clofibric acid both have aromatic nucleus and carboxylic acid group (adapted from Reddy, 2004; Pineau et al., 1996)*

Berger and co-workers (2005), studied PBA in the pharmacological treatment of X-ALD, based on gene redundancy (refer to chapter 2.7.6). It activates the ABCD2 gene by inhibiting HDAC activity. PBA restores peroxisomal β-oxidation of VLCFA, decreasing the levels of accumulated VLCFAs in the plasma of X-ALD patients. The increased number of peroxisomes could therefore contribute to enhanced VLCFA metabolism in X-ALD patients.

3.2 METABOLISM

The metabolism of PBA differs in humans, rats and dogs. As mentioned earlier, PBA is a pro-drug that is converted to phenylacetate (PA) by β-oxidation in the kidney and liver mitochondria. PA is a metabolically active compound that conjugates with glutamine in humans via acetylation to form phenylacetylglutamine (PAGN), which is then excreted in the urine. The known metabolites of phenylbutyrate in humans are phenylacetate, PAGN, and phenylbutyrylglutamine (PBGM) (Comte *et al*., 2002; Batshaw *et al*., 1981).

In rats and dogs PA conjugates with glycine to form phenylacetylglycine (James *et al*., 1972; Ambrose & Sherwin, 1933).

Recently, new metabolites were identified by Kasumov and co-workers (2004). The metabolites were by products originating from the β-oxidation pathway or related to glucuronide conjugates in humans and rats. These metabolites, as well as the metabolic pathway, are shown in Figure 3.2.

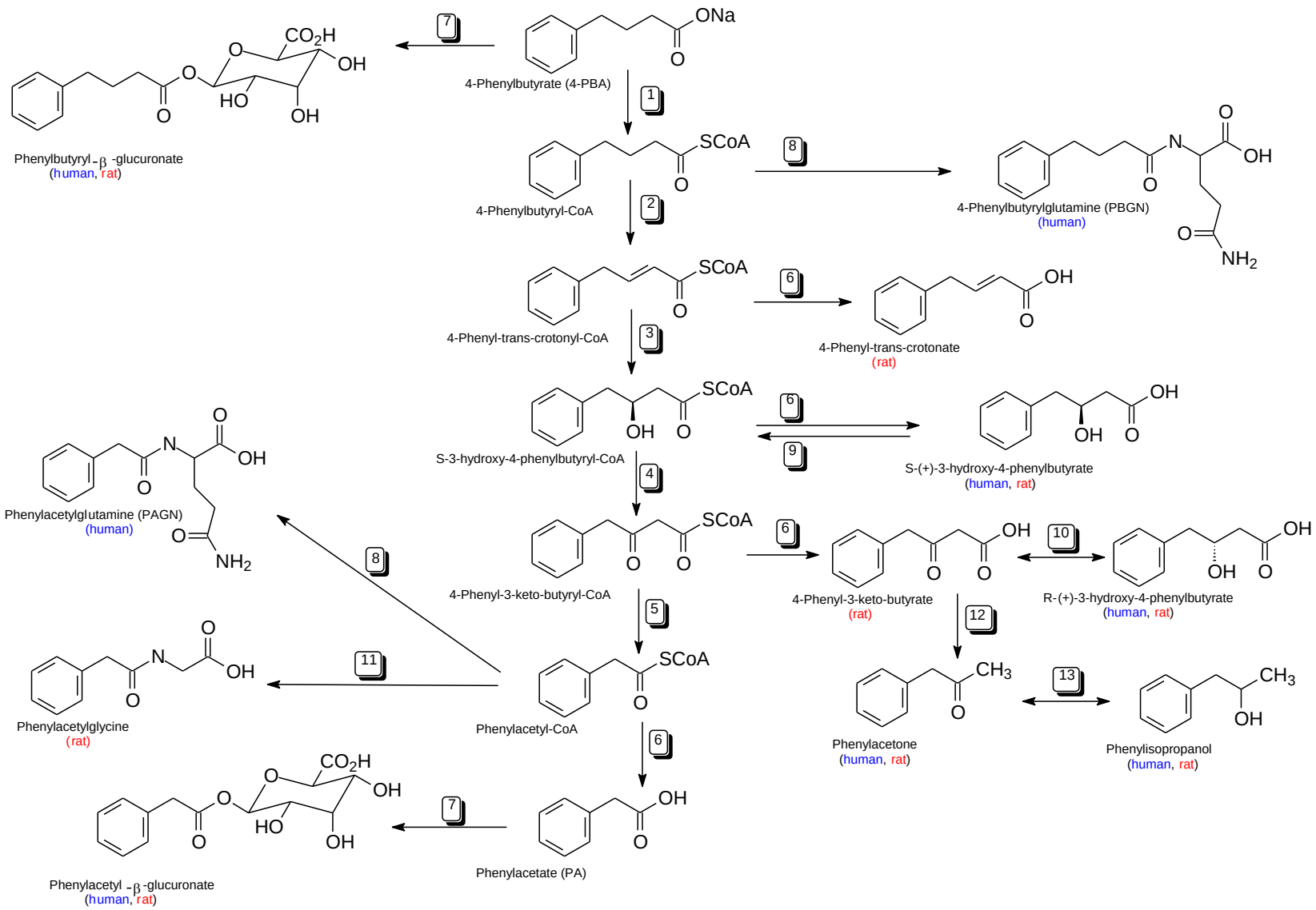

Figure 3.2: *Organic acids discovered in the urine of humans and rats. PBA is β-oxidized to phenylacetate (PA). Most of the metabolites originate from the β-oxidation pathway, using enzymes or conjugating to other products. Enzymes: (1) acyl-CoA synthetase; (2) acyl-CoA dehydrogenase; (3) enoyl-CoA hydratase; (4) S-3-hydroxyacyl-CoA dehydrogenase; (5) 3-ketoacyl-CoA thiolase; (6) acyl-CoA hydrolase; (7) UDP-glucuronyl transferase; (8) acyl-Co-L-glutamine; (9) S-3-hydroxyacyl-CoA-synthetase; (10) R-β-hydroxybutyrate dehydrogenase; (11) glycine N-acylase; (12) spontaneous phenylketobutyrate decarboxylation; (13) alcohol dehydrogenase (adapted from Kasumov et al., 2003)*

3.3 MULTIPLE MECHANISMS OF ACTION OF PBA

3.3.1 PBA, the ammonia scavenger

The urea cycle is the final pathway for the excretion of waste nitrogen in mammals. In the liver, ammonium nitrogen, derived from dietary protein sources or from the breakdown of endogenous proteins, is converted into urea. Urea is non-hazardous, water-soluble and is easily excreted as a part of urine (Deignan *et al*., 2008; Jeng *et al*., 2007; Scaglia *et al*., 2004; Leonard & Morris, 2002).

Urea cycle disorders (UCDs) are caused by the defective enzymatic activities that transfer nitrogen from ammonia to urea. In all UCDs there is accumulation of glutamine and alanine, causing reversible and irreversible disabling symptoms (Deignan *et al*., 2008; Bachmann *et al*., 2004; Scaglia *et al*., 2004; Wilcken, 2004; Leonard & Morris, 2002).

UCDs are treated by diverting nitrogen to alternative disposal routes, for example, PBA is oxidized in the liver to phenylacetate, it is then conjugated with glutamine forming phenylacetyl-glutamine. In this way PBA forms a glutamine trap, which is then excreted in the urine (Figure 3.3) (Deignan *et al*., 2008; Scaglia *et al*., 2004; Qi *et al*., 2004; Leonard & Morris, 2002; Hommes, 1999; Zeitlin, 1999).

Burlina and co-workers (2001) investigated the effect of PBA in the long-term treatment of patients with ornithine transcarbamylase (OTC). OTC is an X-linked disorder that occurs commonly in urea cycle disorders. They found that PBA is well-tolerated at high dosage with little or no adverse effects (Burlina *et al*., 2001).

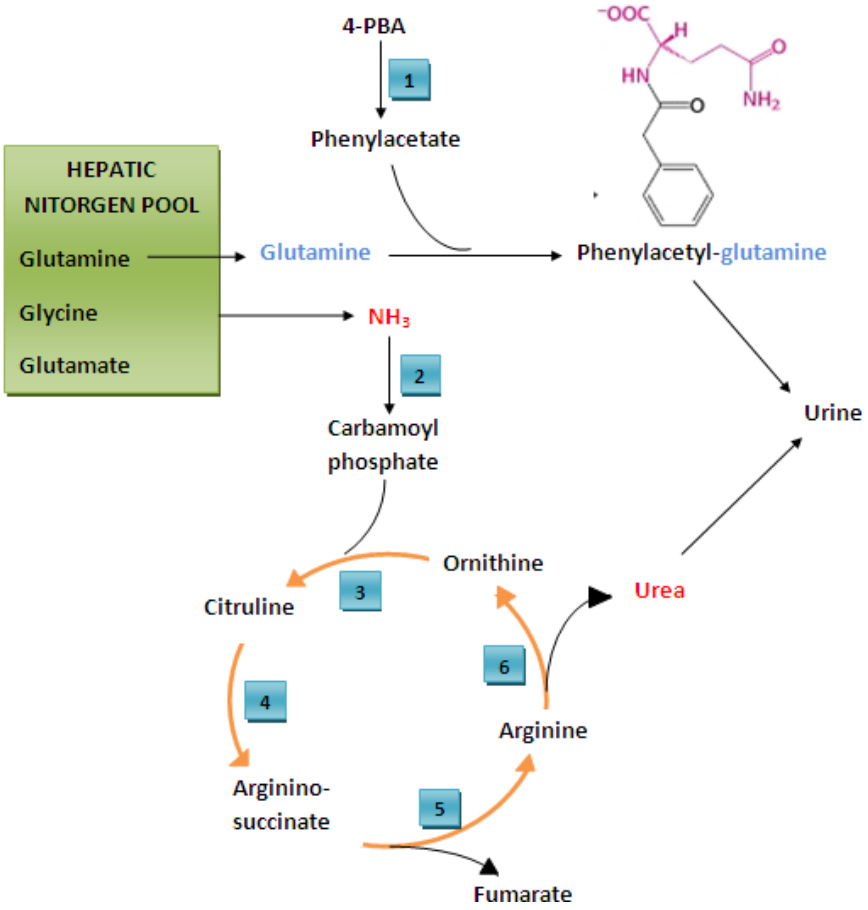

Figure 3.3: *Urea cycle pathway and alternative nitrogen waste removal of PBA. PBA is oxidized to phenylacetate. Phenylacetate conjugates with glutamine and is excreted in the urine. Enzymes involved in the urea cycle: 1. β-oxidation, 2.carbamoyl phosphate synthetase, 3. ornithine transcarbamylase, 4. argininosuccinate synthetase, 5. argininosuccinate lyase, 6. arginase (image modified from Deignan et al., 2008; Leonard & Morris, 2002).*

3.3.2 PBA as a histone deacetylase inhibitor (HDACI)

Histone acetyltransferases (HATs) and histone deacetylases (HDACs) are two enzymes catalizing the acetylation and deacytylase of histones. The histone acelytation opens the chromatin structure for gene transcription. This acetylation also stabilizes and activates transcription factors for a greater activation of target genes. The deacetylation closes the chromatin structure, inhibiting further gene expression. An imbalance between acetylation and deacetylation can cause disarray in proliferation and differentiation in normal cells, initiating the forming of a tumour (Phillips & Griffin, 2007; Bi & Jiang, 2006; Goh *et al*., 2001).

This acetylation homeostasis is a key mechanism in cancer development and heart dysfunction (Daosukho *et al*., 2007; Kennedy *et al*., 2002).

Phenylbutyric acid (PBA) is clinically being tested as an anticancer drug (Bi & Jiang, 2006; Carducci *et al*., 2001). PBA shows little or no toxicity towards the normal tissues and also provides neuro-protection as discussed later in this chapter (Daosukho *et al.*, 2007; Gardian *et al*., 2005). The anticancer activity of PBA is mainly attributed to its function as an HDACI (Burkitt & Ljungman, 2008; Daosukho *et al*., 2007, Phillips & Griffin, 2007; Phuphanich *et al.,* 2005; Davie, 2003).

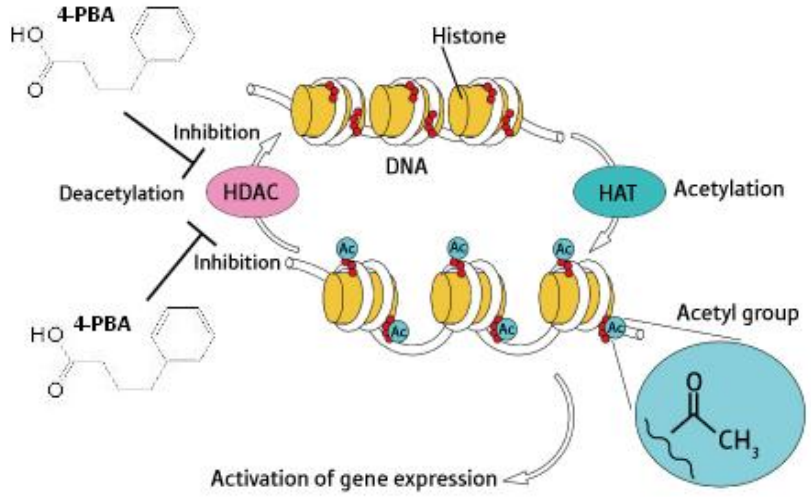

Figure 3.4: *Inhibition of histone deacetylation by PBA. The histone acelytation opens the chromatin structure of DNA for gene transcription. The acetylation is catalized by histone acetyltransferase (HAT). Shortly afterwards, the histones are deacetylated by histone deacetylase, HDAC. This stops the gene expression. PBA inhibits HDAC, leaving the histones acetylated and gene expression activated (adapted from Bi & Jiang, 2007; Davie, 2003)*

Studies done by Kennedy and co-workers (2002) revealed that PBA can be a chemo-preventative candidate for breast cancer, decreasing the risk of breast cancer. After well tolerated treatment of PBA there was a decrease in the production in mammary epithelial cells and a reduced expression of ovarian hormone receptors. PBA showed also great possibility as a growth inhibitor for nasopharyngeal tumors (Hattori *et al*., 2007). PBA in combination with cisplatin, a chemotherapeutic drug, can sensitize drug-resistant head and neck cancer cells to cisplatin (Burkitt & Ljungman, 2008).

Histone deacetylation inhibition leads to the induction of ABCD2 gene and PEX11α observed in PBA-treated fibroblasts (Gondcaille *et al*., 2005). PBA inhibits histone deacetylase to induce the expression of PEX11α and ALDP-related protein.

3.3.3 PBA activates transcription of β-and γ-globin

β-thalassemia, is an anemic disease characterised by an inadequate production of β globin. Sickle-cell anemia is an inherited blood disorder where the red blood cells have a sickle shape causing various complications (Collins *et al*., 1995; Dover *et al*., 1994).

Hudgins and partners (1996) demonstrated that PBA stimulates the production of fetal hemoglobin (HbF). HbF inhibits the polymerization of HbS (sickle hemoglobin). This lowers the tendency of HbS-cells to undergo misformation. PBA increases HbF production by the transcriptional activation of β- and γ-globin gene with well-tolerated dosage.

3.3.4 PBA as a chemical chaperone

Proteostasis disorders are caused by the misregulating or imbalances in the protein homeostasis network, which includes pathways that control protein synthesis, folding, trafficking, aggregation, disaggregation, and degradation or clearance of misfolded proteins. The inability of the proteostasis network to cope with inherited misfolding proteins, aging, metabolic or environmental stress activates or aggravates proteostasis diseases, including cystic fibrosis, Alzheimer's, Parkinson's, and Huntington's disease (Powers *et al*., 2009; Balch *et al*., 2008).

Investigations done by Tveten and colleagues (2007) showed that PBA reduced the misfolding of several proteins. PBA is identified as a chemical chaperone. Chemical chaperones are small molecules that bind to a protein, stabilize the folded state and in so doing reduce protein misfolding. PBA stabilized proteins like α_1-antitrypsin, vasopressin V2 receptor, CFTR, Parkin-associated endothelin receptor-like receptor and aquaporin-2 (Choi *et al*., 2008; Tveten *et al*., 2007).

Roque and co-wokers (2008) studied the ability of PBA to traffic ΔF508-cystic fibrosis transmembrane conductance regulator (CFTR) to the cell membrane and repair CFTR chloride function at the plasma membrane. PBA stimulates and therefore increases the production of proinflammatory cytokine interleukin (IL)-8 in a concentration-dependent manner (Roque *et al*., 2008; Hayashi & Sugiyama, 2007; Zeitlin, 1999; Rubenstein & Zeitlin, 1998).

After PBA exhibited the capability of restoring the reduced cell surface expression of CFTR, further investigations showed a similar response of the progressive familial intrahepatic cholestasis type 2 (PFIC2) to PBA treatment (Hayashi & Sugiyama, 2007).

Tveten and co-workers (2007) also investigated the effect of PBA on familial hyperocholesterolemia. The disease is characterized by defective clearance of lipoproteins because of a mutated gene encoding the low-density lipoprotein receptor (LDLR). The treatment with PBA increased the expression of LDLR restoring its functionality.

Qi and co-workers (2004), concluded in their studies that the therapeutic potential of PBA as a chemical chaperone can be used for treatment of other ER stress-related neurodegenerative diseases.

3.3.5 PBA decrease ER stress

The endoplasmic reticulum (ER) is the principal site for protein synthesis and folding, calcium storage and calcium signalling. The ER lumen has a highly oxidative setting required for these functions. ER stress results from unfolded or misfolded proteins. Activated ER stress initiates the unfolded protein response (UPR) pathway, which produces reactive oxygen species (ROS), leading to cell death (Mulhern *et al*., 2007).

A large number of studies have been done to demonstrate that PBA can decrease ER stress.

Qi and co-workers (2004) studied the prolonged ER stress in the lens epithelial cells (LECs) that result in cataract formation. PBA, diffuse into the ER lumen, stabilized and improved ER folding which postponed cataract development by protecting LECs from ER stress.

Reports of Luo and colleagues (2010) stated that PBA can suppress oxidative stress by decreasing ER stress. They investigated the effects of PBA on induced-diabetic nephropathy by streptozotocin. ER stress is also elevated in the kidney of diabetic nephropathy (DN) animal models. The induction of renal oxidative stress in rats with streptozotocin-induced DN was successfully suppressed after PBA treatment. PBA treatment reduced kidney hypertrophy and effectively stopped the progression and development of DN in animal models (Luo *et al*., 2010).

Palmitate induces the inhibition of glucose-stimulated insulin secretion (GSIS). PBA decreased the palmitate-induced-ER stress and reversed the palmitate-induced GSIS-inhibition (Choi *et al*., 2008).

Wiley and co-workers (2010) also confirmed the capability of PBA to counteract ER stress and promote protein trafficking, demonstrating a neuroprotective mechanism of PBA (Wiley *et al*., 2010; Lui *et al*, 2002).

3.3.6 PBA is neuroprotective

PBA can be used for multiple sclerosis because it reduces the neuro-inflammation and the disease progression (Dasgupta *et al*., 2003). Qi and colleagues (2004) showed that PBA protects the brain from ischemic injury by reducing the infarct volume and hemispheric swelling. The reduced neuronal apoptosis further confirmed the protective effect of PBA. Importantly, PBA provides a wide therapeutic window for treatment to be effective before and after cerebral ischemic development.

Experiments done by Mulhern and co-workers (2007) revealed that pre-treatment of retinal ischemia with PBA can reduce the level of ischemia-associated loss of thickness of the total retina. These results emphasize the neuroprotective effect of PBA on high intraocular pressure-induced ischemia (Jeng *et al*., 2007).

Gardian and co-workers (2005) investigated the promising neuroprotective effect of PBA for treatment of Huntington's disease (HD). Their findings showed that PBA have neuroprotective effects and increased the survival rate in symptomatic HD in transgenic mouse models.

Lui and co-workers (2002) demonstrated that PBA prevents the loss of catalase occurring in ts1 MoMuLV infected astrocytes. The catalase protein levels in brain of ts1-infected mice are maintained by PBA after peroxisome proliferation.

3.3.7 PBA as a nonclassical peroxisomal proliferator

Classical peroxisome proliferators (PPs) such as clofibrate, activates PPARα (refer to chapter 1) and peroxisomal Acyl-CoA oxidase (AOX), causing peroxisome proliferation in rodents treated with PPs. Hertz and co-workers (1987), investigated the possibility of hypolipidemic PP's to induce peroxisomal proliferation in humans. Human hepatoma cells were treated with clofibrates, but it did not induce peroxisomal activities or peroxisome proliferation. Other studies reported peroxisome proliferation in rodents but also not in humans (Gondcaille *et al*., 2005, Gariot *et al*., 1987; Blümcke *et al*., 1983; Hanefeld *et al*., 1983; De La Iglesia *et al*., 1982). Hertz and colleagues (1987) concluded that the nonresponsive human cells to PP's indicate species specificity (Hertz & Bar-Tana, 1998, Hertz *et al*., 1987).

Kemp and co-workers (1998) studied fibroblasts in X-ALD patients and ABCD1 -/- mice (mice without ALDP). They demonstrated that PBA restored the β-oxidation of VLCFA and also increased the expression of ABCD2. There was also a reduction of VLCFA in the brains of ABCD1 -/- mice. The authors revealed an increase in peroxisomes in the X-ALD human fibroblast and control. Gondcaille and partners (2005) demonstrated that PBA induced the expression of ABCD2 in both PPARα +/+ and PPARα -/- fibroblasts, indicating that there is no involvement of PPARα activation of ABCD2. The data indicates that PBA acts as a nonclassical peroxisomal proliferator (Gondcaille *et al*., 2005; McGuinness *et al*., 2001; Kemp *et al*., 1998).

Gondcaille and colleagues (2005) also reported that PPARα activation and peroxisome proliferation of PP's occur early in rodents after the beginning of treatment. In contrast, PBA had no peroxisome proliferation effect with short-term treatment, confirming a different mode of action. However, the lack of gene induction could result from a rapid catabolism of PBA (half life is 1-2h). Therefore they treated rats with high doses of PBA over a period of 6 to 9 weeks. They detected induction of ABCD2 and AOX expression and also noted a change in the shape and distribution of the peroxisomes. Peroxisomes were phi-shaped and clustered, almost touching each other, proposing a fission or budding process (Gondcaille *et al*, 2005).

Mammals have multiple PEX11 genes. Li and co-workers (2002), investigated the PEX11α and PEXβ genes, PMPs, which promote peroxisomal division (refer to chapter 1). The increased expression of either PEX11α or PEX11β is adequate to stimulate peroxisomal division (Islinger *et al*., 2010; Thoms *et al*., 2009; Li *et al*., 2002). They demonstrated that cells without PEX11 are not responsive to the peroxisome proliferation action of PBA and are unable to induce peroxisome synthesis, confirming that PBA stimulates PEX11 for peroxisome proliferation (Li *et al*., 2002).

The necessity of PPARα activation and PEX11α for peroxisome proliferation and the type of cell where peroxisome proliferation occurs, differ for PBA and classical PPs. Both PBA and PP induce PEX11α. PPs induce peroxisome proliferation by activating PPARα and not PEX11. PBA requires PEX11 to induce peroxisome proliferation in humans, initially changing from round vesicles into stretched out tubules, then followed by many small vesicular peroxisomes (Gondcaille *et al*, 2005; Li *et al*., 2002).

The peroxisome proliferation action of PBA led to considerable interest to explore PBA as treatment for X-ALD (Berger *et al*., 2005; McGuinness *et al*., 2001). Pharmacological therapy of X-ALD is based on the functional peroxisomal transporter, ALDRP, to compensate for the loss of ALD protein (Engelen *et al*., 2008; Berger *et al*., 2005). PBA decreases

VLCFA levels in X-ALD patients by increasing peroxisomal β-oxidation causes: (1) over-expression of the ABCD2 gene, (2) increased expression of ALDRP, (3) increased transport of VLCFA into peroxisomes into the β-oxidation pathway, (4) an increase in the number of peroxisomes (also leading to increased number of ALDRP) and (5) a decrease in VLCFA levels in the brain, because phenylacetate can cross the blood-brain barrier (Engelen *et al*., 2008; Berger *et al*., 2005; Gondcaille *et al*, 2005; McGuinness *et al*., 2001; Netik *et al*., 1999)

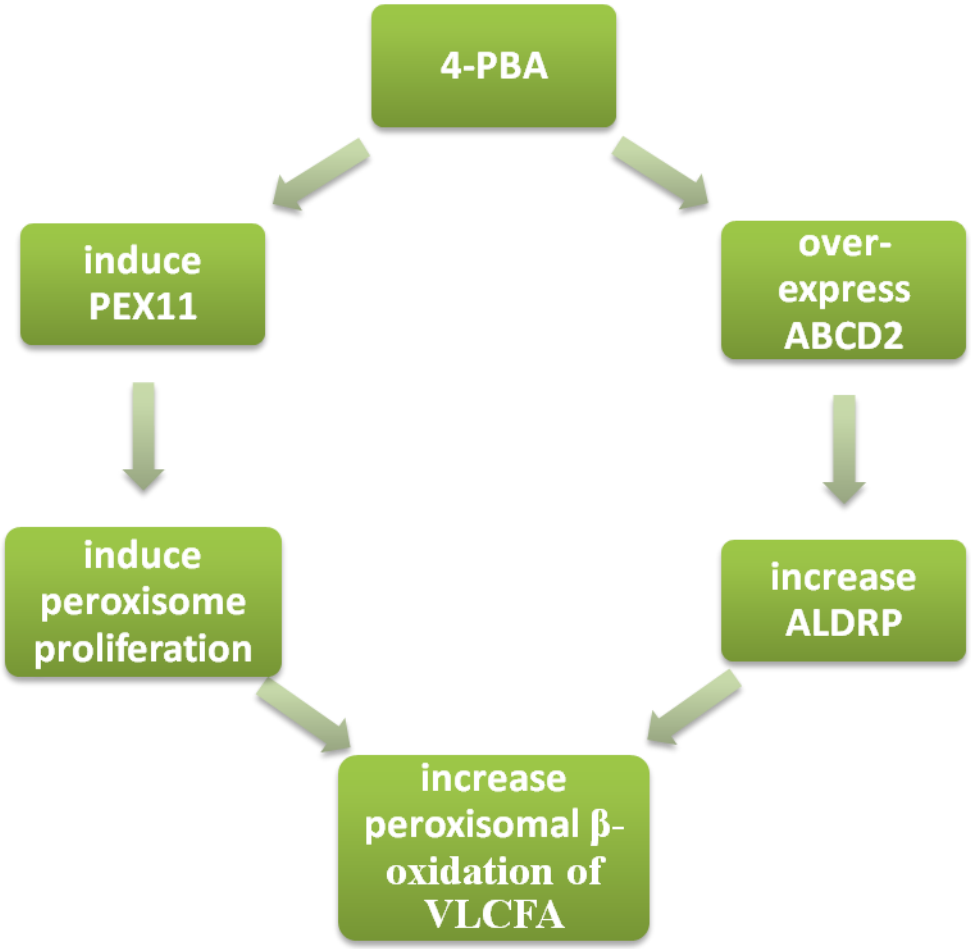

Figure 3.5: *The postulated mechanism of PBA for treating X-ALD is to decrease VLCFA in plasma by increasing peroxisomal β-oxidation of VLCFA (adapted from Engelen et al., 2008; Berger et al., 2005; Gondcaille et al, 2005; McGuinness et al., 2001; Netik et al., 1999)*

3.3.8 PBA, peroxisome proliferator, protects against oxidative stress

Stamer and colleagues (2002), noted that the absence of peroxisomes in cells expose them to oxidative stress, leading to disintegration. They studied Alzheimer's disease, a

neurodegenerative disease. The disease initially starts when the tau protein, the protein that generates and maintains neuritis, accumulates in the neurons. This leads to an enhanced production of the toxic β-amyloid peptide (Aβ) and oxidative stress. They observed the oxidative stress effect of the tau protein and the decreased levels of peroxisomes in tau-transfected cells. The death of cells excelled when tau-expressed cells were exposed to H_2O_2. They experiments demonstrate that the inhibition of catalase intensified the oxidative damage induced by H_2O_2 (Ricobaraza *et al*., 2009; Stamer *et al*., 2002).

Peroxisomal proliferation protects Aβ-dependent toxicity in hippocampal neurons. Experiments revealed that PBA protects the normal shape of hippocampal neurons, axonal processes and neuritis. Catalase plays an important role in neuronal protection. Peroxisome proliferation decreased the elevated level of ROS produced by incubating neurons with Aβ or H_2O_2. These experiment showed that the increased number of peroxisomes protect neurons from Aβ-induced oxidative stress, preventing cell death and morphological changes. These events are mediated by the increase in the number of peroxisomes and catalase activity (Ricobaraza *et al*., 2009; Stamer *et al*., 2002).

3.4 CONCLUSION

Phenylbutyric acid (PBA) is a short-chain fatty acid that is well-tolerated and has a potential beneficial role in the treatment of different diseases. PBA is a multi-drug with numerous biological activities, including HDAC inhibitor, neuroprotector, a chemical chaperone, transcriptor of β-and γ-globin and ammonia scavenger in urea cycle.

Most importantly PBA protects tissues from oxidative stress and is a nonclassical peroxisome proliferator. This mechanism leads to a possible treatment for X-ALD. The increase in peroxisomes and over-expression of ABCD2 gene leads to an increase in the transport of VLCFA into the peroxisome, thus restoring the β-oxidation of VLCFA. The peroxisome proliferation also increases the catalase activities to reduce the oxidative stress that is involved in many neurodegenerative diseases.

It is clear that a substantial fraction of the metabolites of PBA has not yet been identified and compounds resulting from hydroxylation of the benzene ring might also be formed (Kasumov *et al*., 2004) and most important: which metabolites contribute to the proliferation and/or toxicity?

CHAPTER 4

MATERIALS AND METHODS

4.1 INTRODUCTION

The metabolic profile of phenylbutyric acid (PBA) was investigated and its *in vitro* and *in vivo* antioxidant capacity was examined in vervet monkeys and HeLa cells respectively. This study was approved by and done in accordance with the guidelines stipulated by the Ethics Committee for the Use of Experimental Animals at the North-West University, Potchefstroom (0019-09-A5) (see Appendix J).

4.2 EXPERIMENTAL DESIGN

A schematic representation of the experimental design is given in Figure 4.1. HeLa human cervical carcinoma cells were used for the *in vitro* study and were cultivated until ready for the experiments. The antioxidant capacity was determined by measuring the Reactive Oxygen Species (ROS) and lipid peroxidation (LP) with flow cytometry. Additionally apoptosis and cell viability were determined, also using flow cytometry. Fluorescence images were taken to visualize the peroxisome proliferation.

One female vervet monkey (*Cercopithecus aethiops*), was used for the *in vivo* study of which the mass varied between 2.40 and 3.10 kg. The monkey was housed in a squeeze-back stainless steel cage and maintained on a balanced diet, purchased from the Medical Research Council and supplemented with fresh vegetables/fruit. Food was given twice daily (9.00–9.30 am and 3.00–3.30 pm), and water was available *ad libitum*. The monkey was anaesthetized with approximately 10 mg/kg ketamine hydrochloride to enable handling and blood collection.

In vivo, the ROS and LP were determined by flow cytometry. A standardised method, employing gas chromatography-mass spectrometry (GC/MS), was used to analyse the organic acids in the urine and fatty acids in the blood to identify known and new metabolites of PBA in the vervet monkey.

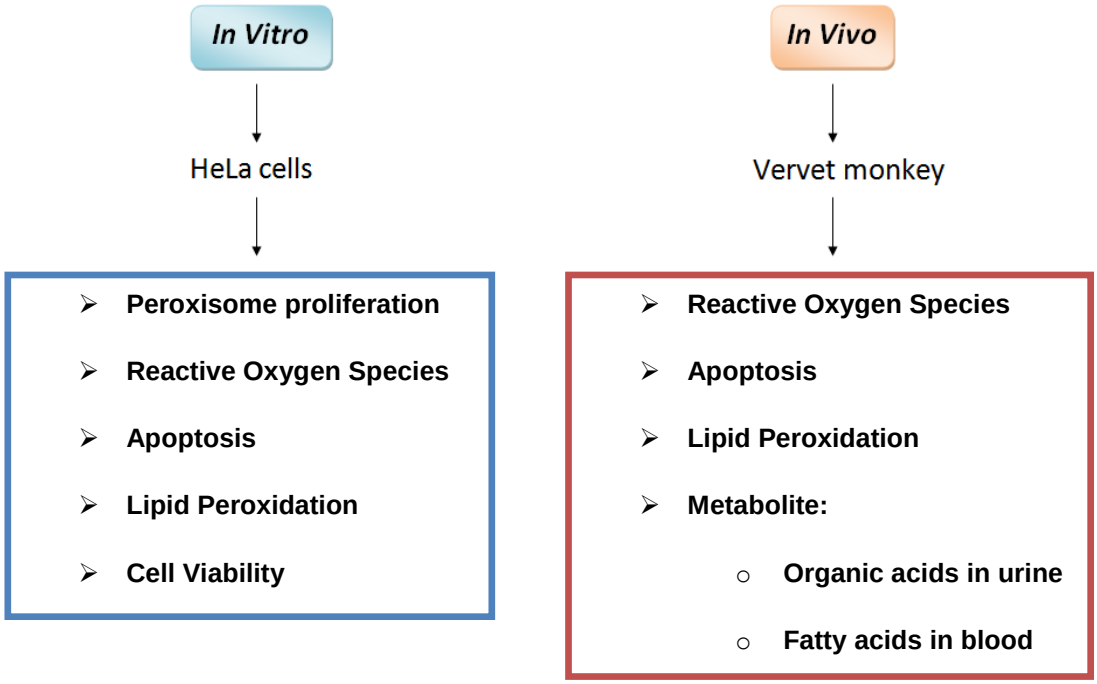

Figure 4.1: *Schematic representation of experimental design*

4.3 IN VITRO ASSAYS

A schematic representation of the different *in vitro* assays is given in Figure 4.2. HeLa cells were cultivated in 75 cm^2 Falcon cultured flasks until the cells were 90% confluent. The cells were then seeded in a 24-well plate or 6-well plate according to each assay. Different concentrations of PBA were added to each well and incubated for 48 hours. After incubation, the ROS, LP, apoptosis and cell viability were analysed by flow cytometry (FACSCalibur^{TM}, Beckton Dickinson) and the peroxisome proliferation by fluorescence microscopy.

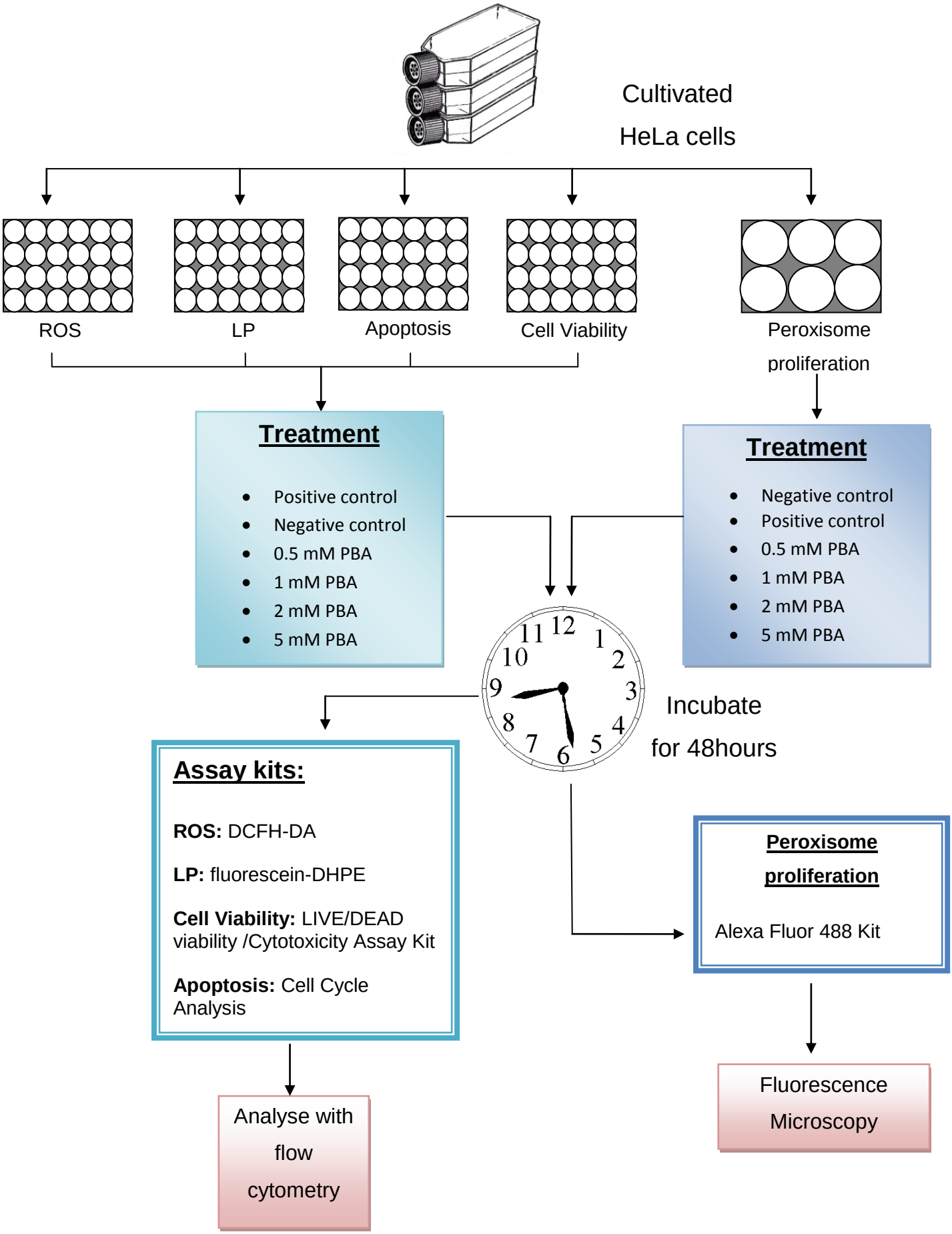

Figure 4.2: *Schematic representation of in vitro cell assays*

4.3.1 Materials

Chemical / Reagent	Supplier
Dulbecco's modified Eagle's medium (DMEM)	Separations
Foetal bovine serum (FBS)	Separations
sodium pyruvate	Separations
penicillin streptomycin	Separations
trypsin	Separations
trypan blue	Separations
HeLa cells	Biochemistry, North-West University
PBA	Nutr-e-volution

4.3.2 Cultivation

Cultures of HeLa cells were grown in 75 cm^2 Falcon cultured flasks with modified Dulbecco's modified Eagle's medium (DMEM). The medium was supplemented with 100 units/ml penicillin, 100 µg/ml streptomycin and with foetal bovine serum (FBS) at a final concentration of 10% and buffered with 1 mM sodium pyruvate. All cultures were maintained in an atmosphere of about 5% CO_2 in air at 37 ^oC. Mass cultures were maintained until the cells were 90% confluent and ready for assays.

When the cells were ready, the medium was aspirated and the cells were detached from the flask bottom surface by means of trypsinization (0.05% Trypsin-EDTA). The 5 ml trypsin-EDTA solution was pre-heated to 37 ^oC and left in contact with the cells for 10 minutes. The cells were shaken into suspension and carried over to a 15 ml Falcon tube. The suspension was centrifuged for 5 minutes at 1000 rpm at room temperature. The trypsin supernatant was aspirated and 1 ml of new medium was added to the cell pellet and dissociated. Fifty µl of the cells suspension were added to 450 µl of Trypan blue and counted.

Depending on the experiment, the cells were seeded either into 24-well plate at a density of 5.0×10^5 cells in 1 ml medium for flow cytometry analysis or 10 µl of cell suspension on 30 mm coverslips placed into 6-well plates with 3 ml of medium for fluorescence microscopy. All the plates were incubated for 24 hours before treatment.

4.3.3 PBA treatment

Stock solutions of PBA were made beforehand: 1 mM, 2 mM, 4 mM and 10 mM. In experiments using the 24-well plate, only 1 ml of each concentration was added to 1 ml cell suspension in the 24-well plates, giving final concentrations of 0.5 mM, 1 mM, 2 mM and 5 mM PBA. In experiments using the 6-well plates, 3 ml of each concentration were added to

3 ml cell suspension in the 6-well plates, giving concentration s of 0.5 mM, 1 mM, 2 mM and 5 mM PBA. All the well-plates were incubated for another 48 hours.

4.4 IN VIVO ASSAYS

A schematic representation of the *in vivo* assays is given in Figure 4.3. The monkey was anaesthetized with ketamine hydrochloride and weighed before treatment. Control blood and urine samples were taken. A single dose of 130 mg/kg PBA, dissolved in 30 ml of normal saline, was given by gavage. Blood samples were taken at 15 minutes, 30 minutes, 1, 2 and 3 hours after treatment. ROS, apoptosis and lipid peroxidation were determined with fluorescein-based flow cytometry. Peroxisome proliferation was examined with a fluorescence microscope. Urine was also collected at 15 minutes, 30 minutes, 1, 2, 3, 7 and 24 hours after treatment. A standardised method, employing gas chromatography-mass spectrometry (GC/MS) was used to determine the organic acids in the urine and fatty acids in the blood.

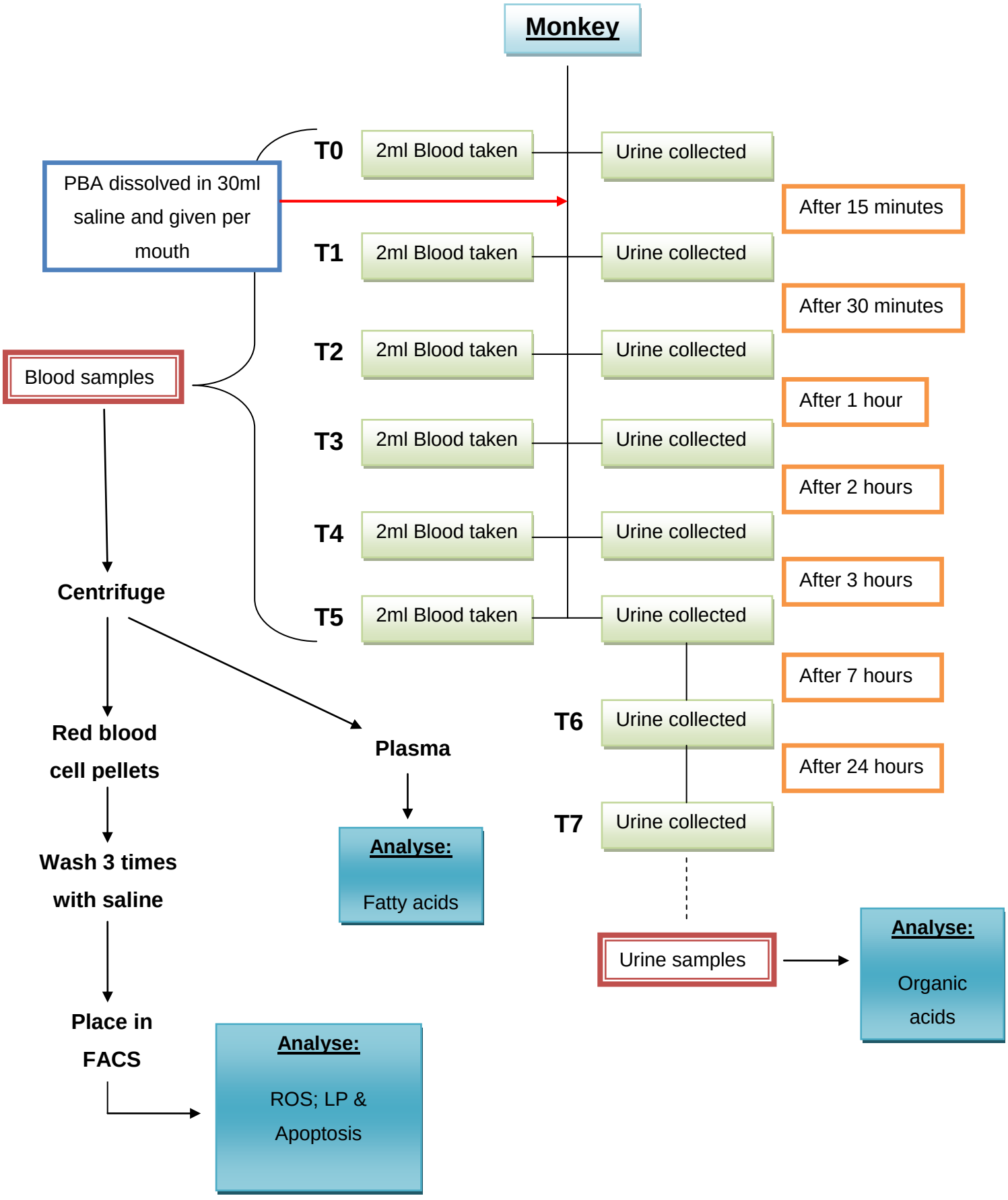

Figure 4.3: *Schematic representation of in vivo assays*

4.5 SAMPLE PREPARATION

4.5.1 In vitro

Experiments with the 24-well plate: The medium with PBA was aspirated from the well plates. Trypsin-EDTA (500 µl) were added to detach the cells and incubated for 5 minutes. The cells were shaken into suspension and then placed into 1.5 ml microtubes. The suspension was washed 3 times with 1 ml of PBS and centrifuged at room temperature for 7 minutes at 1500 rpm. The cells were resuspended in 500 µl of PBS (phosphate buffer solution) and placed into tubes for the flow cytometry assays.

Experiments with the 6-well plate: The medium with PBA was aspirated from the well plates and the sample was ready for the assay.

4.5.2 In vivo

All the blood samples (± 2 ml) were drawn from the femoral vein into EDTA tubes. The 2 ml blood was split into two aliquots of 1 ml each. Blood samples (1 ml) were centrifuged at 5000 rpm for 10 minutes at 37 °C to separate plasma. Plasma was removed using a Pasteur pipette and placed into microtubes and stored at -80 °C until analysis. Red blood cells (RBC) were washed 3 times with an equivalent volume of IV normal saline (0.9% NaCl) and all the non-red blood cell cells were removed after each wash to minimize contamination. The RBC was placed in tubes for the flow cytometry assays.

The other 1 ml blood sample was used to isolate the peripheral blood mononuclear cells (PBMC). Histopaque -1077 (15 ml) was added to the upper chamber of an Accuspin tube and centrifuged at 800 x g for 30 seconds at room temperature. The outside of all securely closed blood tubes were sprayed with 70% isopropyl alcohol before removing the caps carefully to prevent spillage. The blood (1 ml) was transferred to the Accuspin tubes and then centrifuged at 800 x g for 15 minutes at room temperature. Then the Accuspin tubes were removed from the machine. With a pipette, the plasma layer was removed within 1 cm of the interphase containing the mononuclear cells. The interphase was transferred, using a sterile pipette, into a centrifuge tube containing approximately 25 ml of DPBS for subsequent washes. During the first wash, the tubes were centrifuged at 325 x g for 10 minutes. The DPBS was discarded into a waste container. The washing was repeated twice and centrifuged at 275 x g after the two washes for 10 minutes each time. Lastly, the cells were centrifuged at 225 x g for 10 minutes to remove DPBS. The cell pellets were loosened by gently tapping the tube. There were $5 \times 10^5 – 1 \times 10^6$ cells per tube.

Urine samples were collected in urine cups and frozen until analysis.

4.6 METHODS

4.6.1 Reactive oxygen species (ROS)

This method requires that the intracellular oxidant levels are measured with the probe 2',7'-dichlorodihydrofluorescein diacetate (DCFH-DA), where it is deacetylated by esterase to dichlorofluorescin (DCFH) and then oxidized inside the cell to the highly fluorescent dichlorofluorescein (DCF) which is measured at 488/520 nm excitation/emission by a flow cytometer, the FACSCalibur (Amer *et al*., 2004; Sen *et al*., 2007 and du Plessis *et al*., 2010).

4.6.1.1 Materials

Chemical / Reagent	Supplier
DCFH	Invitrogen, Molecular Probes
PBS	Invitrogen
H_2O_2	Sigma-Aldrich

4.6.1.2 Assay

For the assay, approximately 1.0 x 10^5- 2.0 x 10^5 HeLa cells or RBC per 500 µl PBS were collected in tubes. A stock solution of dye at 10 mM in methanol was prepared. The dye was used at 10 µM final concentration per 500 µl. The following controls were prepared and analysed before the experimental sample: a cell control with only HeLa cells in 500 µl PBS; a negative control consisting of cells in 500 µl PBS with 10 µM dye added; a positive control consisting of cells, pre-treated with H_2O_2, in 500 µl PBS with 10 µM dye added (Pre-incubate the cells after adding 4 mM H_2O_2 for 1 hour, before adding the dye). With the experimental samples, 0.5 µl dye were added to the cells which were then incubated for 30 minutes in the dark. The fluorescence was measured at ~488/520 nm excitation/emission.

4.6.2 Lipid peroxidation (LP)

In this assay, the cell lipid peroxidation is measured with the probe N-(fluorescein-5-thiocarboyl)-1,2-diheade-canoyl-sn-glycero-3-phosphoethanolamine, triethylammonium salt (fluorescein-DHPE) (Amer *et al*., 2004; du Plessis *et al*., 2010).

4.6.2.1 Materials

Chemical / Reagent	Supplier
Fluorescein-DHPE	Invitrogen, Molecular Probes

4.6.2.2 Assay

For the assay, approximately 1.0 x 10^5- 2.0 x 10^5 HeLa cells or RBC per 500 µl PBS were collected in tubes. A stock solution of dye (10 mM in ethanol) was prepared. The dye was used at a final concentration of 5 µM per 500 µl. The following controls were prepared and analysed before the experimental sample: a cell control with only HeLa cells in 500 µl PBS; a negative control consisting of cells in 500 µl PBS with 50 µM dye added; a positive control consisting of cells in 500 µl PBS with 50 µM dye added after which the dye was removed by washing with PBS and the cells were treated with 8 mM H_2O_2. With the experimental samples, 2.5 µl dye were added to the cells and incubated 60 minutes in the dark. The fluorescence was analysed at ~488/520 nm excitation/emission.

4.6.3 Cell viability

This is a two-colour fluorescence cell viability assay that can determine live and dead cells simultaneously with two probes that measure intracellular esterase activity and plasma membrane integrity.

4.6.3.1 Materials

Chemical / Reagent	Supplier
LIVE/DEAD Viability/Cytotoxicity kit	Invitrogen, Molecular Probes

4.6.3.2 Assay

The assay was done according to the instructions provided with the kit. Approximately 1.0 x 10^5 – 2.0 x 10^5 HeLa cells per 500 µl PBS were collected in tubes. All the reagents and experimental samples were brought to room temperature. Initially, a 50 µM working solution of calcein AM (component A) in DMSO was prepared, by adding 2 µl of the 4 mM component A to 158 µl DMSO, prior to use. Then 2 µl of the 50 µM calcein AM working solution and 4 µl of the 2 mM ethidium homodimer were added to 1 ml cell suspension and mixed. The cells were incubated for 15-20 minutes at room temperature and protected from light. After incubation, the stained cells were analysed by flow cytometry using 488 nm excitation and measuring green fluorescence emission (~530 nm) for calcein and red fluorescence emission (~610 nm) for ethidium homodimer. The cells separated into two groups: live cell showed green fluorescence and dead cells showed red fluorescence.

4.6.4 Cell cycle analysis / Apoptosis

This assay is used to determine whether PBA modifies the cell cycle of HeLa cells and if the cell inactivation is induced by way of an apoptotic mechanism. Propidium iodide (PI) is a DNA specific dye used to determine DNA content or cell cycle analysis.

4.6.4.1 Materials

Chemical / Reagent	Supplier
PI	Invitrogen, Molecular Probes
RNase	Sigma-Aldrich
Triton X-100	Sigma-Aldrich

4.6.4.2 Assay

For the assay, approximately 1.0 x 10^5 – 2.0 x 10^5 HeLa cells per 500 µl PBS were collected in tubes. For flow cytometry measurement, the cells were fixed by adding 700 µl cold ethanol to 300 µl of cell suspension in PBS while vortexing gently. The cells were kept for 24 hours at 4 ^{o}C. The cells were centrifuged at 1200 rpm at 4 ^{o}C for 5 minutes, washed 1 time with PBS and re-centrifuged. After centrifugation, the cells were resuspended in 0.25 ml of PBS and 5 µl of 10 mg/ml RNase was added. Cells were incubated for 1 hour with the RNase solution at 37 ^{o}C. After incubation, 25 µl of 1 mg/ml PI solution and 25 µl of Triton X-100 were added. The samples were kept in the dark at 4 ^{o}C until analysis. Samples were analysed at ~488/630 nm excitation/emission.

4.6.5 Peroxisome proliferation

This method uses an antibody binding to a high-abundance integral peroxisomal membrane protein (PMP70) that can be visualized by a fluorescence microscopy.

4.6.5.1 Materials

Chemical / Reagent	Supplier
SelectFX® Alexa Fluor ® 488 Peroxisome Labeling Kit	Invitrogen, Molecular Probes

4.6.5.2 Assay

The assay was done according to the instructions provided with the kit. Different stock solutions were prepared: (1) 1 L of PBS solution where 900 ml dH_2O were added to 100 ml of 10 x PBS; (2) a fixative solution when the ampoule (10 ml) of the 4 x fixative solution were added to 30 ml of the PBS; (3) a permeabilization solution of 0.2% Triton X-100 when mixing

1 ml of the100 x permeabilization solution and 99 ml of PBS; (4) a blocking reagent consisting of 10% NGS when mixing 50 ml of the 10 x blocking reagent and 450 ml of PBS; (5) the diluted primary antibody solution by centrifuging (at 4 ^{o}C for 2 minutes at 10 000 x g) the tube containing the anti–PMP 70 antibody and adding 1 µl of the antibody solution to 1 ml of blocking reagent and (6) the diluted secondary antibody solution by centrifuging (at 4 ^{o}C for 2 minutes at 10 000 x g) the tube containing the Alexa Fluor 488-labeled secondary antibody, adding 1 µl of the antibody solution to 1 ml of PBS.

For the assay, 1.0 x 10^5 – 2.0 x 10^5 HeLa cells in the 6-well plates were used. The cells were washed with 1 ml warmed PBS. The cells were fixed by adding 800 µl of the fixative solution to the sample and incubated for 15 minutes at 37 °C. The cells were washed twice with 1 ml PBS. The cells were permeabilized by adding 1 ml of the permeabilization solution to the sample and incubated at room temperature for 5 minutes. The cells were washed twice with 1ml PBS and 1 ml blocking reagent was added to the sample, which was incubated for 1 hour at room temperature. The diluted primary antibody solution (200 µl) was added to the sample, which was incubated at room temperature for 2 hours protected from light. Cells were then washed 4 times with 1 ml of blocking solution. Alexa Fluor 488-labeled secondary antibody (200 µl) was added to the sample and incubated at room temperature for 2 hours protected from light. Cells were washed 4 times with 1 ml PBS. The samples were viewed with a fluorescence microscope (Nikon, TE2000) equipped with appropriate filters.

4.6.6 Flow Cytometric determination

Flow cytometry can measure different properties of individual cells as they flow one by one through a column. The cell is probed with beams of light/lasers. The light scattering or fluorescence emission provides information about the cell. The light scattering analyses the cell's size (forward scatter) and granularity (side scatter). The fluorescence scattering provides information about the specifically selected properties of the cell. The properties are detected by a series of mirrors, detectors and filters. The information of the light scattering or fluorescence emission is collected and analysed by analytical software packages to present data graphically.

4.6.6.1 Experimental design

A schematic overview of the flow cytometry evaluation is given in Figure 4.4. The tube was vortexed and the prepared samples passed through the FACSCalibur Flow Cytometer. The cells passed one by one through the 488 nm argon ion laser (used for excitation) where each sample was counted. The properties were evaluated by the forward scatter (FSC), the side scatter (SCC), FL-1 or green channel filter and FL-2 or yellow channel. Data are presented

as dot plots or histograms. Data were collected with BD CellQuest Pro software and further analysed by FCSExpress software.

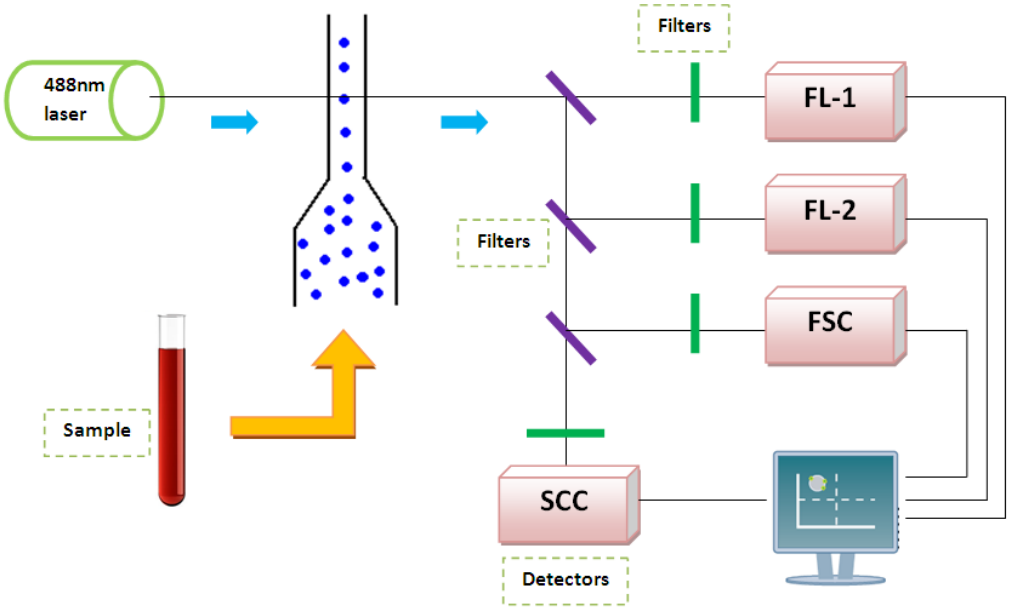

Figure 4.4: *Schematic overview of the flow cytometric evaluation of the different assays (adapted from Herzenberg et al., 2002)*

4.6.6.2 Analysing Mean Fluorescence Intensity (MFI)

All the data obtained from the different assay were measure as mean fluorescence intensity (MFI).

To express the results relative to the control, the following equation were used:

$$\text{Equation 1: } \% = \frac{\text{sample MFI (arbit. units)} \times 100}{\text{Positive control sample}}$$

Equation 1 was used to interpret the ROS, cell viability and apoptosis data.

There is an inverse correlation between lipid peroxidation and mean fluorescence intensity.

$$\text{Equation 2: } LP = \frac{1}{\text{sample MFI (arbit. units)}}.$$

Equation 2 was used to express the data as lipid peroxidation. Equation 1 was then used again to express the lipid peroxidation data relative to the positive control.

4.6.6.3 Statistical Evaluation

Data are presented as mean ± standard error (SE) in tables and graphical form. Data were evaluated for statistically significant differences using GraphPad version 5 software, and data tested for normality and analysed non-parametrically. Data of the ROS, LP and apoptosis assays were analysed with one-way ANOVA followed by Dunnets posttest to compare all treatment groups with the control. Significance was set as $p \leq 0.05$. Data of cell viability was analysed with two-way ANOVA followed by Bonferroni posttest to compare all treatment groups with control. Significance was set as $p \leq 0.001$.

4.6.6.4 Fluorescence Microscopic evaluation

A schematic overview of fluorescence microscopy is given in Figure 4.5. In fluorescence microscopy, the light source (an arc lamp) produces a full-spectrum of light which is passed through a coloured excitation filter to produce the specific excitation radiation. This is reflected by the dichroic mirror, goes through the objective and to the sample. The sample fluoresces and some of the emitted radiation goes back through the objective. The dichroic mirror transmits the longer wavelength light to the emission filter to separate the very bright excitation and the relatively weak fluorescence. The final image is magnified and can be seen or photographed (Lichtman & Conchello, 2005).

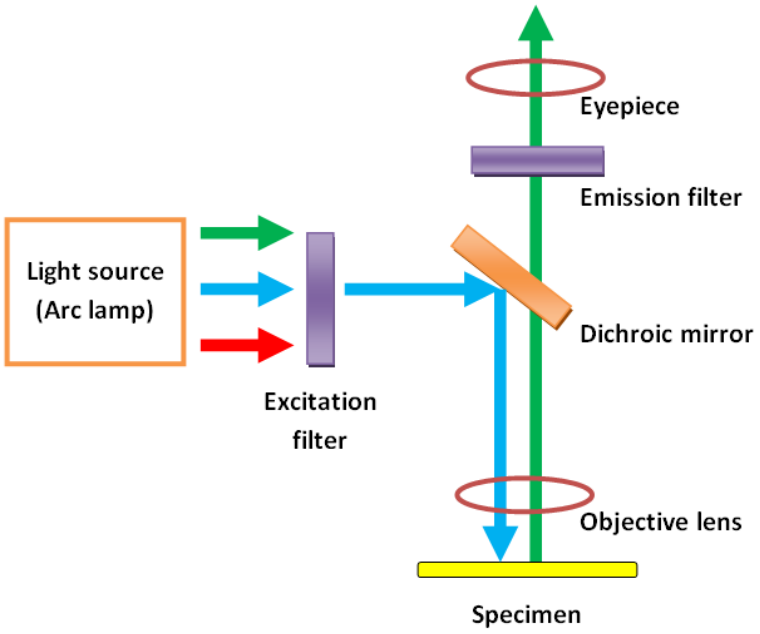

Figure 4.5: *Schematic overview of the fluorescence microscopy (adapted from Lichtman & Conchello, 2005).*

4.6.7 Organic acid analysis

The creatinine levels in urine samples were determined prior to extraction, using a Technicon RA-100 analyser. The urinary organic acid levels were calculated and expressed relative to the creatinine content. Organic acids in urine were determinded using a traditional method employing gas chromatography-mass spectrometry as described by Jooste and co-workers (1994).

4.6.7.1 Materials

Chemical / Reagent	Supplier
Hydrochloric acid	Merck
3-Phenylbutyric acid	Sigma Chemical Company
Ethyl acetate	Merck
Diethyl ether	Merck
Sodium sulphate (anhydrous)	SAARchem (Merck laboratory supplies)
Nitrogen	Afrox
TMCS	Sigma-Aldrich
BSTFA	Sigma-Aldrich

4.6.7.2 Creatinine determinations

The creatinine levels in urine samples were determined prior to extraction. The urinary organic acid levels were calculated and expressed relative to the creatinine content. This allowed eliminating intra individual physiological differences in the monkeys. Creatinine was determined using a Technicon RA-100 analyser. Urine was diluted 10 or 20 times and analysed according to the prescriptions of the manufacturer (Miles Inc., Tarrytown, NY). Creatinine content was expressed in μmol/litre.

4.6.7.3 Organic acid extraction

The volume of urine used for extraction of organic acids was determined according to the creatinine values (mg%) [Equation 3]. For creatinine values < 100 mg%, 1 ml of urine was used, for creatinine values between 100 mg% and 135 mg%, 0.5 ml of urine was used, and for values > 135 mg%, 0.25 ml of urine was used. This volume was transferred to a 15 ml glass tube (Pyrex®) and about 6 drops of HCl (5 M) were added to adjust the pH to 1. Internal standard (3-phenylbutyric acid) was then added [volume IS in µl = 5 X creatinine mg%]. Organic acids were extracted using two solvents: first 6 ml distilled ethyl acetate was added and the samples vigorously shaken for 30 minutes. The samples were centrifuged for 3 minutes at 300 rpm and the organic phases aspirated into clean tubes. Thereafter 3 ml of

distilled diethyl ether was added to the aqueous phase and shaken for 10 minutes. After centrifugation, the organic layer was added to the ethyl acetate phase. The organic phase was dried over two spatulas of Na_2SO_4 and centrifuged, where after it was transferred to clean smaller glass tubes (Kimax®). The organic phase was then evaporated to dryness under nitrogen at 40 ^oC and the dry samples were frozen at –18 ^oC.
Prior to injection into the GC-MS system, BSTFA [Equation 4] and TMCS [Equation 5] were added to the dried samples and incubated at 60 ^oC for 1 hour to form TMS derivatives.

Equation 3: mg% = μmol/litre x 10/1000 x 11.312

Equation 4: volume in μl = 2X mg% creatinine

Equation 5: volume in μl = 0.4X mg% creatinine

4.6.7.4 GC/MS analysis

One microliter of each derivatised sample was injected into a Hewlett Packard 5880 GC equipped with a Hewlett Packard 5988A mass spectrometer (MS). A Macherey-Nagel (MN 30962-52) column was used. The inlet for the GC was splitless while the MS was GC dependent splitless and helium was the carrier gas.

The settings of the GC were as follows: the carrier gas was hydrogen at 2.5 x 100 kPa at a flow rate of 1 ml/min. The makeup gas was nitrogen at a flow rate of 30 ml/min. The final oven temperature was 280 ºC. The carrier gas in the MS was helium.

As each compound has a fragmentation pattern composed of a series of split molecular ions, the mass charge ratios and the abundance were compared with standard mass chromatograms in the NIST (National Institute of Standards and Technology) mass spectra library by the ChemStation Software to identify organic acids.
The concentrations of the organic acids [Equation 6] in urine were determined using WsearchPro® software.

Equation 6: Organic acids (μmol/l) = $\frac{\text{Area of specific organic acid}}{\text{Area of IS}} \times 262.5$

4.6.8 Very-long-chain fatty acid analysis

A modified method from Vreken and co-workers (1998) was used for sample preparation and determination of VLCFAs, phytanic and pristanic acid at the laboratory for Inherited Metabolic Defects, School for Biochemistry, North-West University (Potchefstroom Campus), South Africa.

4.6.8.1 Materials

Chemical / Reagent	Supplier
2,6,10,14-tetramethylpentadecanoic acid (pristanic acid)	Sigma Aldrich
3,7,11,15-tertramethylhexadecanoic acid (phytanic acid);	Sigma Aldrich
dososahexaenoic acid (C22:0)	Sigma Aldrich
tetracosanoic acid (C24:0)	Sigma Aldrich
hexacosanoic acid (C26:0)	Sigma Aldrich
2-methyl-$^{2}H_{3}$,6,10,14-trimethyl)pentadecanoic acid (pristanic acid-d3)	H. ten Brink
3-methyl-$^{2}H_{3}$,7,11,15,trimethyl)hexadecanoic acid (phytanic acid-d3)	H. ten Brink
(3,3,5,5,$^{2}H_{4}$)-docosanoic acid (C22:0-d4)	H. ten Brink
(3,3,5,5,-$^{2}H_{4}$)-tetracosanoic acid (C24:0-d4)	H. ten Brink
(3,3,5,5,-$^{2}H_{4}$)-hexacosanoic acid (C26:0-d4)	H. ten Brink
acetonitrile	Merck
hydrochloric acid	Merck
sodiumhydroxide	Merck
methanol	Merck
potasiumhydroxide	Merck
hexane	Merck
pyridine	Merck
toluene	Merck
N-methyl-N-(tert-butyldimethylsilyl)trifluoroacetamide (MTBSTFA)	Sigma Aldrich

4.6.8.2 Sample preparation

The internal standards used in order to quantify the VLCFA included the fatty acid standards obtained from Sigma Aldrich® and H. Ten Brink® (see section 4.6.8.1). Preparing the internal standards entailed making a solution in toluene by adding all the standards and deuterium labelled standards to comprise of 1 µmol/l pristanic acid; 4 µmol/l phytanic acid; 50 µmol/L C22:0; 50 µmol/l C24:0; 1 µmol/l C26:0; 5 µmol/l pristanic acid-d3; 8 µmol/l phytanic acid-d3; 50 µmol/l C22:0-d4; 50 µmol/l C24:0-d4 and 5 µmol/l C26:0-d4. This mixture was stored at 2 to 8 °C.

The plasma samples were thawed and 100 µl plasma was mixed with 100 µl of the internal standards solution in a clean glass extraction tube. In order for free fatty acids to form, the mixture was treated with an acid and alkali to hydrolyze.

For acid hydrolysis, 2 ml of a 0.5 M HCl in acetonitrile was added, the tube tightly capped and vortexed for approximately 3 seconds, allowed to hydrolyze for about 45 minutes at 110 °C and left to cool down to room temperature. After the mixture cooled, 2 ml of a 1 M NaOH in methanol was added for alkaline hydrolysis. Again the mixture was tightly capped and vortexed for 3 seconds, left for 45 minutes at 110 °C to hydrolyze and cooled down to room temperature.

After cooling, the pH was lowered by adding 400 µl of 0.5 M HCl in acetonitrile. For extraction, 4 ml of hexane was added and the tube shaken for 1 minute. The hexane layer was transferred to a new Kimax® tube.

From a 1 M KOH, 3.7 ml was added to the hexane layer and shaken for 1 minute. The top layer was removed and the pH of the hexane layer lowered by adding 500 µl 0.5 M HCl in acetonitrile. This step enabled the removal of sterols.

Hexane (4ml) was added and the mixture was shaken for 1 minute. The hexane layer was transferred to a clean extraction tube and dried under nitrogen.

Derivatization was accomplished by adding 50 µl MTBSTFA and 50 µl of pyridine to the dried organic layer and by incubating it for 30 minutes at 80 °C. The organic layer was evaporated to dryness under nitrogen and 200 µl hexane added just before GC-MS analysis. .

4.6.8.3 GC/MS analysis

The samples were analyzed on a GC/MS system (Hewlett-Packard model 6890/5973 GC-MS system) equipped with a 120-0132 DB-1ms capillary column (30 m x 0.25 mm i.d. x 0.25 µm film thickness) (Agilent Technologies, Chemetrix, Midrand, South Africa).

One micro litre of the sample was injected into the GC/MS system with splitless mode and the carrier gas was helium (14.99 psi). The electron impact was applied at 0.7 eV and the mass spectrum with single ion monitoring (SIM) mode was used to monitor the characteristic $[M - 57]^+$ ions (Vreken *et al.*, 1998). The oven temperature was programmed to initiate at 60 °C for 1 minute and was increased to 240 ˚C (30 °C/min) then to 270 ˚C (10 °C/min) and was finally increased to 300 °C (4 °C/min) and maintained for 3 minutes. HP-chemstation software was used to quantify the raw data obtained from the GC/MS.

Table 4.1*: A list of the* characteristic $[M - 57]^+$ ions *monitored by single ion monitoring (SIM) via MS (Vreken et al., 1998).*

Compound	$[M - 57]^+$ ions
C22:0	397.4
$^2H_4$]-C22:0	401.4
C24:0	425.4
[$^2H_4$]-C24:0	429.4
C26:0	453.4
[$^2H_4$]-C26:0	457.4

The fatty acid response factor (Rf-value) was determined as follow:

$$\text{Equation 7: } Rf = \frac{\text{Area under curve (IS)}}{\text{Area of under curve (fatty acid)}} \times \frac{\text{Concentration (fatty acid)}}{\text{Concentration (IS)}}$$

The Rf-value was used to establish the concentration of the fatty acids as follow:

$$\text{Equation 8: } [\ ] = \frac{\text{Area under curve (fatty acid)}}{\text{Area of under curve (IS)}} \times \text{Concentration (IS)} \times Rf$$

IS = internal standard and [ ] = concentration of the fatty acids.

CHAPTER 5

RESULTS AND DISCUSSION

5.1 INTRODUCTION

As described in chapter 3, PBA is a pro-drug with numerous biological activities and the question remains which metabolites contribute to the proliferation and/or toxicity. In this study our aim was to determine the antioxidant capacity of PBA *in vitro* and *in vivo* and to identify known and new metabolites of PBA in the vervet monkey. Additionally the cytotoxicity of PBA and its possible influence on peroxisome proliferation was also measured.

There are two different approaches to determining ROS, both *in vitro* and *in vivo,* that include firstly, trapping the species and measuring the levels of the trapped molecules and secondly measuring the levels of oxidative damage done by the species (Halliwell & Whiteman, 2004). In this study the focus was to determine general levels of cellular ROS and ROS induced damage to evaluate the possible antioxidant effects of PBA. The antioxidant results of the different assays are given below with an explanation how the data were interpreted. The results of the each assay are discussed separately for *in vitro* and *in vivo* followed by a short discussion.

The results of the fatty acids in the blood and organic acids in the urine are discussed individually.

5.2 ANTIOXIDANT CAPACITY

5.2.1 Reactive oxidant species (ROS)

ROS contribute to pathogenesis of several disorders because they are by products of metabolism which can oxidize various biomolecules, leading to cell death and tissue injury (Sarkar *et al*., 2005).

The intracellular levels of ROS were determined by DCFH-DA. The conversion chemistry of the dye is complex and is illustrated in Figure 5.1. DCFH-DA is a stable non-fluorescent compound that can be converted to the fluorescent form, DCF, by active radicals within the cells. DCFH-DA is converted to DCFH by intracellular esterase when it crosses the cell membrane and is entrapped inside the cells. ROS oxidizes this non-fluorescent compound

into the highly fluorescent DCF, which upon excitation at 488 nm, emits green fluorescence, proportional to the intracellular level of ROS. Thus, when quantifying the fluorescence, the rate and extent of ROS production is quantified. The change in DCF fluorescence imitates mostly the intracellular accumulation of ROS (Sarkar *et al*., 2005; Amer *et al*., 2004). The fluorescence can be quantified by a fluorometer or fluorescence plate reader, but flow cytometry offers the additional advantage of being able to provide quantitative data on the numbers of cells emitting fluorescence (Halliwell & Whiteman, 2004).

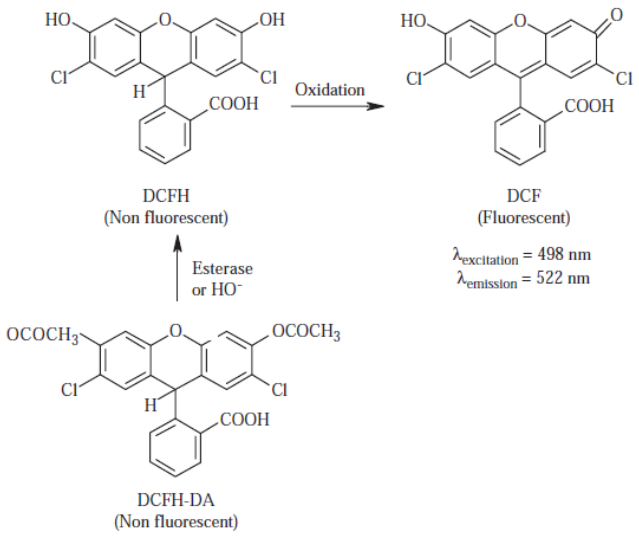

Figure 5.1: *The DCFH-DA non fluorescent compound is converted to DCFH by intracellular esterase when entering the cell. It is then oxidized to DCF, a highly fluorescent compound, by ROS (adapted from Gomes et al., 2005).*

Figure 5.2 shows representative flow cytometry plots of selected controls. A two parameter dot plot of SSC and FSC are used to identify the specific cells of interest (not shown). A FCS/FL1 dot plot was used to identify DCF specific events (Figure 5.2 A). The plot uses a log scale and every dot represents a cell. A gated area is used to selectively visualize the cells of interest. The percentage cells in that area and the geometric mean are used for further analysis. The histogram (Figure 5.2 B) illustrates the fluorescence (FL1) versus the amount of cells gated. There is a clear difference between the normal cells and cells with induced ROS in both the dot plots and the histogram. The geometric mean in the gated area represents the fluorescence intensity measured (MFI) in arbitrary units and directly reflects the intracellular levels of ROS. The MFI of the negative control was 146.81, whereas the MFI of the positive control was 1465.76.

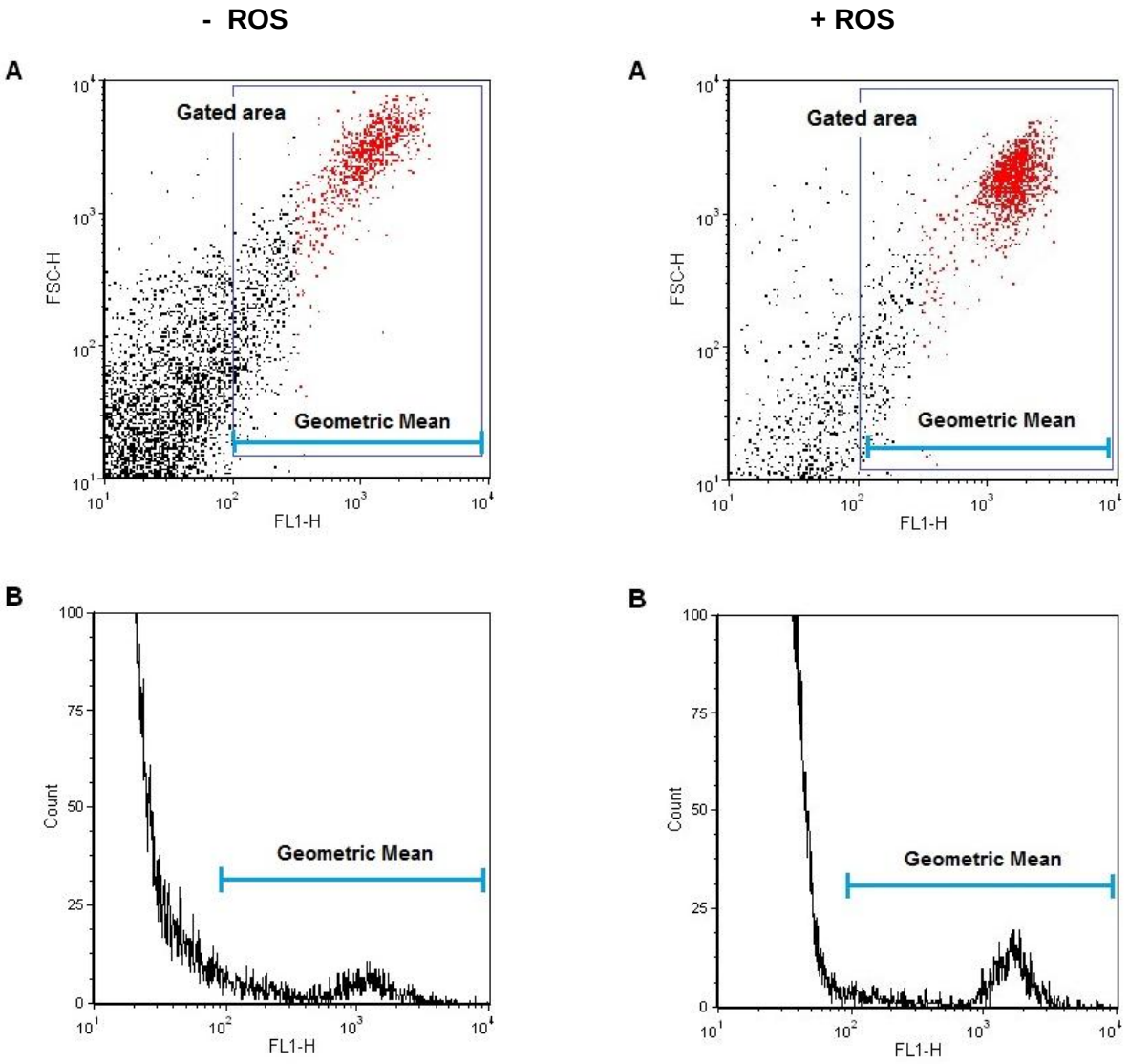

Figure 5.2: *FSC/FL1 dot plots (A) of the negative control consisting of cells only and positive control consisting of cells treated with 8 mM H_2O_2. The histograms (B) show the difference between the normal cells and cells with induced ROS.*

5.2.1.1 In vitro results

The tables represent the data collected from the MFI and the data in the graphs are expressed relative to the positive control (see Appendix A for raw data).

Table 5.1: *Results of the different concentrations of PBA on intracellular levels of ROS*

Concentration of PBA (mM)	MFI (arbit. units)
Positive control	1465.763 ± 38.601
0	146.80 ± 6.83
0.5	225.910 ± 7.549
1	179.653 ± 9.717
2	171.787 ± 4.260
5	148.757 ± 6.921

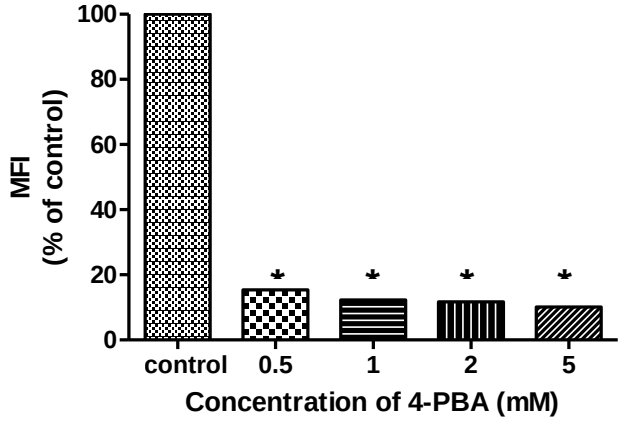

Figure 5.3: *The intracellular levels of ROS in HeLa cells measured as MFI versus different concentrations of PBA. Results are expressed relative to the positive control. * differs significantly from the control ($p \leq 0.05$).*

Table 5.1 give the results of the intracellular levels of ROS in HeLa cells after 48 hours of treatment with PBA. The control cells treated with 8 mM H_2O_2 elicit maximal levels of ROS with high MFI. Treatment with PBA resulted in low levels of intracellular ROS, with the lowest levels at 5 mM. The results in Figure 5.3 illustrate lower percentage intracellular ROS levels in treated cells represented by lower fluorescence measured as MFI, relative to the control. The 0.5 mM PBA decreased ROS levels by 84.59% in HeLa cells; 1 mM PBA decreased ROS levels by 87.74% and 2 mM PBA decreased ROS levels by 88.28%. The 5 mM PBA treated cells decreased ROS levels by 89.85%. ROS levels for all the concentration of 4-PBA was statistically lower than that of the control. Therefore ROS levels tended to decrease with an increase in the concentration of PBA.

5.2.1.2 In vivo results

(See Appendix E for raw data)

Table 5.2: *Results of ROS levels in RBC over time in PBA treated vervet monkeys*

Time of treatment with PBA (min)	MFI (arbit. units)
0 (control)	56.970 ± 5.340
15	119.035 ± 18.605
30	119.065 ± 8.505
60	43.730 ± 0.210
120	32.285 ± 1.975
180	16.910 ± 1.340

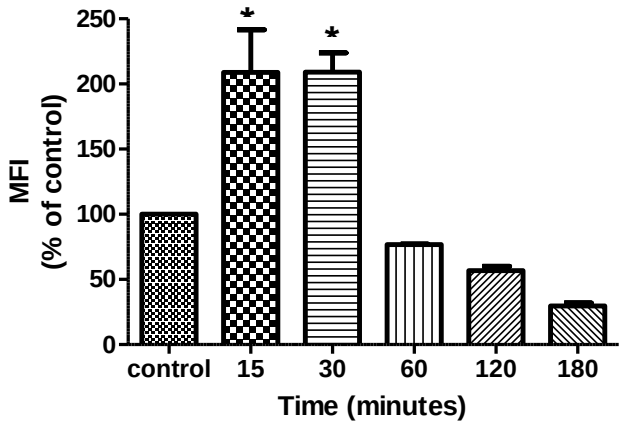

Figure 5.4: *The intracellular ROS levels in RBC measured as MFI over time after a single dose of 130 mg/kg of PBA in vervet monkeys. Results are expressed relative to the control. * differs significantly from the control (p ≤ 0.05).*

Table 5.2 indicates low levels of intracellular ROS levels in RBC after 60 minutes of treatment with PBA. Figure 5.4 indicates an initial higher percentage ROS levels within the first 30 minutes of treatment with PBA, compared to the control. Thereafter ROS levels dropped from 208.94% to 76.75%, compared to the control, between 30 and 60 minutes. After 60 minutes ROS levels decreased by 23.25% relative to the control. After 120 minutes, ROS levels dropped by 43.33% and after 180 minutes ROS levels was lowered by 70.31%. Although the ROS levels did not decrease significantly, there seemed to be a decrease in ROS levels over the time of treatment with PBA in vervet monkeys.

5.2.1.3 Discussion

In vitro there was significant decrease in ROS levels with all the concentrations of PBA after 48 hours. In this study the baseline ROS levels of HeLa cells without additional ROS production or stimulation was measured. This relates to the baseline capacity of cells to

generate ROS. DCF fluorescence is also a measure of generalized oxidative stress, rather than measuring specific ROS (Halliwell & Whiteman, 2004). It therefore seems as if PBA acts as an antioxidant in HeLa cells, by lowering oxidative stress.

In vivo, there were initially elevated levels of ROS levels after 15 minutes of PBA treatment. It is uncertain why these initial high levels of ROS were seen after 15 and 30 minutes. The decreased ROS levels after 60 minutes of treatment could be attributed to the half-life of PBA which is between 1 to 2 hours. At 60 minutes most of the pro-drug is converted to active metabolites which might then affect the antioxidant effect. Another explanation for the sharp increase of ROS and the decrease after 30 minutes, could be the upregulation of antioxidant capacity in adaptation to intrinsic oxidative stress initially caused by PBA. To confirm if PBA is responsible for the initial increase in ROS levels, further studies have to be done, using other mammals and more vervet monkeys. Nevertheless PBA treatment was still capable to significantly lower the ROS levels after 1 hour with even lower levels after 3 hours compared to the control, 15 minutes and 30 minutes values.

These results support the findings of Glod & Grieb (2005) where they used ion-exclusion chromatography for analysis of hydroxyl radicals after spin trapping. They found that 1 mM PBA was a scavenger of both hydroxyl and peroxy radicals.

In summary: these results suggest that the HDAC-inhibitor, PBA, can decrease the ROS levels in PBA treated HeLa cells and in vervet monkeys.

5.2.2 Lipid Peroxidation (LP)

Oxidative stress induced by free radicals such as ROS causes lipid peroxidation, an oxidative degradation of lipids. Initially, after lipid peroxidation, polyunsaturated fatty acids are oxidized by lipid peroxyl radicals and by oxygen-derived free radicals, resulting in the formation of lipid hydroperoxides which can further be metabolised into a mixture of products including ketones and aldehydes. During lipid peroxidation there is a continuous generation of free radicals in the cell membranes (Amer *et al*, 2004; Maulik *et al*., 1998, Makrigiorgos *et al*., 1997).

Lipid peroxidation was assessed by measuring fluorescence of fluor-DHPE (Figure 5.5). Fluorescence was determined by flow cytometry. Fluor-DHPE loses its fluorescence upon the generation of peroxyl radicals (Gomes *et al*., 2005; Amer *et al*., 2004; Maulik *et al*., 1998; Makrigiorgos *et al*., 1997).

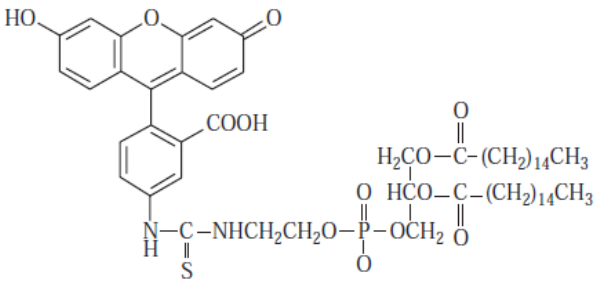

Figure 5.5: *The fluorescent flour-DHPE loses its fluorescence in the presence of peroxyl radicals (adapted from Gomes et al., 2005).*

Figure 5.6 illustrates representative plots of controls. The dot plots (Figure 5.6 A) indicate the decrease in fluorescence when the cells are exposed to ROS, which directly relates to lipid peroxidation. The blue area indicates intense fluorescence measured in the first decade (10^1). These plots use a log scale and every dot represents a cell. A gated area is used to selectively visualize the cells of interest. The histogram (Figure 5.6 B) illustrates the geometric mean in the gated area that represents the fluorescence intensity measured in arbitrary units. There is a clear difference between the normal cells and cells with induced lipid peroxidation. The MFI of the negative control was 2.58, whereas the MFI of the positive control was 9.84.

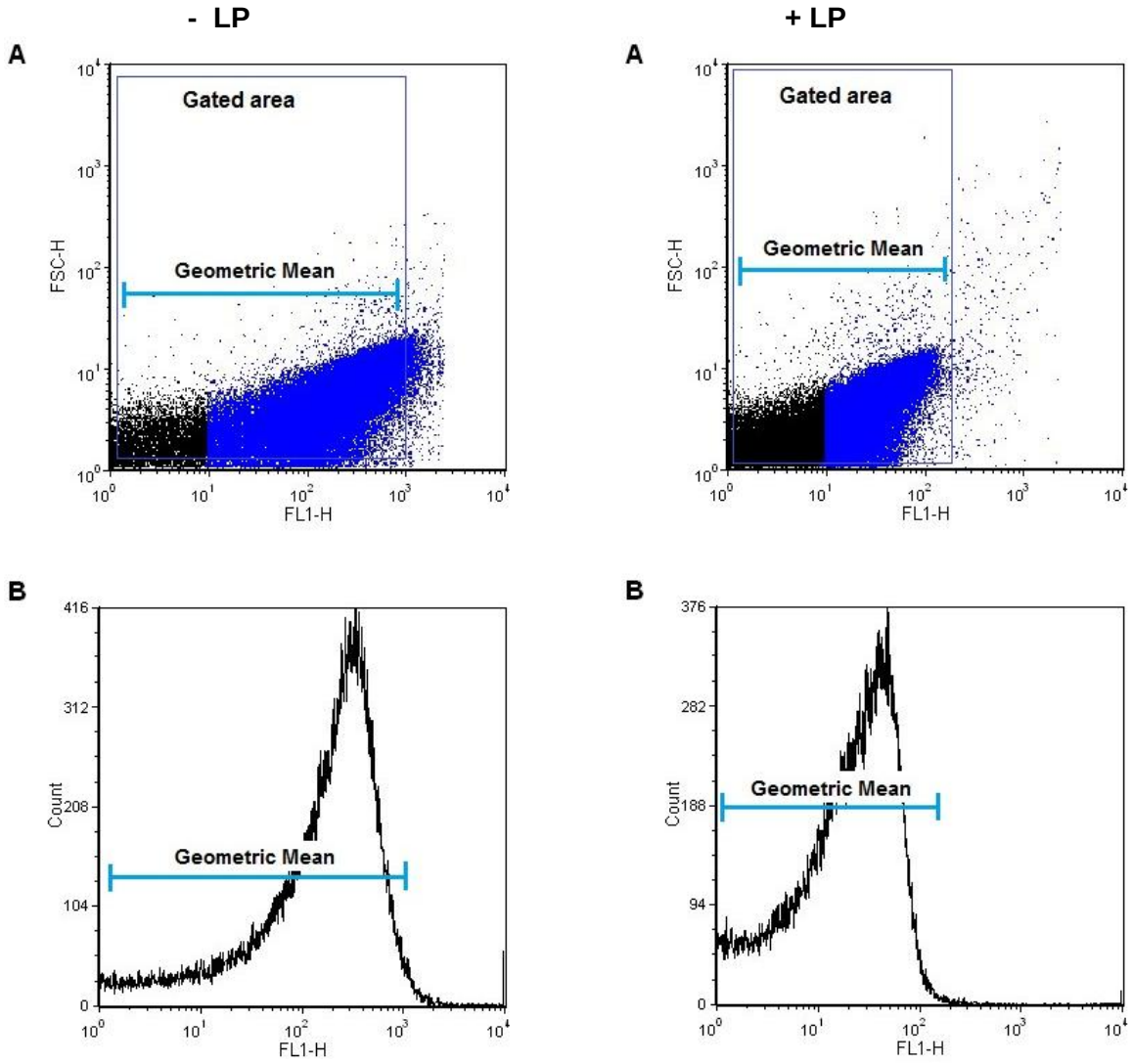

Figure 5.6: *FSC/FL1 dot plots (A) of the negative control that consists only of cells and positive control that represent cells treated with 8 mM H_2O_2. The histograms (B) show the difference between the normal cells and cells with induced lipid peroxidation.*

5.2.2.1 In vitro results

The tables represent the data collected from the MFI and in the graphs the data are expressed relative to the positive control (see Appendix B for raw data).

Table 5.3: *The effect of PBA concentrations on lipid peroxidation in HeLa cells.*

Concentration of PBA (mM)	MFI (arbit. units)
Positive control	9.835 ± 0.085
0	2.574 ± 1.366
0.5	12.510 ± 0.590
1	23.400 ± 0.480
2	33.705 ± 1.885
5	35.975 ± 5.775

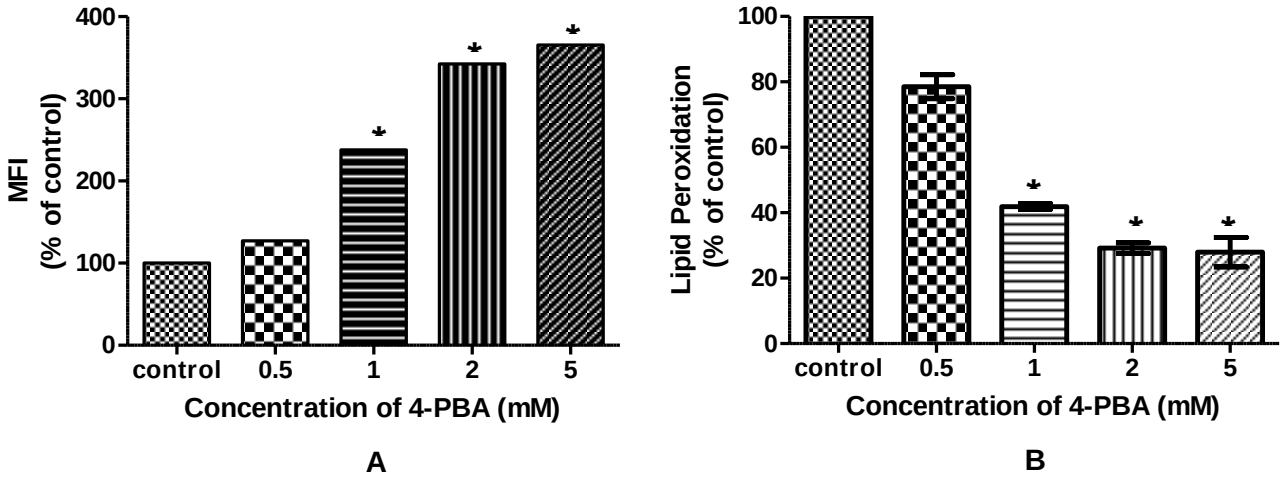

Figure 5.7: *The lipid peroxidation activity (B) in HeLa cells measured as MFI (A), treated with different concentrations of PBA. Results are expressed relative to the positive control. * differs significantly from the control (p ≤ 0.05).*

Table 5.3 gives the results of the lipid peroxidation in HeLa cells after 48 hours of treatment with PBA. The control cells treated with 8 mM H_2O_2 obtained maximal levels of lipid peroxidation (low MFI). Treatment with PBA resulted in decreased levels of lipid peroxidation, with the lowest levels at 5 mM. The results in Figure 5.7 A show an increase in MFI, which is inversely proportional to the lipid peroxidation. Figure 5.7 B illustrates lower percentage lipid peroxidation relative to the control. Treatment of HeLa cells with 0.5 mM, 1 mM, 2 mM and 5 mM PBA decreased lipid peroxidation by 21.46%, 58.09%, 70.82% and 72.02% respectively. Lipid peroxidation at 1, 2 and 5 mM of PBA were statistically lower than the control.

5.2.2.2 In vivo results

(See Appendix A for raw data)

Table 5.4: *Lipid peroxidation in RBC measured over time in PBA treated vervet monkeys*

Time of treatment with PBA (min)	MFI (arbit. units)
0 (control)	31.630 ± 0.180
15	23.925 ± 4.445
30	29.325 ± 0.095
60	35.195 ± 0.085
120	37.715 ± 2.655
180	45.625 ± 0.925

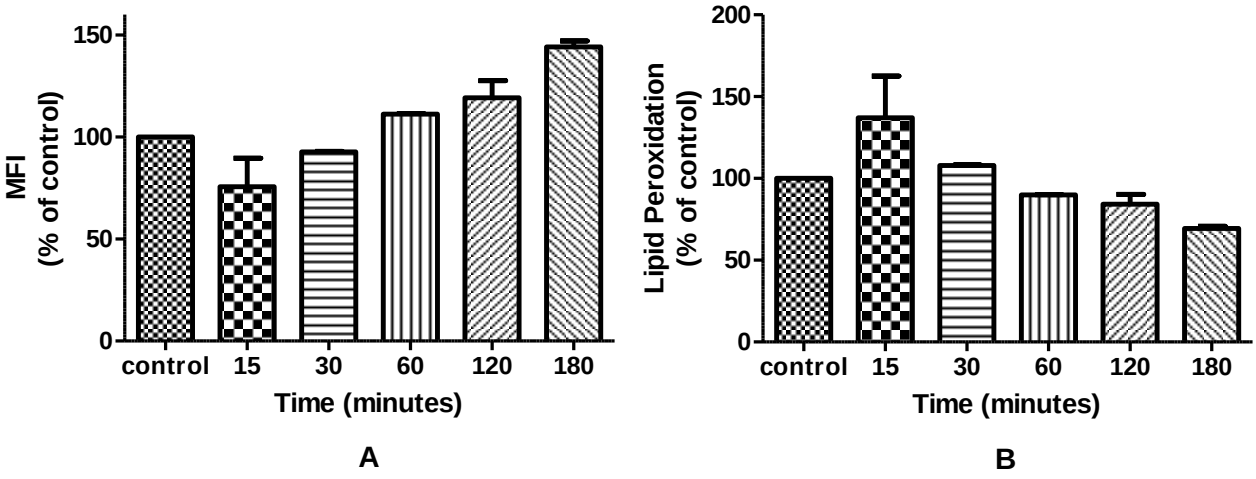

Figure 5.8: *The lipid peroxidation (B) in RBC measured as MFI (A) over time after a single dose of 130mg/kg of PBA. Results are expressed relative to the control.*

Table 5.2 indicates an increase in the MFI, over time, which is inversely proportional to the lipid peroxidation. Figure 5.8 A illustrates a higher percentage of MFI over the time of treatment with PBA. Figure 5.8 B shows an initial increase in lipid peroxidation after 15 minutes of treatment of 37.02%. Lipid peroxidation gradually decreased after 30 min, but was still higher (7.91%) than the positive control. After 60 minutes lipid peroxidation decreased to 10.09% compared to the positive control. After 120 minutes there was a 15.68% decrease and at 180 minutes a 30.61% decrease in lipid peroxidation. Although lipid peroxidation did not decrease significantly, there seemed to be a decrease in lipid peroxidation over the time of treatment with PBA in vervet monkeys

5.2.2.3 Discussion

Increasing concentration of PBA decreased lipid peroxidation within 48 hours. The highest concentration of PBA (5 mM) decreased lipid peroxidation by 72.02%.

In vivo results followed the same pattern as experienced with the ROS levels (Figure 5.4), showing an initial increase in lipid peroxidation after 15 and 30 minutes and a decrease after 60 minutes of treatment. The decrease after 60 minutes may be attributed to the half-life of PBA which is between 1 to 2 hours. At 60 minutes most of the pro-drug was converted to active metabolites which could be responsible for the decrease in ROS. PBA lowered the initial increased lipid peroxidation level by 30.61% and that of the control by 10.09%. It is at this stage uncertain why the initial elevated levels of lipid peroxidation occur. As discussed in 5.2.1.3, the initial increase after 15 minutes and decrease after 30 minutes in lipid peroxidation could be attributed to intrinsic oxidative stress initially caused by PBA leading to an upregulation of antioxidant capacity. The lipid peroxidation in the vervet monkey decreased tended to over time with treatment with PBA.

5.2.3 Apoptosis and cell cycle analysis

Apoptosis, or programmed cell death, is characterized by a series of features including loss of cell volume, clustering of chromatin and nuclear fragmentation into apoptotic bodies (Doszczak *et al*., 2008; Rello-Varona *et al.,* 2006). ROS leads to cellular damage including oxidative DNA damage that may lead to apoptosis (Wu *et* al., 2005; Nunez, 2001; Lee *et al*., 2000, Chang *et al.,* 1999). It is therefore important to determine apoptosis in HeLa cells to accurately determine the possible antioxidant effect of PBA.

Live cells can exclude dyes with their intact membranes whereas dead or damaged cells can easily be penetrated. The most generally used dye for DNA content or cell cycle analysis is the water soluble, PI. PI disrupts the cell membrane and rapidly stains the nuclear chromatin. The PI intercalates into the major groove of the double-stranded DNA and produces a highly fluorescent adduct (ex/em 488/600 nm). PI can also bind to double-strand RNA. Cells are treated with RNase for optimal DNA resolution (Zhang *et al.,* 2007; Cooke *et al*., 2003; Guetens *et al*., 2002).

Flow cytometry can determine the relative cellular DNA content (apoptosis) and can identify cell distribution during the various phases of the cell cycle. Four distinct phases can be observed in a proliferating cell population; The G1-, S- (DNA synthesis), G2- and M (mitosis)-phases. The emitted fluorescence of PI (FL2) generates an electronic signal that can be

recorded as high intensity of staining (FL2-H), as well as pulse-area (FL2-A) and pulse-width (FL2-W). Figure 5.9 illustrates representative plots of controls. The histogram shows the FL2H fluorescence versus the amount of cells. From this plot the different phases of the cell cycle can be distinguished. In the dot plot (FL2-W/FL2-A) a gate is set around a single population that discriminate the apoptotic cells. The graphs show a clear difference between the two controls: MFI of the negative control was 17.90 and the positive control was 27.80. The percentage of cells present in the apoptosis (APOP) cycle is represented by MFI.

- Apoptosis

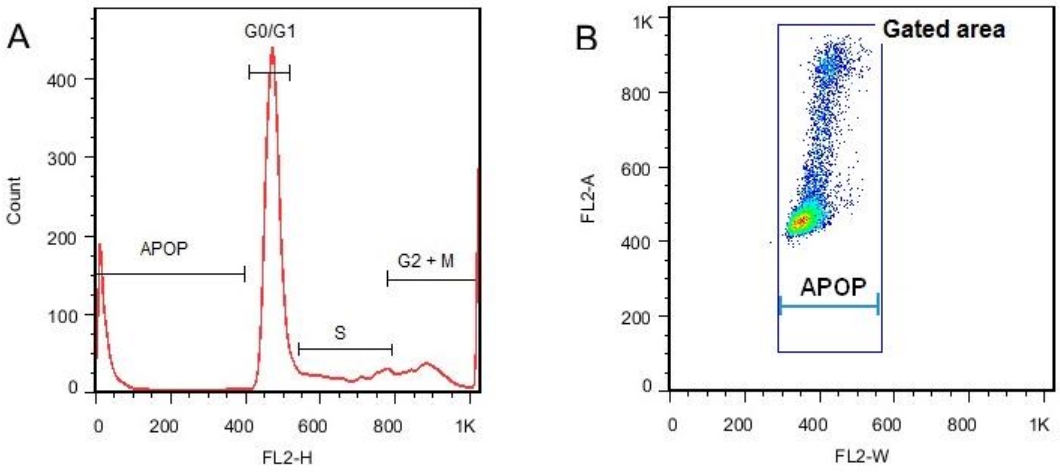

+ Apoptosis

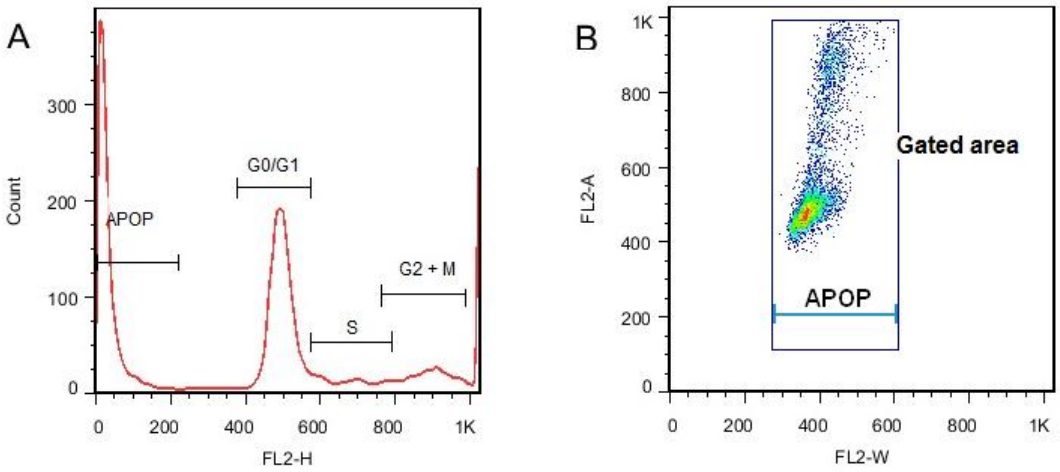

Figure 5.9: *Negative and positive control for apoptosis and cell cycle analysis. The histogram (A) represents cells in apoptosis (APOP), G0/G1, S and G2 + M of the cycle that were sorted based on DNA contents staining with propidium iodide (PI). The FL2-A/FL2-W dot plots illustrate only the cells in apoptosis.*

5.2.3.1 In vitro results

The tables represent the data collected from the MFI and the graphs express the data relative to the positive control (see Appendix D for raw data).

Table 5.5: *The effect of different PBA concentrations on apoptosis.*

Concentration of PBA (mM)	MFI (arbit. units)
Positive control	27.800 ± 6.274
0	17.90 ± 3.700
0.5	20.700 ± 2.500
1	17.700 ± 3.400
2	15.550 ± 5.450
5	12.717 ± 3.819

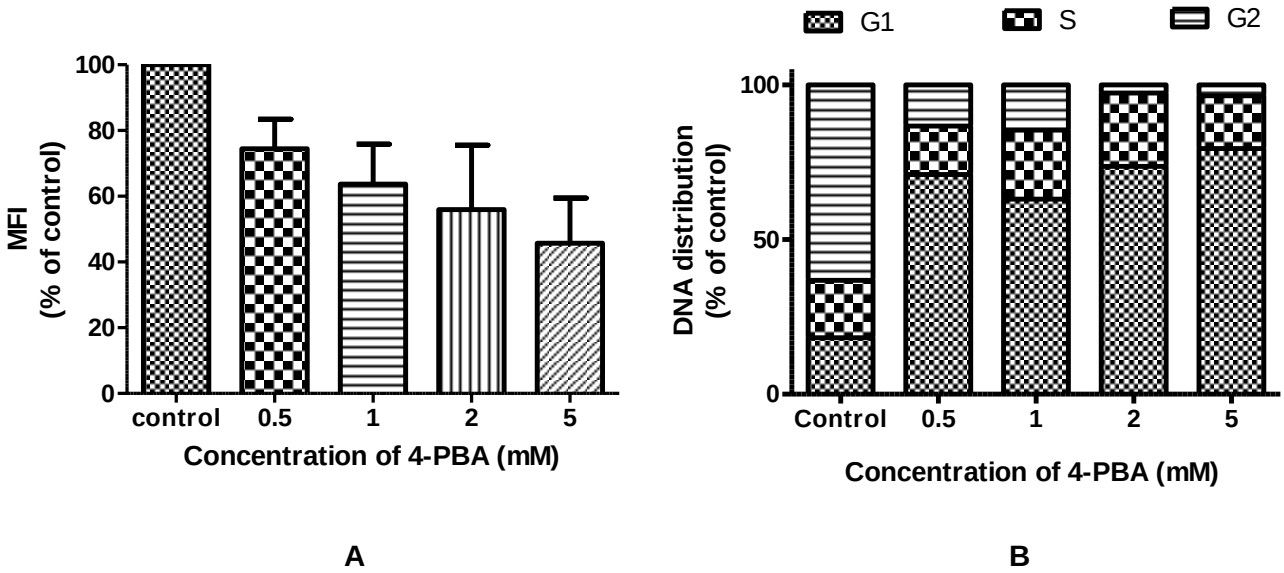

A **B**

Figure 5.10: *The rate of apoptosis in HeLa cells (A) measured as MFI at different concentrations of PBA. The cell cycle analysis in HeLa cells (B) expressed as percentage DNA distribution across the different phases. Results are expressed relative to the positive control.*

Table 5.5 illustrates that treatment with PBA resulted in lower apoptotic levels, with the lowest levels at 5 mM PBA. The results in Figure 5.10 A demonstrate lower percentage apoptosis (lower fluorescence) measured as MFI relative to the control. The 0.5 mM PBA decreased apoptosis by 25.54%, 1 mM PBA by 36.33%, 2 mM PBA by 44.07% and the 5 mM concentration decreased cell death by 54.26%. Although no significant decrease was seen in apoptosis, there seemed to be a decrease in apoptosis with increasing dosis of PBA in HeLa cells.

Figure 5.10 B illustrates the cell cycle analysis and distribution of DNA across the different phases, G0/G1, S and G2/M. The control cells, treated with H_2O_2 (8 mM), show cell cycle arrest at the G2/M phase, which is indicative of oxidative DNA damage. Cells treated with different concentrations of PBA show no cell cycle arrest.

5.2.3.2 In vivo results

(See Appendix G for raw data)

Table 5.6: *Apoptotic effect over time of treatment with PBA*

Time of treatment with PBA (min)	MFI (arbit. units)
0 (control)	2.125 ± 0.048
15	2.900 ± 0.500
30	1.00 ± 0.100
60	3.100 ± 0.600
120	1.050 ± 0.250
180	0.500 ± 0.200

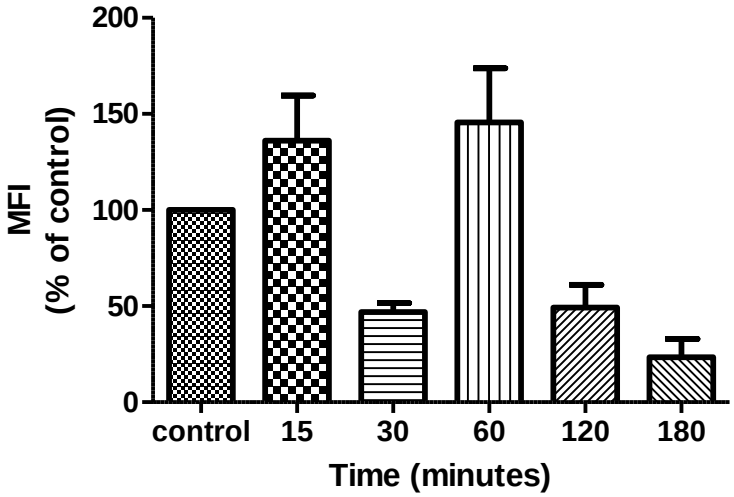

Figure 5.11: *The rate of apoptosis or cell death was in RBC measured as MFI over time of treatment with PBA. Results expressed relative to the positive control.*

Table 5.6 illustrates that over the treatment period of 3 hours, PBA did not statistically significantly influence apoptosis results. Figure 5.11 displays the effect of PBA on apoptosis over the treatment time of 3 hours. Initially, apoptosis increased by 36.15% 15 minutes after treatment with PBA in the vervet monkey compared to the control. After 30 minutes a reduction in cell death of 46.95% was measured. However, after 60 minutes of treatment another induction of cell death occurred to a 45.54% higher level than the control. A decrease in cell death after 2 and 3 hours of 49.30% and 23.47% respectively compared to

the control was seen. Although no significant differences were seen, an overall decrease in cell death was seen after 3 hours of treatment with PBA in vervet monkeys.

5.2.3.3 Discussion

In vitro apoptosis decreased with an increase in the concentration of PBA. 5mM PBA showed the most promising result with a 54.26% reduction of apoptosis in HeLa cells. There were no changes in the cell cycle with different concentrations of PBA. Although there was no clear pattern of decrease in apoptosis during the first 30 minutes of treatment with PBA *in vivo,* apoptosis did decrease after 2 and 3 hours. A reason for this observation might be that *in vivo* inhibition of apoptosis by PBA is initiated over a longer period of time (see 3.3 for a discussion of 4-PBA mechanisms). Studies may be done by treating the monkeys over a longer period to fully establish the effect of PBA on apoptosis.

These results support the findings of Vilatoba and co-workers (2005) who subjected C57BL/6 mice to ischemia and by given PBA 1 hour before and 12 hours after reperfusion. They found a greater than 45 % reduction in apoptosis. Qi and co-workers (2004) induced hypoxia in C57BL/6 mice and treated them with PBA intraperitoneally. They found that PBA protected against ischemic brain injury by suppressing ER stress-mediated apoptosis by 40%. They found no change in normal mice treated with PBA.

Our results with the apoptosis experiments illustrate that PBA has protective properties.

5.2.4 Cell Viability

Increased levels of ROS lead to lipid peroxidation, which in turn leads to changes in cell membrane fluidity that may cause cell death (Wu *et* al., 2005; Yakes & Van Houten, 1997). The cell viability assay measures the amount of live and dead cells at the same time, using two probes. The two probes measure intracellular esterase activity and plasma membrane integrity.

Live cells have intracellular esterase that converts the nonfluorescent, cell-permeable calcein acetoxymethyl (calcein AM) to the extremely fluorescent calcein. The polyanionic dye, calcein, is well maintained within live cells, creating an intense uniform green fluorescence in live cells (ex/em ~495/515 nm).

The ethidium homodimer-1 (EthD-1) enters those cells with damaged membranes and becomes fluorescent upon binding to the nucleic acids, producing a bright red fluorescence

in dead cells (ex/em ~495/635 nm). EthD-1 cannot pass through the plasma membrane of live cells.

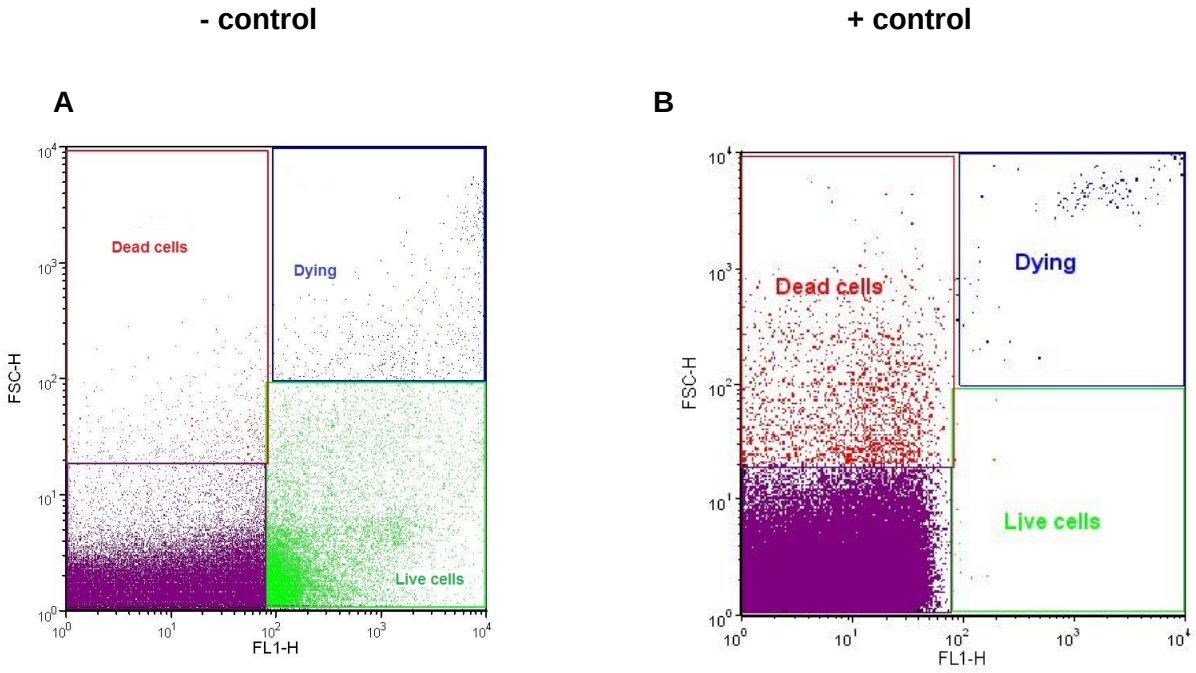

Figure 5.12: *FSC/FL1 dot plots represent the negative control (A) and the positive control (B) used to evaluate the number of live (green dots), dying (blue dots), dead (red dots) and unstained cells (purple dots).*

Figure 5.12 illustrates flow cytometry dot plots of representative controls used to analyse the cell viability. The positive control cells were treated with methanol (100%) to effect cell death. Every dot represents a cell. Live cells produced green fluorescence and dead cells red fluorescence. Unstained cells (purple dots) could also still be viable. The data of the positive and negative controls were compared by adding the live, dying and unstained percentages and by expressing the live and viable cells as a percentage of this accumulated number of cells. The graphs show a clear difference between the number of the live cells between the two controls (green dots). However, the viable cells for the negative control were 98.93% and 87.76% for the positive control.

The HeLa cells were treated with different concentrations of 4-PBA and analysed by flow cytometry (see 4.6.3)

5.2.4.1 In vitro results

The tables represent the data collected from the MFI and the data in the graphs are expressed relative to the positive control (see Appendix C for raw data).

Table 5.7: *Calculated cell viability with different concentrations of PBA*

Concentration of PBA (mM)	Cell Viability (%)	
	Live	Dead
Positive control	87.763 ± 6.289	12.243 ± 6.286
0	98.925 ± 0.035	1.080 ± 0.040
0.5	97.945 ± 0.235	2.060 ± 0.240
1	97.165 ± 0.375	2.835 ± 0.375
2	97.963 ± 0.188	2.037 ± 0.193
5	99.120 ± 0.136	0.880 ± 0.136

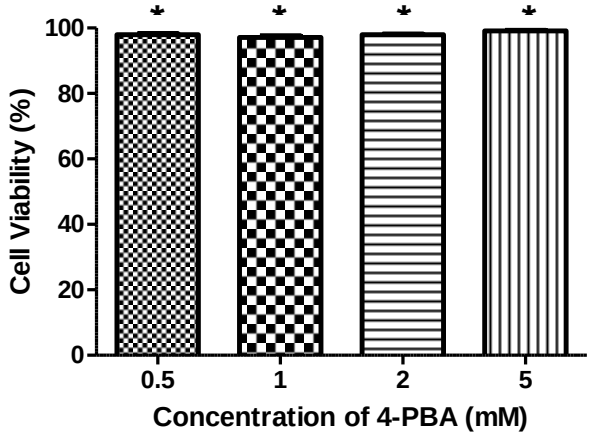

A

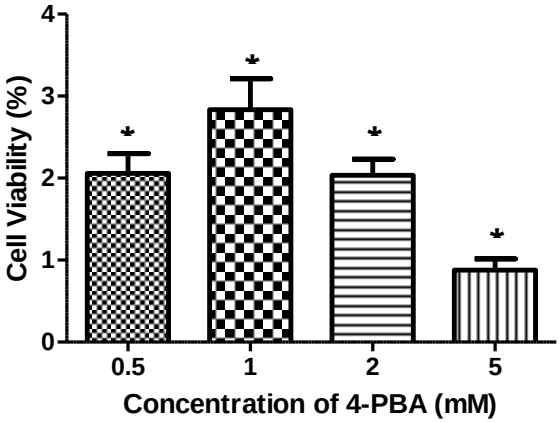

B

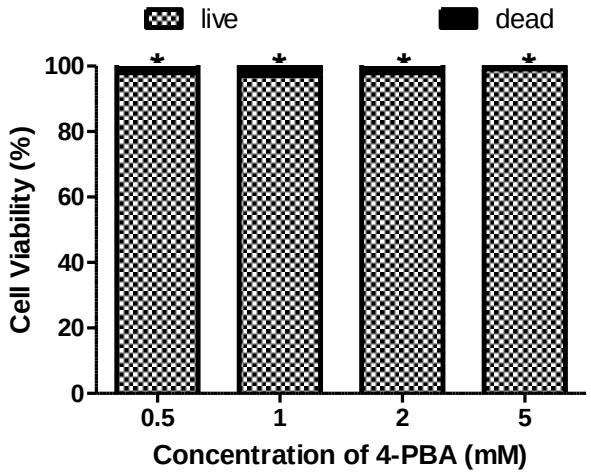

C

Figure 5.13: *The cell viability of the HeLa cells after treatment with different concentrations of PBA. Results are expressed relative to the specific control. (A) Live cells at different concentrations, (B) Dead cells at different concentrations and (C) comparison between live and dead cells at different concentration. * differs significantly from the control ($p \leq 0.001$).*

Table 5.7 illustrates that a high number of cells are viable with an increase in the concentration of PBA. In Figure 5.13 A 97.945% cells remained alive at 0.5 mM PBA, 97.165% at 1 mM PBA, 97.963% at 2 mM and 99.120% at 5 mM PBA. In Figure 5.13 B the percentage of dead cells at 0.5 mM, 1 mM, 2 mM and 5 mM PBA were 2.060%, 2.835%, 2.037% and 0.880% respectively. Figure 5.13 C is a summarized comparison between the live and dead cells at 0.5, 1, 2 and 5 mM, confirming that at a concentration of 5 mM PBA the smallest percentage of cell loss occurred. The percentage cell viability for all concentrations of PBA was statistically higher than that of the control.

5.2.4.2 Discussion

Our results confirmed that PBA retains a high percentage of viable cells. This outcome, together with its attenuation of apoptosis strongly suggests that PBA will provide cell protection.

5.2.5 Peroxisome proliferation

Peroxisomes were detected using an antibody directed against peroxisomal membrane protein 70 (PMP70), which is a high-abundance integral-membrane component of peroxisomes. Imaging was done with a light and fluorescence microscope and peroxisomes were identified by the green fluorescence produced.

HeLa cells were treated with different concentration of PBA and viewed with the microscopes (see 4.6.5).

5.2.5.1 In vitro results

Every dot in Figure 5.14 represents a peroxisome. A and B represent the untreated HeLa cells; C and D 0.5 mM PBA treated cells; E and F 1 mM PBA treated cells; G and H 2 mM PBA treated cells and I and J 5 mM PBA treated cells.

The images of 0.5 mM PBA, 1 mM PBA and 2 mM PBA show an increase in the number of peroxisomes with increasing concentration of PBA. The 5 mM PBA showed the most promising proliferation effect as can be seen by the high number of peroxisomes in Figure 5.14 (J) as well as the phi-shape of the cells which is also an indication of proliferation.

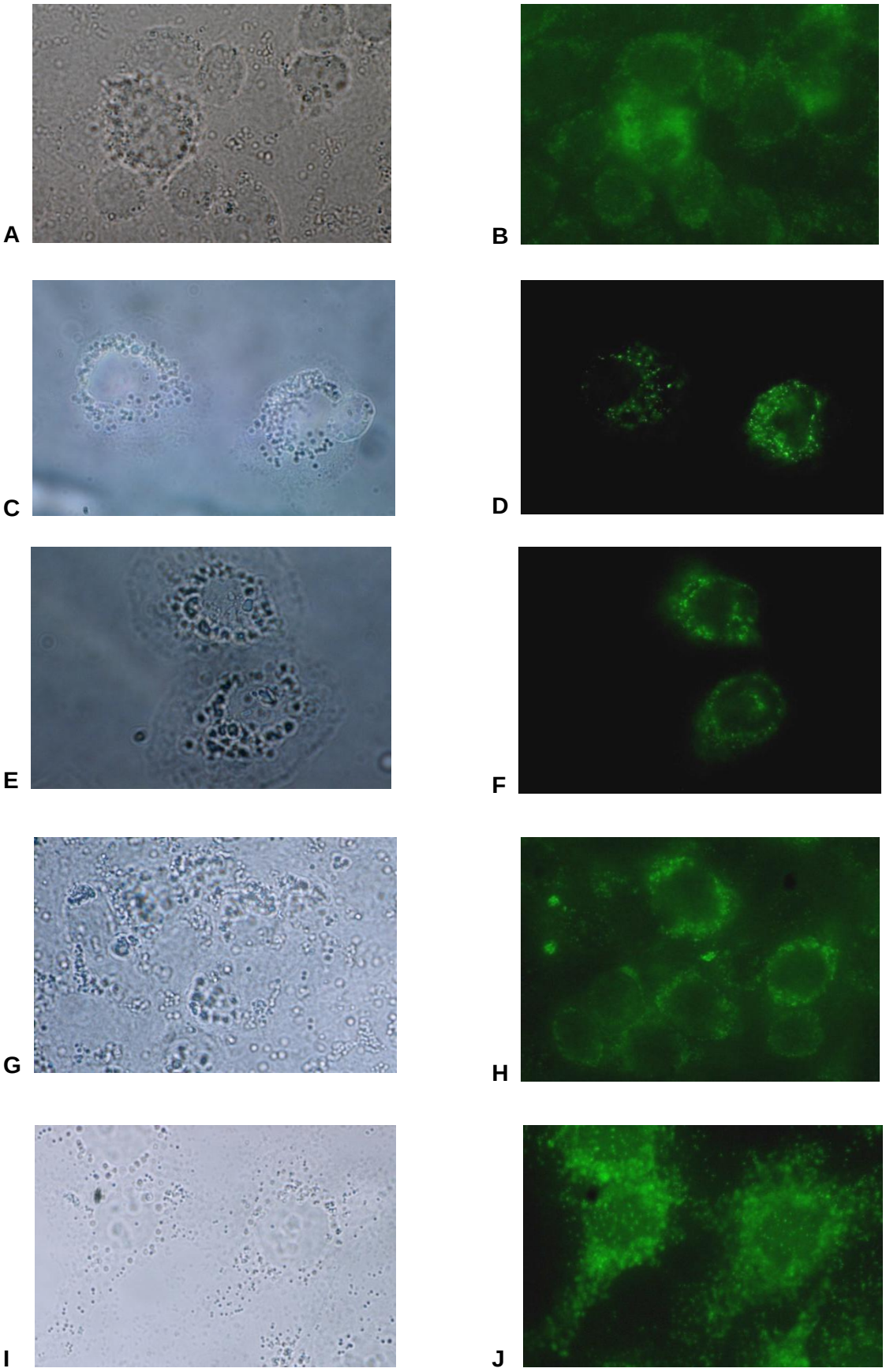

Figure 5.14: *A, C, E, G and I are light microscopic images. B, D, F, H and J are fluorescence microscopic images (60 x magnification)*

5.2.5.2 Discussion

In vitro, 5 mM PBA showed the highest tendency fro peroxisome proliferation as is evident from its intensified fluorescence, having visually the most number of peroxisomes and the phi-shape of the cells (refer to section 3.3.7). These results support the findings of Gondcaille and colleagues (2005) who injected rats with PBA and stained the peroxisomes with anti-catalase protein A-gold immunolabeling. Peroxisomes were observed in the livers of the control rat and those of PBA-treated rats by light microscopy. Microscopy images showed that the livers of the PBA-treated rats contained peculiar shape, phi-bodies. These phi-bodies were found in several fragments of the same liver but no phi-bodies were seen in control livers.

In vivo experiments for peroxisome proliferation could not be conducted, because matured red blood cells do not have peroxisomes (chapter 1). Studies to examine the peroxisome proliferation effect of PBA *in vivo* would require a liver biopsy.

5.2.6 Very-long-chain fatty acids (VLCFA)

The VLCFAs in blood were analysed by GC/MS. We evaluated the effect of PBA on the fatty acids C22:0, C24:0 and C26:0 3 hours after treatment. The concentrations were calculated as described in paragraph 4.6.8 (see Appendix H).

5.2.6.1 Results

The concentration of C22:0 and C26:0 (Figure 5.15) showed an initial decrease after 15 minutes of treatment (for C22:0 from 29.57 µmol/L to 28.58 µmol/L), followed by a slight increase after 30 and 60 minutes and another decrease after 2 and 3 hours. Values remained below the control. The ratio C26:0/C22:0 showed the same pattern with an initial decrease after 15 minutes (from 0.0149 to 0.0105), a slight increase and then a decrease with values lower than the control (0.0107).

C24:0 only showed a slight decrease after 15 minutes whereafter values remained unchanged. There was no change in the C24:0/C22:0 ratios.

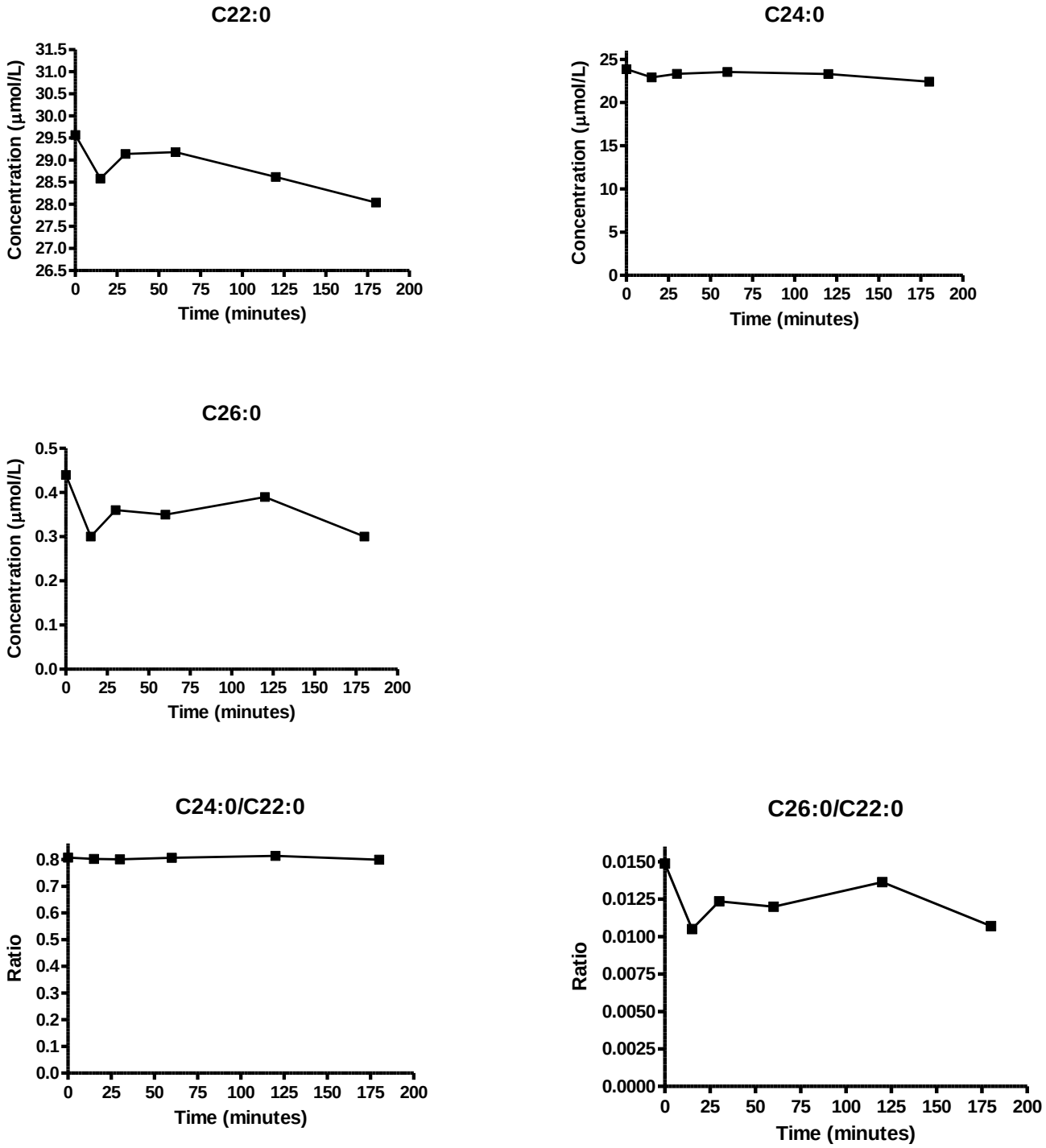

Figure 5.15: *The concentration of the fatty acids (22:0, C24:0 and C26:0 evaluated over the time of treatment with PBA.*

5.2.6.2 Discussion

There were only slight differences in all the fatty acids measured. A noteworthy effect is that there was an initial decrease of all fatty acids at 15 minutes after PBA was given. This shows that PBA has an effect on the peroxisomal β-oxidation of the fatty acids. The

increased effect that occurred between 30 and 120 minutes could be caused by the β-oxidation of PBA to active metabolites. PBA is β-oxidized by mitochondria of the liver and kidneys and the inhibiting effect might only occur when PBA is converted to other metabolites. At 180 minutes another decrease in the fatty acids concentrations occurred, which might be caused by one of the active metabolites stimulating the peroxisomal β-oxidation of fatty acids.

These results show that PBA initially stimulated β-oxidation and that this stimulation was mediated after 3 hours by one of the metabolites that originated from the β-oxidation pathway which can be attributed to an induction that regulates gene expression rather than activation. Further investigation including longer time evaluation as well as chronic treatment would answer many questions.

5.2.7 Summary

In addition to fatty acid metabolism, peroxisomes are a major site of ROS inactivation and thus provide protection against free radicals.

In vitro proliferation results showed that PBA increased the number of peroxisomes in HeLa cells. Based upon the *in vitro* and *in vivo* results showing that PBA caused a decrease in ROS levels, a reduction in lipid peroxidation and a decrease in apoptotic cell death we conclude that PBA shows promise as an antioxidant agent, protecting against oxidative stress in normal tissue. Its low toxicity adds to the feasibility to employ PBA as antioxidant.

5.3 ORGANIC ACIDS IN URINE

The organic acids were analysed by GC/MS over a time of 24 hours of PBA treatment as described in section 4.6.7 (see Appendix I).

5.3.1 Known metabolites

Kasumov and co-workers (2003) identified new metabolites of phenylbutyrate in urine of normal humans and in rat liver (refer to Figure 3.2). In our study we found spectra of more than 200 metabolites in the vervet monkey, confirmed the presence of the metabolites found in the study by Kasumov and also identified new metabolites in the monkey.

The known metabolites identified in humans and rats, that were also present in the vervet monkey are: phenylbutyryl-β-glucuronate, 4-phenylbutyryl-CoA, 4-phenyl-trans-crotonyl-CoA, S-3-hydroxy-4-phenylbutyryl-CoA, 4-phenyl-3-keto-butyryl-CoA, phenylacetyl-CoA, phenylacetate (PA), phenylacetyl-β-glucuronate, S-(+)-3-hydroxy-4-phenylbutyrate, R-(+)-3-hydroxy-phenylbutyrate, phenylacetone and phenylisopropanol. The known metabolites

identified only in rats but also present in small amounts in the vervet monkey are phenylacetylglycine, 4-phenyl-trans-crotonate and 4-phenyl-3-keto-butyrate (see Figure 5.17). The known metabolites only present in humans but also identified in the monkey are phenylacetylglutamine and 4-phenylbutyrylglutamine (see Figure 5.17).

Figure 5.16 shows the concentration over time of a few metabolites in the vervet monkey that originate from the β-oxidation pathway of PBA. These metabolites are 4-phenyl-3-hydroxybutyric acid, 4-phenyl-3-ketobutyric acid, phenylacetic acid, phenylacetylglycine and phenylacetylglutamine

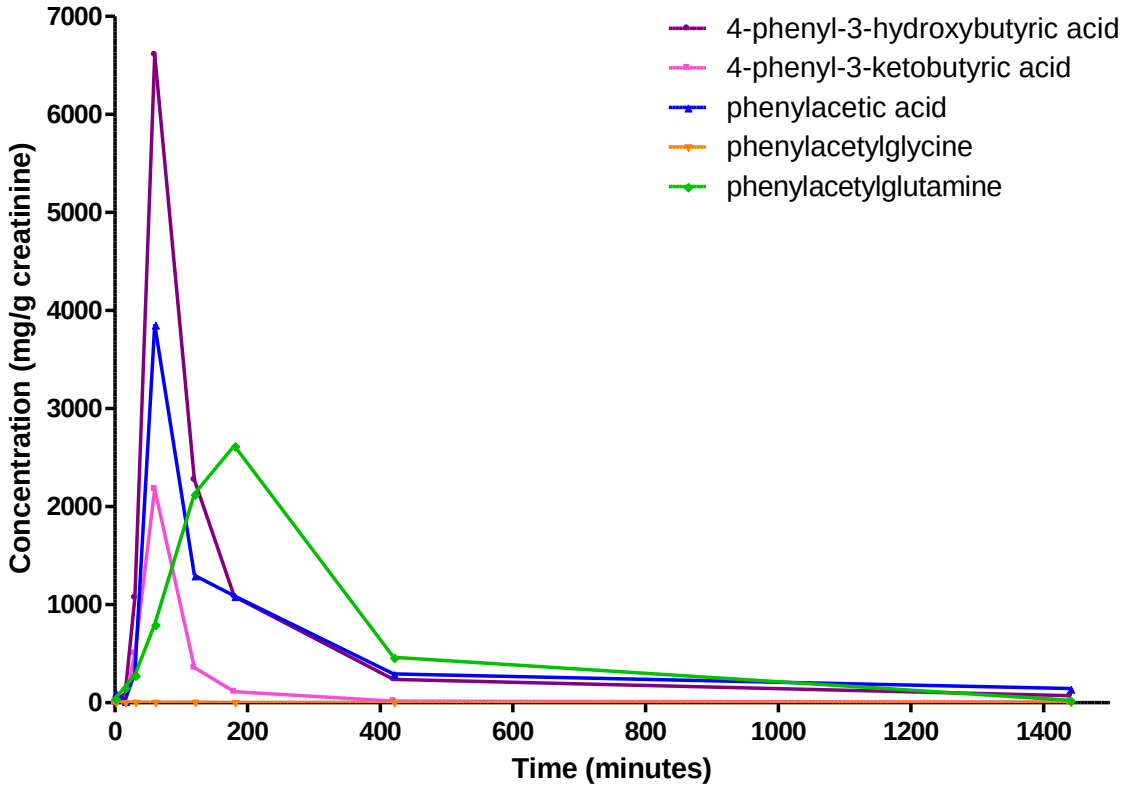

Figure 5.16: *The concentration (mg/g creatinine) of 4-phenyl-3-hydroxybutyric acid, 4-phenyl-3-ketobutyric acid, phenylacetic acid, phenylacetylglycine and phenylacetylglutamine, in the vervet monkey over the period of treatment.*

The concentration of 4-phenyl-3-hydroxybutyric acid, 4-phenyl-3-ketobutyric acid and phenylacetic acid peaked at 60 minutes, with values of 6609.47, 2179.98 and 3859.03 mg/g creatinine respectively. The concentration of phenylacetylglutamine peaked at 180 minutes with a value of 2620.23 mg/g creatinine. The phenylacetylglycine concentration was very low and peaked at 120 minutes with a value of 5.02 mg/g creatinine. After 400 minutes all the metabolites returned to baseline values.

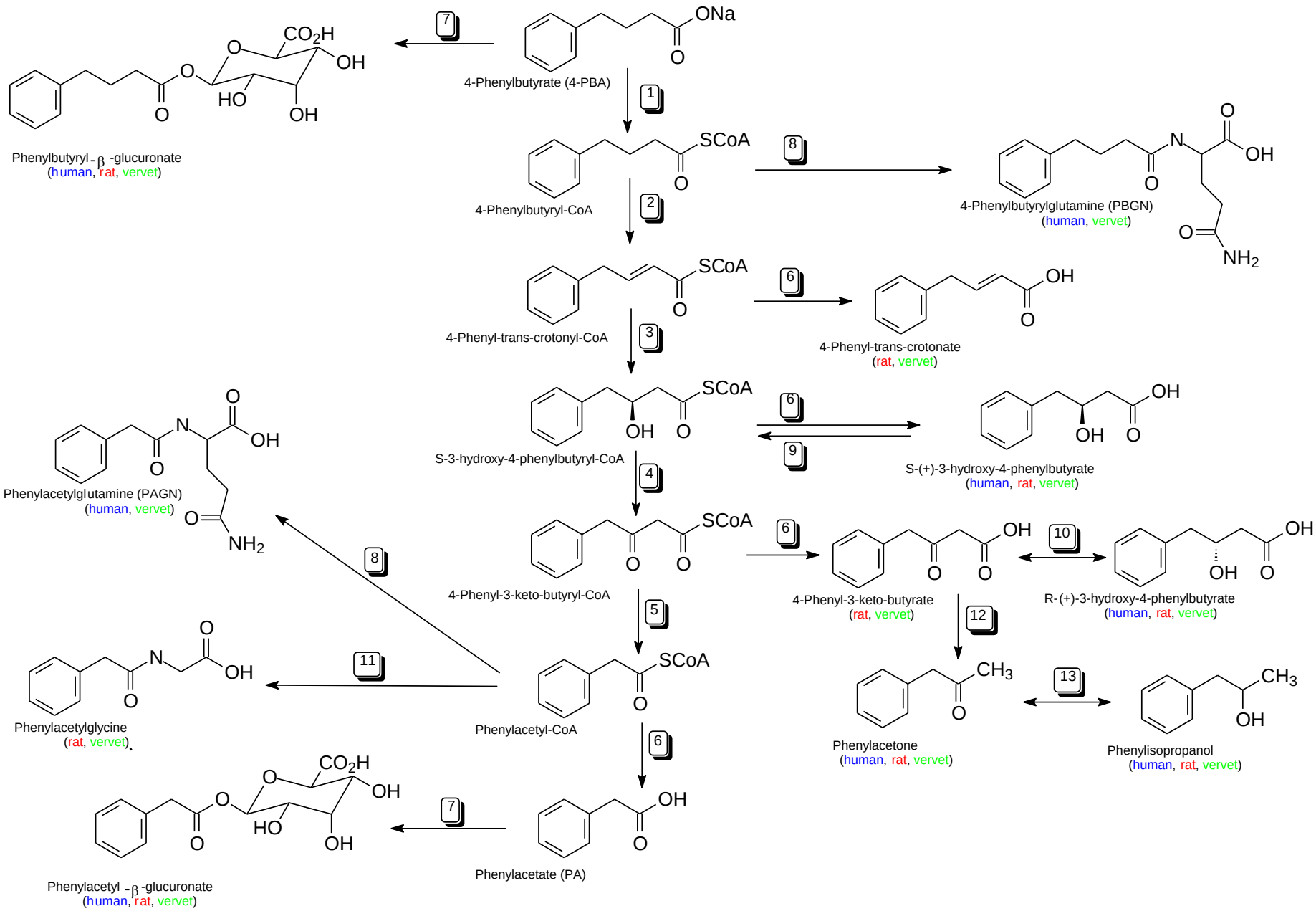

Figure 5.17: *Metabolites of PBA identified in the vervet monkey that correlates with human and rat metabolites*

5.3.1.1 Discussion

PBA is converted into a number of active metabolites. The metabolism of PBA is different in humans and rats. The metabolic profile of PBA in the vervet monkey correlated with the metabolites in humans and rats identified by Kasumov and co-workers in 2003.

PBA has a half-life in vervet monkeys between 1 and 2 hours. This can be seen in Figure 5.16 where most of the metabolites reached a peak at 60 minutes after PBA treatment. Phenylacetylglutamine and phenylacetylglycine peaked at 180 and 120 minutes respectively, because conjugation with glycine and glutamine only takes place after PBA is metabolized to phenylacetic acid.

5.3.2 New metabolites

There were also new metabolites discovered in the vervet monkey treated with PBA and a metabolic pathway is proposed with the likely enzymes involved.

Figure 5.18 illustrates the known metabolites that occur via the β-oxidation pathway together with the new metabolites identified. Two of the new metabolites identified were **3-(4-phenylbutylamino) piperidine-2,6-dione,** which is likely formed via the enzyme N-phenylacetyl-glutamine synthases from phenylbutylglutamine, and **N-(2,6-dioxopiperidin-3-yl)-2-phenylacetamide** probably formed by N-phenylacetyl-glutamine synthases from N-phenylacetylglutamine.

In Figure 5.18 a new monooxygenase pathway is proposed with identified metabolites: (E)-4-phenylbut-3-enoic acid, 4-hydroxy-4-phenylbutanoic acid, phenyl-4-ketobutyric acid and mandelic acid. 4-Hydroxy-4-phenylbutanoic acid can also be metabolized to γ-phenyl-γ-butyrolactone and phenyl-4-ketobutyric acid to benzoic acid which in turn can be metabolized to hippuric acid likely via N-phenylacetyl-glutamine synthases. 3-Hydroxyphenylbutyric acid, that results from hydroxylation of PBA via tyrosine hydroxylation, was also identified. 3-Hydroxyphenylbutyric acid could also undergo β-oxidation and monooxygenase, but such metabolites were not identified in this study.

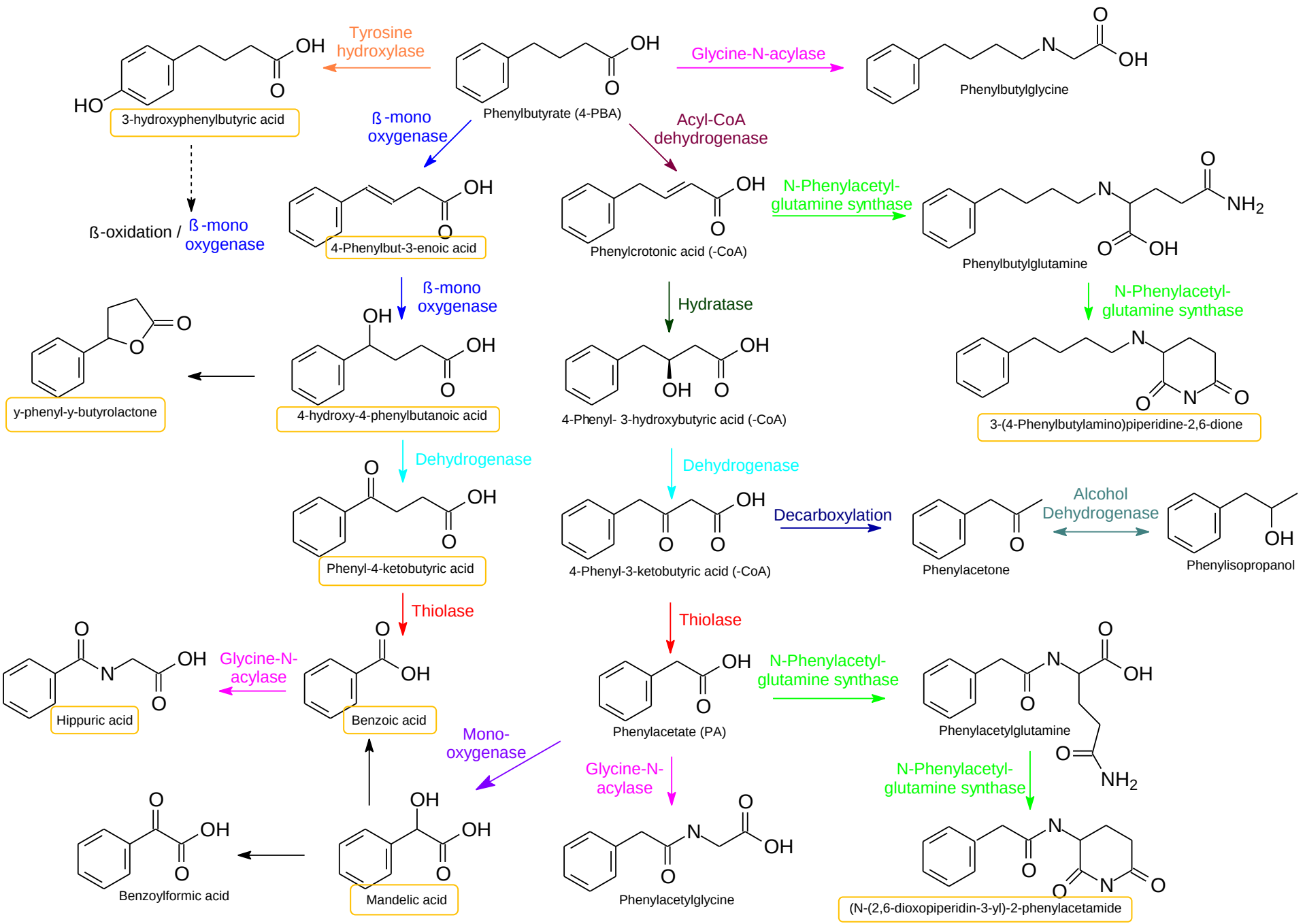

Figure 5.18: *New metabolites (boxed in yellow) identified in the vervet monkey*

Figures 5.19 and 5.20 show the concentration over time of a few of the metabolites formed by the monooxygenase pathway.

.

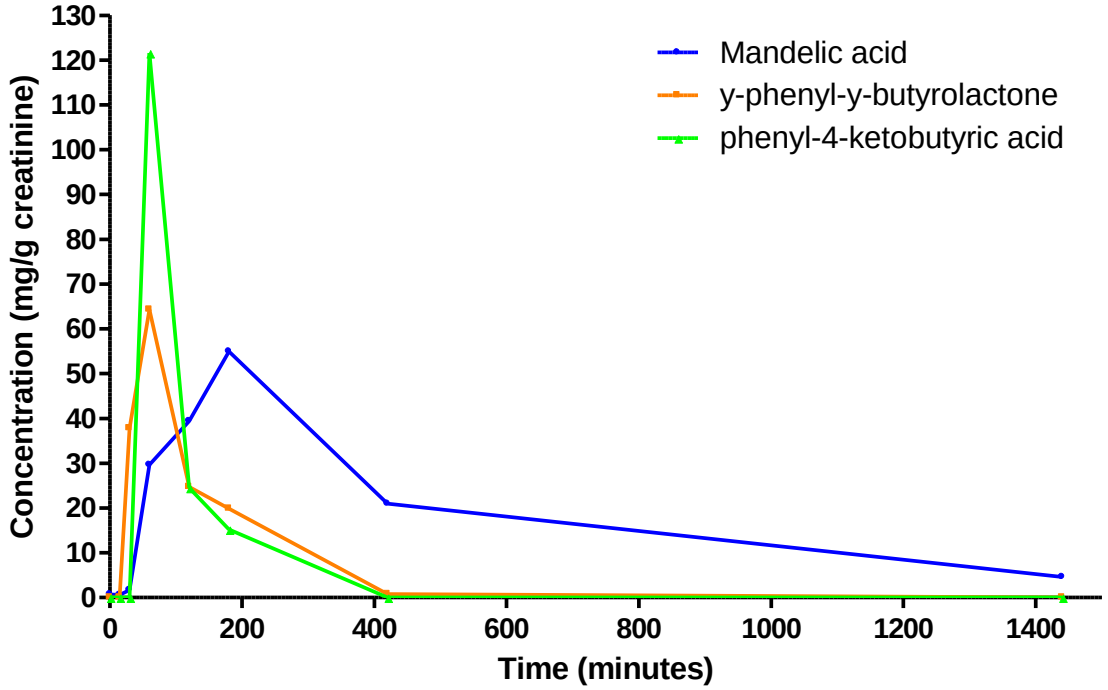

Figure 5.19: *The concentration (mg/g creatinine) of newly identified metabolites, mandelic acid, γ-phenyl-γ-butyrolactone and phenyl-4-ketobutyric acid, in the vervet monkey over the treatment period*

The concentrations of γ-phenyl-γ-butyrolactone and phenyl-4-ketobutyric acid peaked at 60 minutes with values of 64.28 and 121.61 mg/g creatinine respectively. The concentration of mandelic acid increased at 60 minutes to 29.64 mg/g creatinine and peaked at 180 minutes at 54.98 mg/g creatinine. After 400 minutes the concentrations of all the metabolites returned to base values.

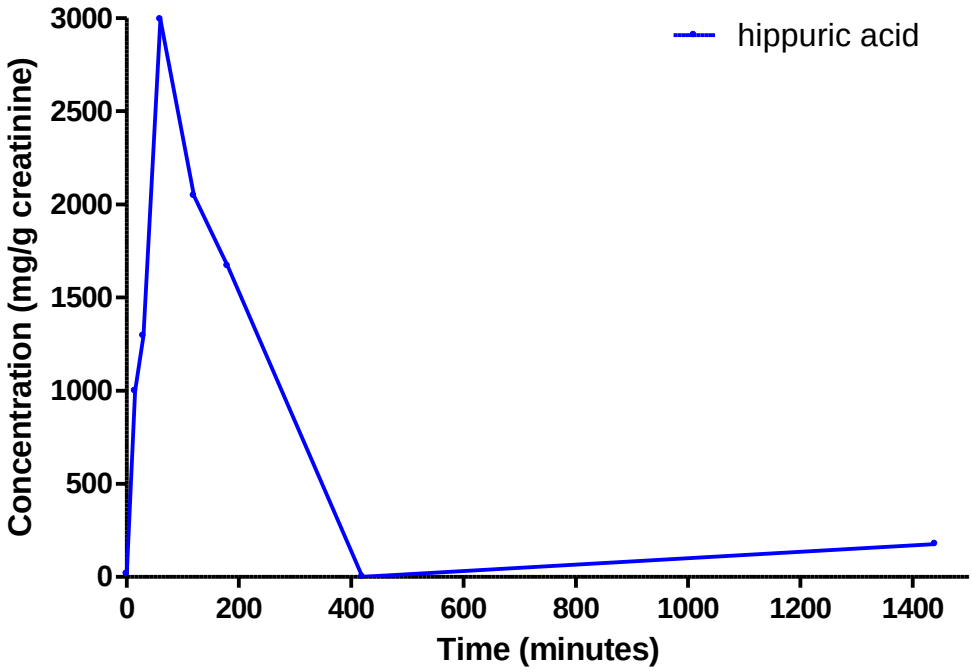

Figure 5.20: *The concentration (mg/g creatinine) of hippuric acid in the vervet monkey over the treatment period.*

Hippuric acid is formed from phenyl-4-ketobutyric acid (Figure 5.20). The concentration of hippuric acid peaked at 60 minutes with 2993.00 mg/g creatinine. At 420 minutes there was no hippuric acid present, but thereafter it appeared again and started to increase and at 1440 minutes its concentration was 177.11 mg/g creatinine.

5.3.2.1 Discussion

Figures 5.17 and 5.18 show the metabolites of PBA, including the new compounds identified and those formed by the monooxygenase pathway in this study. This investigation demonstrated that PBA forms more metabolites that were originally identified by Kasumov and co-workers (2003). We identified a metabolite resulting from hydroxylation of the benzene ring of PBA (3-hydroxyphenylbutyric acid) and are presently searching for PBA metabolites resulting from β-oxidation and monooxygenase. Two metabolites formed by α-hydroxylating monooxygenase, 4-phenylbut-3-enoic acid and 4-hydroxy-4-phenylbutanoic acid were also identified. Driscoll and co-workers (2000) revealed that 4-phenyl-3-butenoic acid inhibited peptidylglycine-α-hydroxylating monooxygenase *in vivo.* In addition they also reported that 4-phenylbut-3-enoic acid itself serves as a substrate resulting in hydroxylated products, eg., 2-hydroxy-4-phenyl-3-butenoic acid and 4-hydroxy-4-phenyl-2-butenoic acid, which we did not find in our experiments. We had, however, identified 4-hydroxy-4-

phenylbutanoic acid, a compound not isolated by Driscoll, which we propose is formed via α-hydroxylating monooxygenase of 4-phenylbut-3-enoic acid. This is followed by a dehydrogenase step, with the formation of phenyl-4-ketobutyric acid, followed by benzoic acid (via a thiolase step) and the glycine-N-acylase step resulting in hippuric acid. Mandelic acid was another metabolite identified that could also originate via α-hydroxylation monooxygenase from phenylacetic acid. Mandelic acid can be further metabolized to benzoylformic acid (not identified).

This variety of metabolites could contribute to the broad spectrum of clinical uses of PBA. The newly suggested monooxygenase pathway revealed new metabolites which could be investigated for their role in peroxisome proliferation.

5.3.3 Secondary metabolites

Secondary metabolites, resulting from other pathways were also identified. These metabolites are most likely to have indirect effects. Figures 5.21 and 5.22 show the time accumulation of 5 secondary metabolites that were found in the urine of the vervet monkey after treatment with a single oral dosage of PBA.

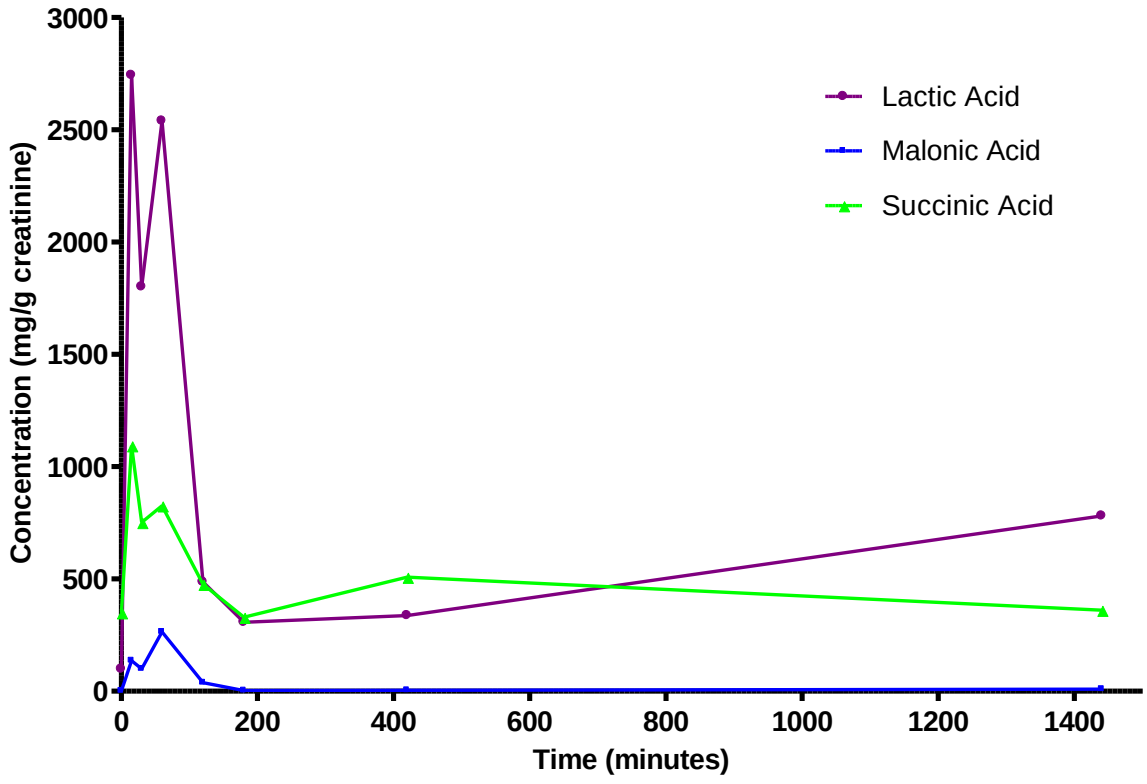

Figure 5.21: *The concentration (mg/g creatinine) of lactic acid, malonic acid and succinic acid over time of treatment.*

Lactic acid increased after 15 minutes to 2742.50 mg/g creatinine and decreased to 1801.38 mg/g creatinine after 30 minutes and increased again after 60 minutes to 2539.70 mg/g creatinine. Thereafter, the concentration decreased over a 6 hour period but started to increase to 780.89 mg/g creatinine after 24 hours.

Malonic acid increased after 15 minutes to 136.54 mg/g creatinine and decreased to 99.45 mg/g creatinine after 30 minutes and increased again to 264.23 mg/g creatinine after 60 minutes. Thereafter, the concentration decreased over a 6 hour period and showed an increase to 9.86 mg/g creatinine again after 24 hours.

Succinic acid showed an initial increase of 1093.00 mg/g creatinine after 15 minutes and a decrease to 751.73 mg/g creatinine after 30 minutes. After 60 minutes the levels increased again to 825.58 mg/g creatinine. Thereafter, the concentration decreased over a 3 hour period and increased to 508.65 mg/g creatinine after 7 hours of treatment which gradually decreased after 24 hours.

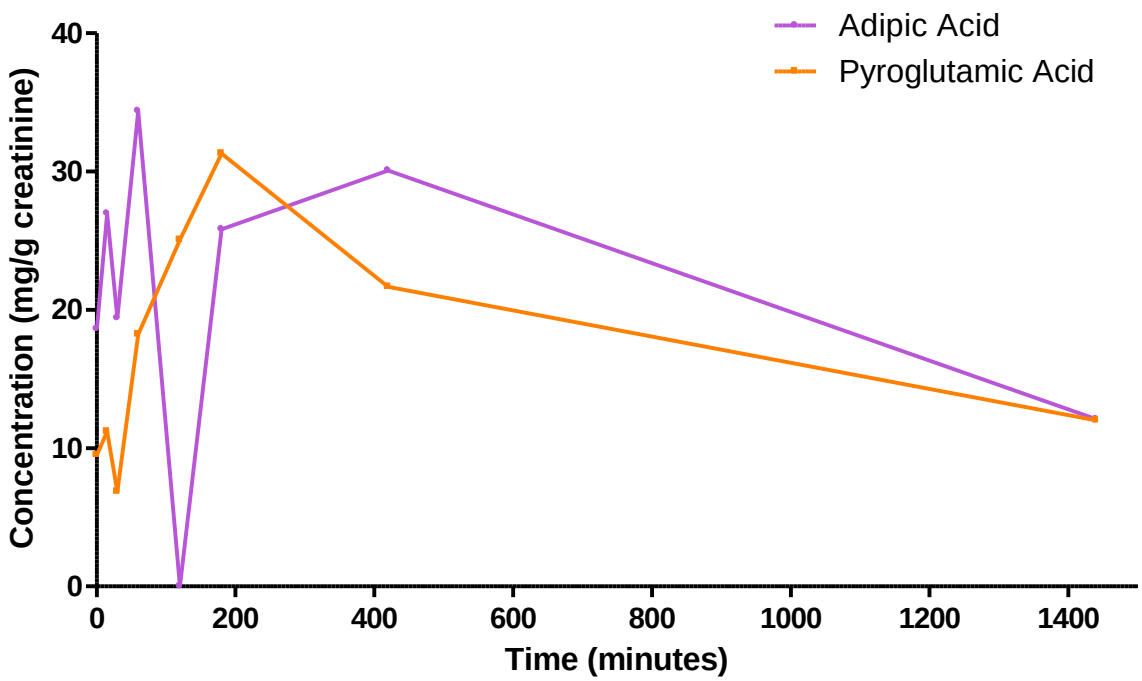

Figure 5.22: *The concentration (mg/g creatinine) of adipic acid and pyroglutamic acid over time of treatment.*

The **adipic acid** concentration increased to 26.96 mg/g creatinine after 15 minutes, decreased to 19.41 mg/g creatinine after 30 minutes and increased again at 60 minutes to 34.38 mg/g creatinine. Levels decreased to zero after 120 minutes and increased again after 180 and 420 minutes to 25.82 and 30.07 mg/g creatinine respectively. Concentrations decreased gradually after 24 hours.

Pyroglutamic acid showed a slight increase of 11.19 mg/g creatinine after 15 minutes of treatment with PBA. Concentrations slightly decreased to 6.85 mg/g creatinine after 30 minutes and then dramatically increased to 31.29 mg/g creatinine at 180 minutes. The levels then decreased gradually to 12.00 mg/g creatinine after 24 hours.

5.3.3.1 Discussion

These secondary metabolites show that PBA could have indirect effects on different biological activities.

Lactic acid or lactate originates from pyruvate, after the conversion of glucose to pyruvate via glycolysis. The results show an initial increase in the concentration of lactic acid, thus leading to the stimulation of the degradation of glucose. **Malonic acid** originates from acetyl-CoA and forms part of the lipid biosynthetic pathway. During the formation of hexanoic acid, an intermediate, **adipic acid,** is produced by ω-oxidation. The initial increase of malonic acid shows stimulation in the lipid biosynthesis. Adipic acid followed the same pattern as malonic acid in Figure 5.21 and when malonic acid decreased at 120 minutes, the levels of adipic acid also dropped (Figure 5.22). **Succinic acid** is produced during the Krebs cycle. The initial increase in succinic acid can also be contributed to the stimulation of the degradation of glucose to produce energy. **Pyroglutamate** is created in the γ-glutamyl cycle, a pathway highly active in renal tubules and anywhere that there is a high demand for glutathione (Chen *et al*, 2003; Pitt *et al*, 1990). The increase in pyroglutamic acid at 180 minutes after treatment with PBA indicates a turnover in glutathione. Glutathione is an essential antioxidant required for the antioxidant enzyme activities of glutathione peroxidase, glutathione reductase and glutathione transferase. Glutathione peroxidases are members of the family of antioxidant enzymes that scavenge hydrogen peroxide in the presence of reduced glutathione. Glutathione peroxidase is present in peroxisomes and plays a novel role in the cellular antioxidant responses to various oxidative stress conditions (Lapenna *et al*, 1998).

Although we could not determine peroxisome proliferation *in vivo,* because there is no peroxisome in RBCs, several studies have shown that PBA is a peroxisome proliferator (Gondcaille *et al*., 2005; McGuinness *et al*., 2001; Kemp *et al*., 1998). The increase in

peroxisomes leads to an increase in pyroglutamic acid (Figure 5.22) 180 minutes after treatment, which reflects an increase in glutathione, which in return leads to radical scavenging via glutathione peroxidases. These effects can be seen in our results, where the lowest ROS levels *in vivo* was seen 180 minutes after PBA treatment (Figure 5.4) and lipid peroxidation *in vivo* was decreased (Figure 5.8) 180 minutes after PBA treatment.

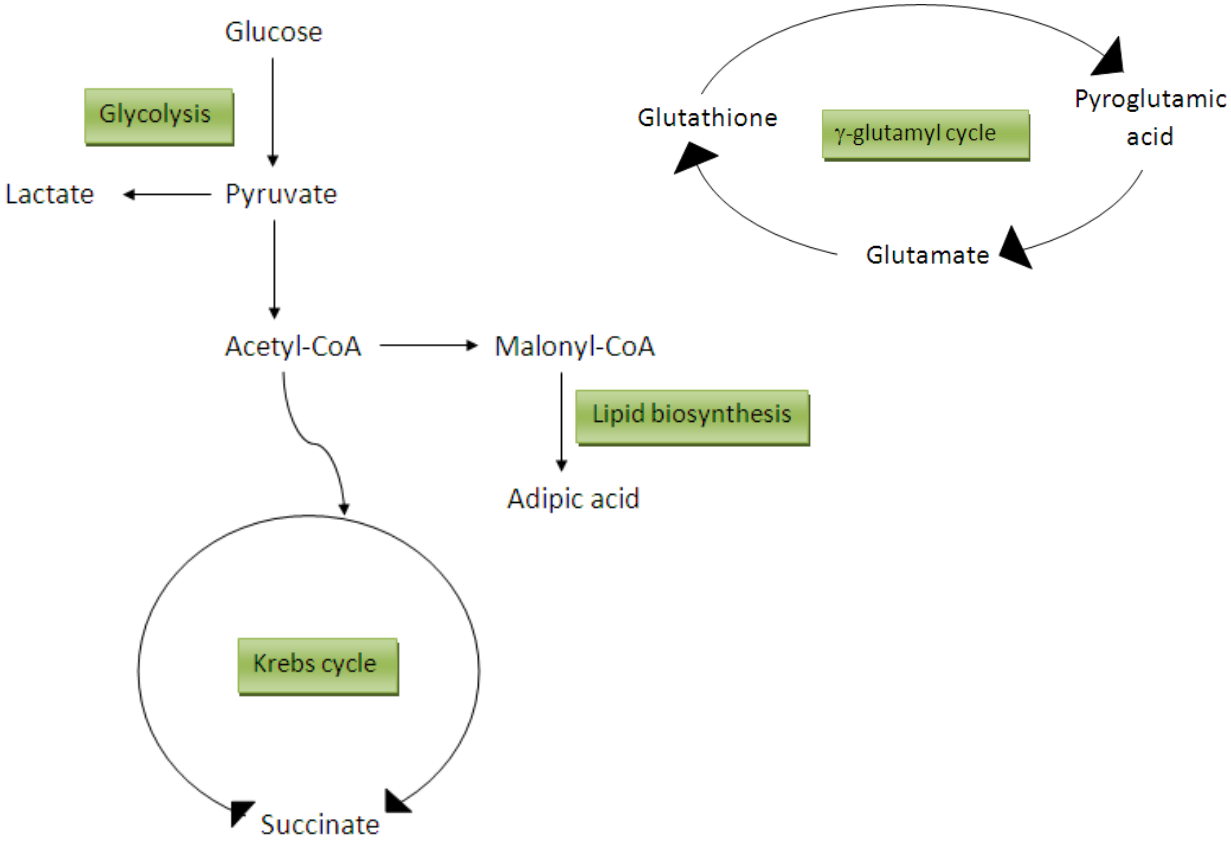

Figure 5.23: *Secondary metabolites of PBA that originate from other pathways and their role in biological activities (adapted from Hertz et al, 2007)*

CHAPTER 6

CONCLUSION

X-linked adrenoleukodystrophy is the most common peroxisomal enzyme deficiency disorder and is caused by mutations in the ABCD1 gene leading to a clinical spectrum of progressive neurodegeneration. (Berger *et al*., 2010; Fidaleo, 2009; Moser, 2006; Guimarãea *et al*., 2002; Weinhofer *et al*., 2002).

In cerebral adrenoleukodystrophy (cALD), an accumulation of very-long-chain fatty acids (VLCFA) stems from a defect of the peroxisomal ALD protein (ALDP) and results in the loss of myelin/oligodendrocytes, induction of inflammatory disease and mental deterioration. Khan and co-workers (2008) observed not only increased levels of VLCFA in brain white matter of cALD patients, but also reduced levels of plasmenylethanolamine and increased levels of reactive oxygen species (ROS) (Khan *et al*., 2008).

The dysfunctional ABCD1 gene leads to the impaired transport of VLCFAs (refer to chapter 2). ABCD1 defect is also associated with faulty oxidative stress homeostasis. This oxidative damage and stress are early events, which lead to neuro-deterioration, because the brain has lower levels of antioxidant defenses and a high substance of lipids, which are very vulnerable to reactive oxygen species assault. (Eichler & Aubourg, 2008; Fourcade, 2008; Moser, 2006; Guimarãea *et al*., 2002). Over-expression of adrenoleukodystrophy-related protein, an ALDP homologue encoded by the ABCD2 (*adrenoleukodystrophy-related*) gene, can compensate for ALDP deficiency. Phenylbutyrate (PBA) has been shown to induce both ABCD2 expression and peroxisome proliferation in human fibroblasts.

PBA is a pro-drug that is converted to phenylacetate by β-oxidation in liver and kidney mitochondria, which in turn can cross the blood-brain barrier. PBA is a known peroxisome proliferator and increasing the number of peroxisomes could contribute to improved VLCFA metabolism in X-ALD patients as described in chapter 3. Peroxisome proliferation can occur by activating the peroxisome proliferator-activated receptor, α (PPARα), or induction of PEX11 protein, involved in peroxisomal proliferation (Engelen *et al*., 2008; Berger *et al*., 2005; Gondcaille *et al*, 2005; McGuinness *et al*., 2001; Netik *et al.,* 1999).

The aim of this study was to determine the antioxidant capacity of PBA *in vivo* and *in vitro* using flow cytometry assays and to identify known and new metabolites of PBA in the vervet

monkey. ROS and oxidative damage can be measured in various cell types *in vitro* and *in vivo* as well as in biological fluids (Halliwell & Whiteman, 2004). In this study, natural occuring levels of ROS were determined in HeLa cells and RBC after treatment with PBA. The use of RBC from the vervet monkey is an ideal model because they contain haemoglobin that participates and facilitates formation of ROS and lipid peroxidation (Maulik *et al*., 1998). The amount of apoptosis was determined in HeLa cells and PBMC to determine whether PBA could protect against cell death.

In some cases, the results obtained in the *in vivo* assays in animals correlated well with those obtained in the short-term *in vitro* assays in controlled sterile environments. Because *in vitro* studies may have implications for regulatory decisions, it is critical that any *in vitro* screening process should be validated by comparisons with the effects in animal models, and where possible, by controlled human exposures. From the economic, efficiency, and ethical points of view, *in vitro* techniques have considerable appeal; however, no *in vitro* technique will ever have the complexity of the whole animal or person.

The *in vitro* results showed a dose-dependent decrease in ROS levels, lipid peroxidation and apoptosis after treatment with PBA. The *in vivo* results showed a time-dependent decrease in ROS levels and lipid peroxidation in the vervet monkey after treatment with PBA. *In vitro* PBA showed weak cytotoxicity towards the cells. Although apoptosis *in vivo* fluctuated, an overall reduction in apoptosis was found after 3 hours of treatment. A possible explanation could be that PBA takes longer *in vivo* to reduce apoptosis. It was demonstrated that PBA retained a high percentage of viable cells and together with a decreased effect on apoptosis, provided protection to the cells. An *in vitro-in vivo* correlation for antioxidant capacity (ROS and lipid peroxidation) of PBA treatment in HeLa cells and the vervet monkey has been demonstrated. Our results confirmed previous reports, that PBA protects normal tissues against oxidative stress (Qi *et al*., 2004; Luo *et al*., 2010).

The fluorescent microscopy images confirmed that there was *in vitro* peroxisome proliferation when treated with PBA but because of a lack of peroxisomes in matured red blood cells, peroxisome proliferation could not be confirmed *in vivo*.

The results of the short term, single dose effect of PBA on VLCFA levels in the vervet monkeys showed an initial decrease in C22:0, C26:0 and C26:0/C22:0 15 minutes and again 60 minutes after treatment. The initial observed reduction of VLCFA by PBA may be caused by the induction of peroxisomal proliferation through a mechanism common to other peroxisome proliferators. This was also observed in studies done by Kemp and colleagues

(1998) where an increase in the expression of PPARα was coincidental with the increase in peroxisomes in mouse cells. The decrease in VLCFA levels after 60 minutes could be attributed to one of the other metabolites of PBA, demonstrating a long term mechanism involving the induction of PEX11α responsible for peroxisome proliferation. To confirm the decrease in VLCFA in the vervet monkey, further studies should include chronic treatment over a longer time period.

In the present study, we reported the identification of additional metabolites of PBA in the vervet monkey. Metabolites identified by Kasumov and co-workers (2003) in humans and rats were also confirmed in the vervet monkey (Figure 5.17). Three new metabolites identified are 3-(4-phenylbutylamino) piperidine-2,6-dione and N-(2,6-dioxopiperidin-3-yl)-2-phenylacetamide probably resulting from N-phenylacetyl-glutamine synthases and 3-hydroxyphenylburyric acid likely resulting from hydroxylation of PBA (tyrosine hydroxylase) (Figure 5.18). Other newly identified metabolites include (E)-4-phenylbut-3-enoic acid 4-hydroxy-4-phenylbutanoic acid, phenyl-4-ketobutyric acid, mandelic acid, benzoic acid, hippuric acid an γ-phenyl-γ-butyrolactone. A monooxygenase pathway was also proposed with the likely enzymes involved. These new metabolites release the potential for further studies to investigate the possibility that one or more of these active metabolites might be responsible for some of the activities of PBA. If such metabolite(s) could be isolated and synthesized, the maximum peroxisome proliferation effect could be obtained with the minimum dosage.

Secondary metabolites, resulting from an indirect effect on other pathways were also identified which could lead to positive effects in the body. The results showed a stimulation of the lipid biosynthesis, resulting in an increase in malonic and adipic acid and a stimulation of the degradation of glucose which caused an increase in lactic and succinic acid levels. The increase in pyroglutamic acid reflects increased glutathione levels leading to radical scavenging which also supports our antioxidant results.

Phenylbutyrate (PBA) is a promising agent that might be useful to to ameliorate or prevent the severe cerebral inflammatory demyelinating phenotype of adrenoleukodystrophy. PBA treatment also may exert an additive therapeutic effect on several other peroxisomal biogenesis disorders.

Future research should include:

- Using cell-lines other than HeLa cells with oxidative challenge (H_2O_2) and to determine the antioxidant capacity of PBA

- A comparison of the antioxidant capacity of PBA with other known antioxidants.
- Elucidation and identification of the metabolite structures resulting from the β-oxidation and monooxygenase pathway of 3-hydroxyphenylbutyric acid.
- Synthesise of the metabolites identified and determination of which metabolite(s) contribute(s) to the proliferation and/or toxicity of PBA.

REFERENCES

AMBROSE, A.M. & SHERWIN, C.P. 1933. Further studies on the detoxication of phenylacetic acid. *Journal of Biology Chemistry,* 101**:**669–675.

AMER, J., GOLDFARB, A. & FIBACH, E. 2004. Flow cytometric analysis of the oxidative status of normal and thalassemic red blood cells. *Cytometry Part A*, 60A: 73-80.

BALCH, W.E., MORIMOTO, R.I., DILLIN, A. & KELLY, J.W. 2008. Adapting proteostasis for disease intervention. *Science*, 319: 916-919.

BACHMANN, C., BRAISSANT, O., VILLARD, A-M., BOULAT, O. & HENRY, H. 2004. Ammonia toxicity to the brain and creatine. *Molecular Genetics and Metabolsim*, 81: S52-S57.

BATSHAW, M.L., THOMAS, G.H. & BRUSILO, S.W. 1981. New approaches to the diagnosis and treatment of inborn errors of urea synthesis, *Pediatrics* 68**:** 290–297.

BERGER, J., FORSS-PETTER, S., OEZEN, I., WEINHOFER, I. 2005. Pharmacological treatment based on gene redundancy: a novel therapeutic approach for X-linked adrenoleukodystrophy. (*In* Understanding and Treating of X-linked adrenoleukodystrophy: Present State and Future Prospectives. SPS-Publications. p.216-227). http://www.meduniwien.ac.at/typo3/fileadmin/Hirnforschung/pdf-downloads/pathobiol/X-ALD_SPS.pdf. [Date accessed: 10 February 2010].

BERGER, J. & GÄRTNER, J. 2006. X-linked adrenoleukodystrophy:clinical, biochemical and pathogenetic aspects. *Biochimica et Biophysica Acta*, 1763:1721-1731.

BI, G. & JIANG, G. 2006. The molecular mechanism of HDAC inhibitors in anticancer effects. *Cellular & Molecular Immunology*, 3(4): 285-290.

BLÜMCKE, S., SCHWARTZKOPFF, W., LOBECK, H., EDMONDSON, N.A., PRENTICE, D.E. & BLANE, G.F. 1983. Influence of fenofibrate on cellular and subcellular liver structure in hyperlipidemic patients. *Atherosclerosis*, 46**:**105–116.

BRITES, P., MOOYER, P.A.W., MRABET, L.E., WATERHAM, H.R. & WANDERS, R.J.A. 2009. Plasmalogens participate in very-long-chain fatty acid-induced pathology. *Brain*, 132: 482-492.

BURKITT, K. & LJUNGMAN, M. 2008. Phenylbutyrate interferes with the Fanconi anemia and BRCA pathway and sensitizes head and neck cancer cells to cisplatin. *Molecular Cancer*, 7(24): 1-9

BURLINA, A.B., OGIER, H., KORALL, H. & TREFZ, F.K. 2001. Long-term treatment with sodium phenylbutyrate in Ornithine Transcarbamylase-deficient patients. *Molecular Genetics and Metabolism*, 72: 351-355.

CARDUCCI, M.W., GILBERT, J., BOWLING, M.K., NOE, D., EISENBERGER, M.A., SINIBALDI, V., ZABELINA, Y., CHEN, T-L., GROCHOW, L.B. & DONEHOWER, R.C. 2001. A phase 1 clinical and pharmacological evaluation of sodium phenylbutyrate on an 120-h infusion schedule. *Clinical Cancer Research*, 7: 3047-3055.

CHANG, M-Y., BERGMARK, C., LAURILA, A., HÖRKKO, S., HAN, K-H., FRIEDMAN, P., DENNIS, E.A. & WITZTUM, J.L. 1999. Monoclonal antibodies against oxidized low-density lipoprotein bind to apoptotic cells and inhibit their phagocytosis by elicited macrophages: evidence that oxidation-specific epitopes mediate macrophage recognition. *Proceedings of the National Academy of Sciences*, 96: 6353-6358.

CHEN, X., SCHOLL, T.O., LESKIW, M.J., DONALDSON, M.R. & STEIN, T.P. 2003. Association of glutathione peroxidase activity with insulin resistance and dietary fat intake during normal pregnancy. *The Journal of Clinical Endocrinology & Metabolism*, 88: 5936-5968.

CHOI, S-E., LEE, Y-J., JANG, H-J., LEE, K-W., KIM, Y-S., JUN, H-S., KANG, S.S., CHUN, J. & KANG, Y. 2008. A chemical chaperone PBA ameliorates palmitate-induced inhibition of glucose-stimulated insulin secretion (GSIS). *Archives of Biochemistry and Biophysics*, 475: 109-114.

COLLINS, A.F., PEARSON, H.A., GIARDINA, P., MCDONAGH, K.T., BRUSILOW, S.W. & DOVER, G.J. 1995. Oral sodium phenylbutyrate therapy in homozygous β thalassemia: a clinical trial. *Blood*, 85(1): 43-49.

COMTE, B., KASUMOV, T., PIERCE, B.A., PUCHOWICZ, M.A., SCOTT, M.E., DAHMS, W., KERR, D., NISSIM, I. & BRUNENGRABER, H. 2002. Identification of phenylbutyrylglutamine, a new metabolite of phenylbutyrate metabolism in humans. *Journal of Mass Spectrometry,* 37**:**581–590.

COOKE, S., EVANS, M.D., DIZDAROGLU, M. & LUNEC, J. 2003. Oxidative DNA damage: mechanisms, mutations, and disease. *FASEB Journal*, 17:1195-1214.

COUTURE, L., NASH, J.A. & TURGEON, J. 2006. The ATP-binding cassette transporters and their implication in drug disposition: a special look at the heart. *Pharmacological Reviews*, 58(2): 244-258.

DAVIE, J.R. 2003. Inhibition of Histone Deacetylase activity by butyrate. *The Journal of Nutrition*, 133: 2485S-2493S.

DAOSUKHO, C., CHEN, Y., NOEL, T., SOMPOL, P., NITHIPONGVANITCH, R., VELEZ, J.M., OBERLEY, T.D. & ST. CLAIR, D.K. 2007. Phenylbutyrate, a histone deactylase inhibitor, protects against Adriamycin-induced cardiac injury. *Free Radical Biology & Medicine*, 42(12): 1818-1825.

DASGUPTA, S., ZHOU, Y., JANA, M., BANIK, N.L. & PAHAN, K. 2003. Sodium phenylacetate inhibits adoptive transfer of experimental allergic encephalomyelitis in SJL/J mice at multiple steps. *The Journal of Immunology*, 170: 3874-3882.

DEIGNAN, J.L., CEDERBAUM, S.D. & GRODY, W.W. 2008. Contrasting features of urea cycle disorders in human patients and knockout mouse models. *Molecular Genetics and Metabolism*, 93: 7-14.

DEON, M., SITTA, A., BARSCHAK, A.G., COELHO, D.M., TERROSO, T., SCHMITT, G.O., WANDERLEY, H.Y.C., JARDIM, L.B., GIUGLIANI, R., WAJNER, M. & VARGAS, C.R. 2008. Oxidative stress is induced in female carriers of X-linked adrenoleukodystrophy. *Journal of Neurological Sciences*, 266:79-83.

DEON, M., WAJNER, M., SIRTORI, L.R., FITARELLI, D., COELHA, D.M., SITTA, A., BARSCHAK, A.G., FERREIRA, G.C., HAESER, A., GIUGLIANI, R. & VARGAS, C.R. 2006. The effect of Lorenzo's oil on oxidative stress in X-linked adrenoleukodystrophy. *Journal of Neurological Sciences,* 247:157-164.

DE DUVE, C. & BAUDHUIN, P. 1966. Peroxisomes (microbodies and related particles). *Physiology review*, 46: 323-357.

DE LA IGLESIA, F.A., LEWIS, J.E., BUCHANAN, R.A., MARCUS, E.L. & MCMAHON, G. 1982. Light and electron microscopy of liver in hyperlipoproteinemic patients under long-term gemfibrozil treatment. *Atherosclerosis,* 43**:**19–37.

DOSZCZAK, M., PIERZCHALSKI, A., GRZENKOWICZ, J., STASILOJC, G. & BIGDA, J.J. 2008. Cytocidal effect of interleukin 1 (IL-1) on HeLa cells is mediated by both soluble and transmembrane tumor necrosis factor (TNF). *Cytokine,* 42: 243-255.

DOVER, G.J., BRUSILOW, S. & CHARACHE, S. 1994. Induction of fetal hemoglobin production in subjects with sickle cell anemia by oral sodium phenylbutyrate. *Blood*, 84(1): 339-343.

DRISCOLL, W.J., KÖNIG, S., FALES, H.M., PANNELL, L.K., EIPPER, B.A. & MULLER, G.P. 2000. Peptidylglycine-α-hydroxylating monoxygenase generates two hydroxylated products from its mechanism-based suicide substrate, 4-phenyl-3-butenoic acid. *Biochemistry*, 39: 8007-8016.

DU PLESSIS, L.D., LAUBSER, P., JOOSTE, J., DU PLESSIS, J., FRANKEN, A., VAN AARDE, N. & ELOFF, F. 2010. Flow cytometric analysis of the oxidative status in human peripheral blood mononuclear cells of workers exposed to welding fumes. *Journal of Occupational and Environmental Hygiene*, 7: 367-374.

EICHLER, F. & AUBOURG, P. 2008. Therapeutics of X-linked adrenoleukodystrophy. *Drug Discovery Today: Therapeutic Strategies*, 5(4): 237-242.

ENGELEN, M. & KEMP, S. 2009. Facts on X-Linked Adrenoleukodystrophy (X-ALD). http://www.x-ald.nl/facts.htm [Date accessed: 23 March 2010]

ENGELEN, M., OFMAN, R., MOOIJER, P.A.W., POLL-THE, B.T., WANDERS, R.J.A. & KEMP, S. 2008. Cholesterol-deprivation increases mono-unsaturated very long-chain fatty acids in skin fibroblasts from patients with X-linked adrenoleukodystrophy. *Biochimica et Biophysica Acta*, 1781: 105-111.

FAWCETT, D.W. 1981. The cell. 2nd edition. Philadelphia: Saunders. 784p.

FERDINANDUSSE, S., DENIS, S., VAN ROERMUND, C.W.T., WANDERS, R.J.A. & DACREMONT, G. 2004. Identification of the peroxisomal β-oxidation enzymes involved in the degradation of long-chain dicarboxylic acids. *Journal of Lipid Research*, 45: 1104-1111.

FIDALEO, M. 2009. Peroxisomes and peroxisomal disorders: the main facts. *Experimental and Toxicologic Pathology*: 2-11.

FOURCADE, S., LÒPEZ-ERAUSCKIN, J., GALINO, J., DUVAL, C., NAUDI, A., JOVE, M., KEMP, S., VILLARROYA, F., FERRER, I., PAMPLONA, R., PORTERO-OTIN, M. & PUJOL, A. 2008. Early oxidative neurodegeneration in X-adrenoleukodystrophy. *Human Molecular Genetics*, 17(12): 1762-1773.

FOURCADE, S., RUIZ, M., GUILERA, C., HAHNEN, E., BRICHTA, L., NAUDI, A., PORTERO-OTIN, M., DACREMONT, G., CARTIER, N., WANDERS, R., KEMP, S., MANDEL, J.L., WIRTH, B., PAMPLONA, R., AUBOURG, P. & PUJOL, A. 2010. Valproic acid induces antioxidant effects in X-linked adrenoleukodystrophy. *Human Molecular Genetics*: 1-10.

GALLAND, N. & MICHELS, P.A.M. 2010 Comparison of the peroxisomal matrix protein import system of different organisms: Exploration of possibilities for developing inhibitors of the import system of trypanosomatids for anti-parasite chemotherapy. *European Journal of Cell Biology*: 1-17.

GARDIAN, G., BROWNE, S.E., CHOI, D-K., KLIVENYI, P., GREGORIO, J., KUBILUS, J.K., RYU, H., LANGLEY, B., RATAN, R.R., FERRANTE, R.J. & BEAL, M.F. 2005. Neuroprotective effects of phenylbutyrate in the N171-82Q transgenic mouse model of Huntington's disease. *The Journal of biological Chemistry*, 280(1): 556-563.

GARIOT, P., BARRAT, E., DROUIN, P., GENTON, P., POINTEL, J.P., FOLIGUET, B., KOLOPP, M. & DEBRY, G. 1987. Morphometric study of human hepatic cell modifications induced by fenofibrate. *Metabolism*, 36:203–210.

GLOD, B.K. & GRIEB, P. 2005. Estimation of antioxidant properties of phenylacetic acids using ion-exclusion chromatography. *Acta Chromatographica*, 15: 258-268.

GOH, M., CHEN, F., PAULSEN, M.T., YEAGER, A.M., DYER, E.S. & LJUNGMAN, M. 2001. Phenylbutyrate attenuates the expression of Bcl-X_L, DNA-PK, Caveolin-1, and VEGF in prostate cancer cells. *Neoplasia*, 3(4): 331-338.

GOMES, A., FERNANDES, E. & LIMA, J.L.F.C. 2005. Fluorescence probes used for detection of reactive oxygen species. *Journal of Biochemistry & Biophysical Methods*, 65: 45-80.

GONDCAILLE, C., DEPRETER, M., FOURCADE, S., LECCA, M.R., LECLERCQ, S., MARTIN, P.G.P., PINEAU, T., CADEPOND, F., ELETR, M., BERTRAND, N., BELEY, A., DUCLOS, S., DE CRAEMER, D., ROELS, F., SAVARY, S. & BUGAUT, M. 2005. Phenylbutyrate up-regulates the adrenoleukodystrophy-related gene as a nonclassical peroxisome proliferator. *The Journal of Cell Biology*, 169(1): 93-104.

GOULD, S.J., RAYMOND, G.V. & VALLE, D. 2008. The peroxisome biogenesis disorders. (*In* Schriver's OMMBID: the online metabolic & molecular bases of inherited diseases. McGraw Hill. p.1-6. http://www.ommbid.com/OMMBID/ the_online_metabolic_and_molecular_bases_of_inherited_disease/b/fulltext/part15/ch129 [Date of access: 20 October 2009].

GUETENS, G., DE BOECK, G., HIGHLEY, M., VAN OOSTEROM, A.T. & DE BRUIJN, E.A. 2002. Oxidative DNA damage: biological significance and methods of analysis. *Critical Reviews in Clinical Laboratory Sciences*, 39(4&5): 331-457.

GUIMARÃES, C.P., LEMOS, M., SÁ-MIRANDA, C. & AZEVEDO, J.E. 2002. Molecular characterization of 21 X-ALD Portuguese families: identification of eight novel mutations in the ABCD1 gene. *Molecular Genetics and Metabolism*, 76: 62-67.

HALLIWELL, B. & WHITEMAN, M. 2004. Measuring reactive oxygen species and oxidative damage *in vivo* and in cell culture: how should you do it and what do the results mean? *British Journal of Pharmacology*, 421: 231-255.

HANEFELD, M., KEMMER, C., & KADNER, E. 1983. Relationship between morphological changes and lipidlowering action of *p*-chlorphenoxyisobutyric acid (CPIB) on hepatic mitochondria and peroxisomes in man. *Atherosclerosis,* 46:239–246.

HATTORI, Y., FUKUSHIMA, M. & MAITANI, Y. 2007. Non-viral delivery of the connexin 43 gene with histone deacetylase inhibitor to human nasopharyngeal tumor cells enhances gene expression and inhibits *in vivo* tumor growth. *International Journal of oncology*, 30: 1427-1439.

HAYASHI, H. & SUGIYAMA, Y. 2007. 4-Phenylbutyrate enhances the cell surface expression and the transport capacity of wild-type and mutated bile salt export pumps. *Hepatology*, 45(6): 1506-1516.

HEBERLE, L.C., ABDULLA, J.K.I., TAWARI, A.A.A.I., OFHMAN, N.A.I. & MAZIDI, Z.A.I. 2001. Peroxisomal disorders: short review with four case reports. *Kuwart Medical Journal*, 33(4): 348-352.

HEMMING, W., KEMP, S., MCGUINNESS, M.C., MOSER, A.B. & KIRBY, D.S. 1999. Pharmacological induction of peroxisomes in peroxisome biogenesis disorders. *Annals of Neurology*, 47(3): 286-296.

HERTZ, L., PENG, L. & DIENEL, G.A. 2007. Energy metabolism in astrocytes: high rate of oxidative metabolism and spatiotemporal dependence on glycolysis/glycogenolysis. *Journal of Cerebral Blood Flow & Metabolism*, 27: 219-249.

HERTZ, R., ARNON, J., HOTER, A., SHOUVAL, D. & BAR-TANA, J. 1987. Clofibrate does not induce peroxisomal proliferation in human hepatoma cell lines PLC/PRF/5 and SK-HEP-1. *Cancer Letter*, 34(3): 263-272.

HERTZ, R. & BAR-TANA, J. 1998. Peroxisome proliferator-activated receptor (PPAR) alpha activation and its consequences in humans. *Toxicology Letters*, 102-103: 85-90.

HERZENBERG, L.A., PARKS, D., SAHAF, B., PEREZ, O., ROEDERER, M. & HERZENBERG, L.A. 2002. The history and future of the fluorescence activated cell sorter and flow cytometry: a view from Stanford. *Clinical Chemistry*, 48(10): 1819-1827.

HOLDEN, P.R. & TUGWOOD, J.D. 1999. Peroxisome proliferator-activated receptor alpha: role in rodent liver cancer and species differences. *Journal of Molecular Endocrinology*, 22: 1-8.

HOMMES, F.A. 1999. The assay of phenylacetic acid and 4-phenylbutyric acid in physiological fluids. *Clinica Chimica Acta*, 284: 109-111.

HUDGINS, W.R., FIBACH, E.F., SAFAYA, S., RIEDER, R.F., MILLER, A.C. & SAMID, D. 1996. Transcriptional upregulation of γ-globin by phenylbutyrate and analogous aromatic fatty acids. *Biochemical Pharmacology*, 52: 1227-1233.

ISLINGER, M., CARDOSO, M.J.R. & SCHRADER, M. 2010. Be different – The diversity of peroxisomes in the animal kingdom. *Biochimica et Biophysica Acta*: 1-17.

JAMES, M.O., SMITH, R.L., WILLIAMS, R.T. & REIDENBERG, M. 1972. The conjugation of phenylacetic acid in man, sub-human primates and some non-primate species. *Proceedings of the Royal Society B: Biological Sciences*, 182:25–35.

JANSEN, G.A., OFMAN, R., DENIS, S., FERDINANDUSSE, S., HOGENHOUT, C.J. & WANDERS, R.J.A. 1999. Phytanoyl-CoA hydroxylase from rat liver: protein purification and cDNA cloning with implications for the subcellular localization of phytanic acid α-oxidation. *Journal of Lipid Research*, 40: 2244-2254.

JANSEN, G.A., VAN DEN BRINK, D.M., OFMAN, R., DRAGHICI, O., DACREMONT, G. & WANDERS, R.J.A. 2001. Identification of pristanal dehydrogenase and activity in peroxisomes: conclusive evidence that the complete phytanic acid α-oxidation pathway is localized in peroxisomes. *Biochemical and Biophysical Research Communications*, 283(3): 674-679.

JENG, Y-Y., LIN, N-T., CHANG, P-H., HUANG, Y-P., PANG, V.F., LIU, C-H. & LIN, C-T. 2007. Retinal ischemic injury rescued by sodium 4-phenylbutyrate in a rat model. *Experimental Eye Research*, 84: 486-492.

JOHNSON, T.L. & OLSEN, L.J. 2001. Building new models for peroxisome biogenesis. *Plant Physiology*, 127: 731-739.

JOOSTE, S., ERASMUS, E., MIENIE, L.J., DE WET, W.J. & GIBSON, K.M., 1994. The detection of 3-methylglutarylcarnitine and a new dicarboxylic conjugate, 3-methylglutaconylcarnitine, in 3-methylglutaconic aciduria. *Clinica Chimica Acta*, 230: 1-8.

KASUMOV, T., BRUNENGRABER, L.L., COMTE, B., PUCHOWICZ, M.A., JOBBINS, K., THOMA, K., DAVID, F., KINMAN, R., WEHRLI, S., DAHMS, W., KERR, D., NISSIM, I. & BRUNENGRABER, H. 2003. New secondary metabolites of phenylbutyrate in humans and rats. *Drug Metabolism and Disposition*, 32(1): 10-19.

KEMP, S. & WANDERS, R.J.A. 2007. X-linked adrenoleukodystrophy: very long-chain fatty acid metabolism, ABC half-transporters and the complicated route to treatment. *Journal of Molecular Genetics and Metabolism*, 90:268-276.

KEMP, S., WEI, H-M., LU, J-F., BRAITERMAN, L., MCGUINNESS, M.C., MOSER, A.B., WATKINS, P.A. & SMITH, K.B. 1998. Gene redundancy and pharmacological gene therapy: implications for X-linked adrenoleukodystrophy. *Nature Medicine*, 4(11): 1261-1268.

KENNEDY, C., BYTH, K., CLARKE, C.L. & DEFAZIO, A. 2002. Cell proliferation in the normal mouse mammary gland and inhibition by phenylbutyrate. *Molecular Cancer Therapeutics*, 1: 1025-1033.

KHAN, M., SINGH, J. & SINGH, I. 2008. Plasmalogen deficiency in cerebral adrenoleukodystrophy and its modulation by lovastatin. *Journal of Neurochemistry*, 106(4): 1766-1779.

KLIEWER, S.A., XU, H.E., LAMBERT, M.H. & WILLSON, T.M. 2001. Peroxisome proliferator-activated receptors: from genes to physiology. *Recent progress in hormone research*, 56: 239-265.

LAPENNA, D., DE GIOIA, S., CIOFANI, G., MEZZETTI, A., UCCHINO, S., CALAFIORE, A.M., NAPOLITANO, A.M., DI ILLIO, C. & CUCCURULLO, F. 1998. Glutathione-related antioxidant defenses in human atherosclerotic plaques. *Circulation*, 97(19): 1930-1934.

LEE, H-C., YIN, P-H., LU, C-Y. CHI, C-W. & WEI, Y-H. 2000. Increase of mitochondria and mitochondrial DNA in response to oxidative stress in human cells. *Biochemistry* Journa, 348: 425-432.l

LEONARD, J.V. & MORRIS, A.A.M. 2002. Urea cycle disorders. *Seminars in Neonatology*, 7:27-35.

LI, X., BAUMGART, E., DONG, G-X., MORRELL, J.C., JIMENEZ-SANSHEZ, G., VALLE, D., SMITH, K.D. & GOULD, S.J. 2002. PEX11α is required for peroxisome proliferation in response to 4-phenylbutyrate but is dispensable for peroxisome proliferator-activated receptor alpha-mediated peroxisome proliferation. *Molecular and Cellular Biology*, 22(23): 8226-8240.

LICHTMAN, J.W. & CONCHELLO, J-A. 2005. Fluorescence microscopy. *Nature Methods*, 2(12): 910-919.

LIN, T., ISLAM, O. & HEESE, K. 2006. ABC transporter, neural stem cells and neurogenesis – a different perspective. *Cell Research*, 19: 857-871.

LUI, N., KUANG, W., THUILLIER, P., LYNN, W.S. & WONG, P.K. 2002. The peroxisome proliferator phenylbutyric acid (PBA) protects astrocytes from ts1 MoMuLV-induced oxidative cell death. *Journal Neurovirology*, 8(4): 318-325.

LUO, Z-F., FENG, B., MU, J., QI, W., GUO, Y-H., PANG, Q., YE, Z-L., LIU, L. & YUAN, F-H. 2010. Effects of 4-phenylbutyrate acid on the process and development of diabetic nephropathy induced in rats by streptozotocin: regulation of endoplasmic reticulum stress-oxidative activation. *Toxicology and Applied Pharmacology*, 246: 49-57.

MAKRIGIORGOS, G.M., KASSIS, A.I., MAHMOOD, A., BUMP, E.A. & SAVVIDES, P. 1997. Novel fluorescein-based flow-cytometric method for detection of lipid peroxidation. *Free Radical Biology & Medicine*, 22: 93-100.

MAULIK, G., KASSIS, A.I., SAVVIDES, P. & MAKRIGIORGOS, G.M. 1998. Fluoresceinated phosphoethanolamine for flow-cytometric measurement of lipid peroxidation. *Free Radical Biology & Medicine*, 25(6): 645-653.

MCDONOUGH, M.A., KAVANAGH, K.L., BUTLER, D., SEARLS, T., OPPERMANN, U. & SCHOFIELD, C.J. 2005. Structure of human phytanoyl-CoA 2-hydroxylase identifies molecular mechanism of Refsum disease. *Journal of Biology Chemistry*, 280(49): 41101-41110.

MCGUINNESS, M.C., LU, J-F., ZHANG, H-P., DONG, G-X., HEINZER, A.K., WATKINS, P.A., POWERS, J. & SMITH, K.D. 2003. Role of ALDP (ABCD1) and mitochondria in X-linked adrenoleukodystrophy. *Molecular and Cellular Biology*, 23(2): 744-753.

MCGUINNESS, M.C., ZHANG, H-P. & SMITH, K.D. 2001. Evaluation of pharmacological induction of fatty acid β-oxidation in X-linked adrenoleukodystrophy. *Molecular Genetics and Metabolism*, 74: 256-263.

MOSER, H.W. 1997. Adrenoleukodystrophy: phenotype, genetics, pathogenesis and therapy. *Brain*, 120:1485-1508.

MOSER, H.W. 2006. Therapy of X-linked adrenoleukodystrophy. *Journal of the American Society for Experimental NeuroTherapeutics*, 3:246-253.

MOSER, H.W., SMITH, K.D., WATKINS, P.A., POWERS, J. & MOSER, A.B. 2008. X-linked adrenoleukodystrophy. (*In* Schriver's OMMBID: the online metabolic & molecular bases of inherited diseases. McGraw Hill. p.1-98 http://www.ommbid.com/OMMBID/the_online_metabolic_and_molecular_bases_of_inherited_disease/b/fulltext/part15/ch131 [Date of access: 20 April 2009].

MULHERN, M.L., MADSON, C.J., KADOR, P.F., RANDAZZO, J. & SHINOHARA, T. 2007. Cellular osmolytes reduce lens epithelial cell death and alleviate cataract formation in galactosemic rats. *Molecular Vision*, 13: 1397-1405.

NETIK, A., FORSS-PETTER, S., HOLZINGER, A., MOLZER, B., UNTERRAINER, G. & BERGER, J. 1999. Adrenoleukodystrophy-related protein can compensate functionally for adrenoleukodystrophy protein deficiency (X-ALD): implications for therapy. *Human Molecular Genetics*, 8(5): 907-913.

NUNEZ, R. 2001. DNA measurement and cell cycle analysis by flow cytometry. *Current Issues on Molecular Biology*, 3(3): 67-70.

PHILLIPS, J.A. & GRIFFIN, B.E. 2007. Pilot study of sodium phenylbutyrate as adjuvant in cyclophosphamide-resistant endemic Burkitt's lymphoma. *Transactions of the Royal Society of Tropical Medicine and Hygiene*, 101: 1265-1269.

PHUPHANICH, S., BAKER, S.D., GROSSMAN, S.A., CARSON, K.A., GILBERT, M.R., FISHER, J.D. & CARDUCCI, M.A. 2005. Oral sodium phenylbutyrate in patients with recurrent malignant gliomas: a dose escalation and pharmacologic study. *Neuro-oncology*: 177-182.

PINEAU, T., HUDGINS, R., LIU, L., CHEN, L-C., SHER, T., GONZALEZ, F.J. & SAMID, D. 1996. Activation of human peroxisome proliferator-activated receptor by the antitumor agent phenylacetate and its analogs. *Biochemical Pharmacology*, 52: 659-667.

PINTO, M.P., GROU, C.P., ALENCASTRE, I.S., OLIVEIRA, M.E., SA-MIRANDA, C., FRANSEN, M. & AZEVEDO, J.E. 2006. The import competence of a peroxisomal membrane protein is determined by PEX19p before the docking step. *The Journal of Biology Chemistry*, 281(45): 34492-34502.

PITT, J.J., BROWN, G.K., CLIFT, V. & CHRISTODOULOU, J. 1990. Atypical pyroglutamic aciduria: possible role of paracetamol. *Journal of Inherited Metabolic Disorders*, 13: 755-756.

POWERS, E.T., MORIMOTO, R.I., DILLIN, A., KELLY, J.W. & BALCH, W.E. 2009. Biological and chemical approaches to diseases of proteostasis deficiency. *Annual review of biochemistry*, 78: 959-991.

PUJOL, A., FERRER, I., CAMPS, C., METZGER, E., HINDELANG, C., CALLIZOT, N., RUIZ, M., PAMPOLS, T., GIRÒS, M. & MANDEL, J-L. 2004. Functional overlap between ABCD1 (ALD) and ABCD2 (ALDR) transporters: a therapeutic target for X-adrenoleukodystrophy. *Human Molecular Genetics*, 13(23): 2997-3006.

PUJOL, A., HINDELANG, C., CALLIZOT, N., BARTSCH, U., SCHACHNER, M. & MANDEL, J-L. 2002. Late onset neurological phenotype of the X-ALD gene inactivation in mice: a mouse model for adrenomyeloneuropathy. *Human Molecular Genetics*, 11(5): 499-505.

QI, X., HOSOI, T., OKUMA, Y., KANEKO, M. & NOMURA, Y. 2004. Sodium 4-phenylbutyrate protects against cerebral ischemic injury. *Molecular Pharmacology*, 66: 899-908.

RAAS-ROTHSCHILD, A., WANDERS, R.J.A., MOOIJER, P.A.W., GOOTJES, J., WATERHAM, H.R., GUTMAN, A., SUZUKI, Y., SHIMOZAWA, N., KONDO, N., ESHEL, G., ESPEEL, M., ROELS, F. & KORMAN, S.H. 2002. A PEX6-defective peroxisomal biogenesis disorder with severe phenotype in an infant, versus mild phenotype resembling usher syndrome in the affected parents. *The American Society of Human Genetics*, 70: 1062-1068.

REDDY, J.K. 2004. Peroxisome proliferators and peroxisome proliferator-activated receptor α: biotic and xenobiotic sensing. *American Journal of Pathology*, 164(6): 2305-2321.

RELLO-VARONA, S., GAMEZ, A., MORENO, V., STOCKERT, J.C., CRISTOBAL, J., PACHECO, M., CANETE, M., JUARRANZ, A. & VILLANUEVA, A. 2006. Metaphase arrest and cell death induced by etoposide on HeLa cells. *The International Journal of Biochemistry & Cell Biology*, 38: 2183-2195.

RHODIN, J. 1954. Correlation of ultrastructural organization and function in normal and experimentally changed proximal convoluted tubule cells of the mouse kidney. Thesis. Stockholm: Karolinska Institutet.

RICOBARAZA, A., CUADRADO-TEJEDOR, M., PÉREZ-MEDIAVILLA, A., FRECHILLA, D., DEL RIO, J. & GARCIA-OSTA, A. 2009. Phenylbutyrate ameliorates cognitive deficit and reduces tau pathology in an Alzheimer's disease mouse model. *Neuropsychopharmacology*: 1-12.

ROSEBUSH, P.I., GARSIDE, S., LEVINSON, A.J. & MAZUREK, M.F. 1999. The neuropsychiatry of adult-onset adrenoleukodystrophy. *The Journal of Neuropsychiatry and Clinical Neurosciences*, 11: 315-327.

ROQUE, T., BONCOEUR, E., SAINT-CRIQ, V., BONVIN, E., CLEMENT, A., TABARY, O. & JACQUOT, J. 2008. Proinflammatory effect of sodium 4-phenylbutyrate in ΔF508-cystic fibrosis transmembrane conductance regulator lung epithelial cells: involvement of extracellular signal-regulated protein kinase ½ and c-Jun-NH_2-terminal kinase signaling. *The Journal of Pharmacology and Experimental Therapeutics*, 326(3): 949-956.

RUBENSTEIN, R.C. & ZEITLIN, P.L. 1998. A pilot clinical trial of oral sodium 4-phenylbutyrate (Buphenyl) in ΔF508-homozygous cystic fibrosis patients. *American Journal of Respiratory and critical care medicine*, 157: 484-490.

SANTOS, M.J., QUINTANILLA, R.A., TORO, A., GRANDY, R., DINAMARCA, M.C., GODOY, J.A. & INESTROSA, N. 2005. Peroxisomal proliferation protects from β-Amyloid neurodegeneration. *The Journal of Biological Chemistry*, 280(49): 41057-41068.

SARKAR, M., VARSHNEY, R., CHOPRA, M., SEKHRI, T., ADHIKARI, J.S. & DWARAKANATH, B.S. 2005. Flow-cytometric analysis of Reactive Oxygen Species in peripheral blood mononuclear cells of patients with thyroid dysfunction. *Cytometry Part B*, 70B: 20-23.

SCAGLIA, F., CARTER, S., O'BRIEN, W.E. & LEE, B. 2004. Effect of alternative pathway therapy on branched amino acid metabolism in urea cycle disorder patients. *Molecular Genetics and Metabolism*, 81: S79-S85.

SCOTTO, K.W. 2003. Transcriptional regulation of ABC drug transporters. *Oncogene*, 22: 7496-7511.

SEN, A., CHATTERJEE, N.S., AKBAR, M.A., NANDI, N. & DAS, P. 2007. The 29-kilodalton thiol-dependent peroxidase of *Entamoeba histolytica* is a factor involved in the pathogenesis and survival of the parasite during oxidative stress. *Eukaryotic Cell*, 6(4): 664-673.

SINGH, I., PAHAN, K. & KHAN, M. 1998. Lovastatin and sodium phenylacetate normalize the levels of very long chain fatty acids in skin fibroblasts of X-adrenoleukodystrophy. *FEBS Letters*, 426: 342-346.

STAMER, K., VOGEL, R., THIES, E., MANDELKOW, E. & MANDELKOW, E-M. 2002. Tau blocks traffic organelles, neurofilaments and APP vesicles in neurons and enhances oxidative stress. *The Journal of Cell Biology*, 156(6): 1051-1063.

THIERINGER, H., MOELLERS, B., KUNAU, W-H. & DRISCOLL, M. 2003. Modeling human peroxisome biogenesis disorders in the nematode Caenorhabolitis elegans. *Journal of Cell Science*, 116: 1797-1804.

THOMS, S., GRØNBORG, S. & GÄRTNER, J. 2009. Organelle interplay in peroxisomal disorders. *Trends in Molecular Medicine*, 15(7): 293-302.

TVETEN, K., HOLLA, Ø.L., RANHEIM, T., BERGE, K.E., LEREN, T.P. & KULSETH, M.A. 2007. 4-Phenylbutyrate restores the functionality of a misfolded mutant low-density lipoprotein receptor. *FEBS Journal*, 274: 1881-1893.

VAN GEEL, B.M., ASSIES, J., HAVERKORT, E.B., KOELMAN, J.H.T.M., VERBEETEN, B., WANDERS, R.J.A. & BARTH, P.G. 1999. Progression of abnormalities in adrenomyeloneuropathy and neurologically asymptomatic X-linked adrenoleukodystrophy despite treatment with “Lorenzo’s oil”. *Journal of Neurology Neurosurgery and Psychiatry*, 67: 290-299.

VASILIOU, V., VASILIOU, K. & NEBERT, W.D. 2009. Human ATP-binding cassette (ABC) transporter family. *Human Genomics*, 3(3): 281-290.

VILATOBA, M., ECKSTEIN, C., BILBAO, G., SMYTH, C.A., JENKINS, S., THOMPSON, J.A., ECKHOFF, D.E. & CONTRERAS, J.L. 2005. Sodium 4-phenylbutyrate protects against liver ischemia reperfusion injury by inhibition of endoplasmic reticulum-stress mediated apoptosis. *International journal of surgery*, 138(2): 342-351.

VOORN-BROUWER, T., KRAGT, A., TABAK, H. & DISTEL, B. 2001. Peroxisomal membrane proteins are properly targeted to peroxisomes in the absence of COPI- and COPII-mediated vesicular transport. *Journal of Cell Science*, 114: 2199-2204.

VREKEN, P., VAN LINT, A.E.M., BOOTSMA, A.H., OVERMARS, H., WANDERS, R.J.A. & VAN GENNIP, A.H. 1998. Rapid stable isotope dilution analysis of very-long-chain fatty acids, pristanic acid and phytanic acid using gas chromatography-electron impact mass spectrometry. *Journal of Chromatography B*, 173:281-287.

WANDERS, R.J.A. 2004. Peroxisomes, lipid metabolism and peroxisomal disorders. *Molecular Genetics and Metabolism*, 83: 16-27.

WANDERS, R.J.A., BARTH, P.G. & HEYMANS, H.S.A. 2008. Single peroxisomal enzyme deficiencies. (*In* Schriver’s OMMBID: the online metabolic & molecular bases of inherited diseases. McGraw Hill. p.1-14 http://www.ommbid.com/OMMBID /the_online_metabolic_and_molecular_bases_of_inherited_disease/b/fulltext/part15/ch130 [Date of access: 7 March 2009].

WANDERS, R.J.A., FERDINANDUSSE, S., BRITES, P. & KEMP, S. 2010. Peroxisomes, lipid metabolism and lipotoxicity. *Biochimica et Biophysica Acta*, 1801: 272-280.

WANDERS, R.J.A., VREKEN, P., FERDINANDUSSE, S., JANSEN, G.A., WATERHAM, H.R., VAN ROERMUND, C.W.T. & VAN GRUNSVEN, E.G. 2001. Peroxisomal fatty acid α- and β-oxidation in humans: enzymology, peroxisomal metabolite transporters and peroxisomal diseases. *Biochemical Society Transactions*, 29(2): 250-267.

WANDERS, R.J.A. & WATERHAM, H.R. 2006. Peroxisomal disorders: the single peroxisomal enzyme deficiencies. *Biochimica et Biophysica Acta*, 1763(12): 1707-1720.

WEINHOFER, I., FORS-PETTER, S., ZIGMAN, M. & BERGER, J. 2002. Cholesterol regulates ABCD2 expression: implications for the therapy of X-linked adrenoleukodystrophy. *Human Molecular Genetics*, 11(22): 2701-2708.

WILEY, J.C., MEABON, J.S., FRANKOWSKI, H., SMITH, E.A., SCHECTERSON, L.C., BOTHWELL, M. & LADIGES, W.C. 2010. Phenylbutyric acid rescues endoplasmic reticulum stress-induced suppression in APP proteolysis and prevents apoptosis in neuronal cells. *Plos One*, 5(2): 1-17.

WILCKEN, B. 2004. Problems in the management of urea cycle disorders. *Molecular Genetics and Metabolism*, 81: S86-S91.

WU, X-J., KASSIE, F. & MERSCH-SUNDERMANN, V. 2005. The role of reactive oxygen species (ROS) production on diallyl disulfide (DADS) induced apoptosis and cell cycle arrest in human A549 lung carcinoma cells. *Mutation Research*, 579: 115-124.

YAKES, F.M. & VAN HOUTEN, B. 1997. Mitochondrial DNA damage is more extensive and persists longer than nuclear DNA damage in human cells following oxidative stress. *Proceedings of the National Academy of Sciences*, 94: 514-519.

YAMADA, T., SHINNOH, N., TANIWAKI, T., OHYAGI, Y., ASAHARA, H., HORIUCHI, I. & KIRA, J. 2000. Lovastatin does not correct the accumulation of very long-chain fatty acids in tissues of adrenoleukodystrophy protein-deficient mice. *Journal of Inherited Metabolic Disease*, 23: 607-614.

ZEITLIN, P.L. 1999. Novel pharmacologic therapies for cystic fibrosis. *The Journal of Clinical investigation*, 103(4): 447-452.

ZHANG, Q., CHEN, Y., WANG, B-D., HE, P. & SU, Y.A. 2007. Differences in apoptosis and cell cycle distribution between human melanoma cell lines UACC903 and UACC903(+6), before and after UV irradiation. *International Journal of Biological Sciences*, 3(6): 342-348.

APPENDIX A

RAW DATA: REACTIVE OXYGEN SPECIES OF HELA CELLS

Data	Description	Geometric mean
data.013	Positive control	1390.99
data.014	Positive control	1486.51
data.015	Positive control	1519.79
data.016	negative control	155.04
data.017	negative control	133.26
data.018	negative control	152.18
data.019	0.5mM	222.77
data.020	0.5mM	240.27
data.021	0.5mM	214.69
data.022	1mM	192.42
data.023	1mM	185.96
data.024	1mM	160.58
data.025	2mM	175.49
data.026	2mM	176.58
data.027	2mM	163.29
data.028	5mM	161.86
data.029	5mM	146.07
data.030	5mM	138.34

APPENDIX B

RAW DATA: LIPID PEROXIDATION OF HELA CELLS

Data	Description	Geometric mean
data.001	negative control	25.38
data.002	negative control	82.83
data.003	Positive control	9.75
data.004	Positive control	9.92
data.005	0.5mM	13.10
data.006	0.5mM	11.92
data.007	1mM	22.92
data.008	1mM	23.88
data.009	2mM	35.59
data.010	2mM	31.82
data.011	5mM	41.75
data.012	5mM	30.20

APPENDIX C

RAW DATA: CELL VIABILITY OF HELA CELLS

Data	Description	Dead (%)	Dying (%)	Live (%)	Unstained (%)	Total Live (%)
data.001	Positive control	3.83	0.12	0.01	96.05	96.18
data.002	Positive control	24.54	2.18	0.05	73.23	75.46
data.003	Positive control	8.36	0.61	0.03	91.01	91.65
data.004	negative control	1.12	4.35	12.63	81.91	98.89
data.005	negative control	1.04	3.95	11.65	83.36	98.96
data.006	0.5mM	2.30	3.84	4.57	89.3	97.71
data.007	0.5mM	1.82	5.05	7.74	85.39	98.18
data.008	1mM	2.46	5.14	4.33	88.07	97.54
data.009	1mM	3.21	3.73	2.17	90.89	96.79
data.010	2mM	1.89	3.52	2.49	92.1	98.11
data.011	2mM	2.42	4.72	2.59	90.28	97.59
data.012	2mM	1.80	2.39	2.89	92.91	98.19
data.013	5mM	1.15	2.39	3.37	93.09	98.85
data.014	5mM	0.77	2.56	2.00	94.67	99.23
data.015	5mM	0.72	3.61	4.58	91.09	99.28

APPENDIX D

RAW DATA: APOPTOSIS OF HELA CELLS

Data	Description	FL2-H subset (%)
data.001	negative control	14.20
data.002	negative control	21.60
data.003	negative control	9.40
data.004	Positive control	40.30
data.005	Positive control	20.60
data.006	Positive control	22.50
data.007	0.5mM	18.20
data.008	0.5mM	23.20
data.009	1mM	21.10
data.010	1mM	14.30
data.011	2mM	21.00
data.012	2mM	10.10
data.013	5mM	20.20
data.014	5mM	7.65
data.015	5mM	10.30

APPENDIX E

RAW DATA: REACTIVE OXYGEN SPECIES OF VERVET MONKEY

Data		Time	Geometric mean	% cells	% ROS
data.001	To	control	8.10	0.13	62.31
data.002	To	control	8.26	0.16	51.63
data.003	T1	15 min	23.10	0.23	100.43
data.004	T1	15 min	30.28	0.22	137.64
data.005	T2	30 min	17.86	0.14	127.57
data.006	T2	30 min	17.69	0.16	110.56
data.007	T3	60 min	13.49	0.31	43.52
data.008	T3	60 min	14.06	0.32	43.94
data.009	T4	120 min	17.13	0.50	34.26
data.010	T4	120 min	18.79	0.62	30.31
data.011	T5	180 min	15.33	0.84	18.25
data.012	T5	180 min	15.73	1.01	15.57

APPENDIX F

RAW DATA: LIPID PEROXIDATION OF VERVET MONKEY

Data	Time		Geometric mean
data.001	To	control	31.81
data.002	To	control	31.45
data.003	T1	15 min	19.47
data.004	T1	15 min	28.38
data.005	T2	30 min	29.23
data.006	T2	30 min	29.42
data.007	T3	60 min	35.11
data.008	T3	60 min	35.28
data.009	T4	120 min	40.37
data.010	T4	120 min	35.06
data.011	T5	180 min	46.55
data.012	T5	180 min	44.70

APPENDIX G

RAW DATA: APOPTOSIS OF VERVET MONKEY

Data	Time		Freq of parent	% apoptosis
data.001	To	control	97.80	2.20
data.002	To	control	97.80	2.20
data.003	To	control	98.00	2.00
data.004	To	control	97.90	2.10
data.005	T1	15 min	96.60	3.40
data.006	T1	15 min	97.60	2.40
data.007	T2	30 min	98.90	1.10
data.008	T2	30 min	99.10	0.90
data.009	T3	60 min	96.30	3.70
data.010	T3	60 min	97.50	2.50
data.011	T4	120 min	98.70	1.30
data.012	T4	120 min	99.20	0.80
data.013	T5	180 min	99.30	0.70
data.014	T5	180 min	99.70	0.30

APPENDIX H

RAW DATA: CONCENTRATION OF VERY-LONG-CHAIN FATTY ACIDS (VLCFAS)

Time	*C22:0*	*C24:0*	*C26:0*	*C24:0/C22:0*	*C26:0/C22:0*	*Phytanic acid*	*Pristanic acid*
To: control	*29.57*	*23.87*	*0.44*	*0.81*	*0.0149*	*0*	*0*
T1: 15min	*28.58*	*22.92*	*0.3*	*0.8*	*0.0105*	*0*	*0*
T2: 30min	*29.14*	*23.33*	*0.36*	*0.8*	*0.0124*	*0.04*	*0*
T3: 60min	*29.18*	*23.54*	*0.35*	*0.81*	*0.0120*	*0.03*	*0*
T4: 120min	*28.62*	*23.3*	*0.39*	*0.81*	*0.0136*	*0.12*	*0*
T5: 180min	*28.04*	*22.41*	*0.3*	*0.8*	*0.0107*	*0.03*	*0*

APPENDIX I

RAW DATA: CONCENTRATION OF ORGANIC ACIDS

Time	4-Phenol	Benzoic-Acid	Phenylacetic-Acid	Phenylpropionic-Acid	3-Methoxy-4-hydroxycinnamic-acid
T0	30.06	1435.57	104.95	0.41	35.36
T1	4.97	194.87	18.36	0.00	23.48
T2	0.53	426.83	305.21	0.44	4.38
T3	0.99	602.94	3859.03	2.21	0.00
T4	13.13	1023.14	1300.74	0.90	29.58
T5	12.00	949.81	1089.17	0.45	20.59
T6	4.17	637.26	294.65	0.36	16.56
T7	2.95	648.28	144.79	2.37	6.82

Time	Phenylacrylic-Acid	Phenyllactic-Acid	Phenylhydracrylic-Acid	3-Hydroxy-phenylacetic-Acid	N-Phenylacetyl-glutamine
T0	10.73	17.15	38.86	108.72	46.11
T1	0.00	19.31	36.74	495.02	160.60
T2	6.07	11.84	49.64	395.43	281.60
T3	9.86	0.00	193.66	788.85	799.70
T4	0.00	11.92	83.66	618.54	2129.68
T5	0.00	7.22	0.00	563.47	2620.23
T6	0.00	0.00	0.00	231.69	462.71
T7	0.00	0.00	17.87	152.51	23.56

Time	4-Hydroxyphenyl-acetic-Acid	3-Hydroxyphenyl-propionic-Acid	4-Hydrocinnamic-Acid	Vanillic-Acid	4-Hydroxyhippuric-Acid
T0	107.37	40.16	6.88	8.83	39.65
T1	248.76	53.59	13.14	11.75	179.88
T2	203.14	79.07	20.99	8.55	101.36
T3	319.19	294.93	115.70	11.18	102.03
T4	238.74	127.68	32.05	12.45	115.91
T5	227.21	92.29	15.98	9.74	73.16
T6	105.25	28.18	6.07	11.55	37.35
T7	168.48	28.71	5.36	4.68	54.87

Time	Mandelic-acid	4-Hydroxbenzoic-Acid	4-Hydroxymandelic-Acid	Hippuric-Acid	3,4-Dihydroxyphenyl-acetic-Acid
T0	0.70	55.95	14.25	16.89	77.84
T1	0.59	23.16	0.00	996.62	18.58
T2	1.70	28.54	18.42	1293.49	5.19
T3	29.64	57.95	23.97	2993.00	0.00
T4	39.39	0.00	13.93	2046.44	24.11
T5	54.98	33.98	12.23	1668.91	20.59
T6	20.94	67.88	55.31	0.00	6.01
T7	4.60	23.98	0.00	177.11	9.02

Time	3-Hydroxyphenyl-hydracrylic-Acid	3-Methoxy-4-Hydroxyphenyl-propionic-Acid	4-Hydroxy-phenyllactic-Acid	4-Hydroxy-cinnamic-Acid	3-Methoxy-4-Hydroxyphenylhydracrylic-Acid
T0	21.69	37.49	6.40	2.90	0.58
T1	0.00	142.83	20.92	3.03	20.45
T2	0.00	126.62	20.84	4.79	0.00
T3	147.77	376.22	46.45	26.65	15.72
T4	39.01	223.00	16.12	6.00	28.08
T5	0.00	145.35	14.98	3.28	17.07
T6	0.00	46.56	0.00	5.11	18.33
T7	0.00	20.83	0.00	3.29	37.35

Time	3-Methoxy-4-Hydroxyphenyllactic-Acid	4-Methoxy-3-Hydroxycinnamic-Acid	4-Methylmandelic-Acid	y-Phenyl-y-Butyrolactone	N-Phenylacetyl-glycine
T0	0.00	0.00	0.00	0.00	0.00
T1	1.49	25.93	1.04	0.00	0.00
T2	1.26	0.00	0.00	37.85	4.45
T3	3.44	0.00	2.50	64.28	3.28
T4	3.18	0.00	13.40	24.75	5.02
T5	2.98	0.00	14.24	19.84	0.00
T6	0.00	21.95	0.00	0.79	0.00
T7	0.00	0.00	0.00	0.00	4.54

Time	4-Hydroxy-cyclohexane-carboxylic-Acid	4-phenyl-3-hydroxybutyric acid	4-Phenyl-3-ketobutyric acid	Homovanillic-Acid	4-Methoxy-mandelic-Acid	3-Hydroxyphenyl-butyric-Acid
T0	0.00	0.00	0.00	0.00	0.00	0.00
T1	24.22	60.58	11.17	118.87	1.03	0.66
T2	12.98	1071.64	503.53	93.76	0.00	41.75
T3	19.81	6609.47	2179.98	194.34	4.09	354.49
T4	24.27	2274.36	359.06	120.04	2.67	0.00
T5	19.60	1084.41	112.82	111.67	1.53	4.40
T6	9.92	238.29	15.89	47.42	0.85	0.00
T7	2.73	72.11	4.22	73.47	2.46	0.00

Time	3,4-Dihydroxy-phenyl-propionic-Acid	3-Hydroxy-cinnamic-Acid	3-Hydroxy-benzoylglycine	2-Keto-benzeneacetic acid	Phenyl-4-Ketobutyric-Acid	4-Hydroxy-benzoylglycine
T0	0.00	0.00	0.00	0.00	0.00	0.00
T1	2.30	0.00	0.00	0.00	0.00	0.00
T2	1.94	6.50	1.70	0.00	0.00	0.00
T3	0.00	0.00	60.00	0.72	121.61	0.00
T4	0.00	8.19	135.43	9.68	24.49	44.12
T5	0.00	5.27	173.50	15.58	15.21	70.77
T6	0.00	0.00	16.46	7.91	0.00	0.00
T7	0.00	0.84	73.55	1.40	0.00	0.00

APPENDIX J

ETHICS APPROVAL

NORTH-WEST UNIVERSITY
YUNIBESITI YA BOKONE-BOPHIRIMA
NOORDWES-UNIVERSITEIT

Private Bag X6001, Potchefstroom
South Africa 2520

Dr. G Terre'Blanche

Tel: (018) 299-4900
Faks: (018) 299-4910
Web: http://www.nwu.ac.za

Ethics Committee
Tel +27 18 299 4850
Fax +27 18 293 5329
Email Ethics@nwu.ac.za

28 September 2009

ETHICS APPROVAL OF PROJECT

The North-West University Ethics Committee (NWU-EC) hereby approves your project as indicated below. This implies that the NWU-EC grants its permission that, provided the special conditions specified below are met and pending any other authorisation that may be necessary, the project may be initiated, using the ethics number below.

Project title : The metabolic profile of phenylbutyric acid in vervet monkeys
Student working on this project: Elmien van der Linde

Ethics number: N W U - 0 0 1 9 - 0 9 - A 5
(Institution - Project Number - Year - Status)
Status: S = Submission; R = Re-Submission; P = Provisional Authorisation; A = Authorisation

Approval date: 15 September 2009 **Expiry date**: 14 September 2013

Special conditions of the approval (if any): None

General conditions:

While this ethics approval is subject to all declarations, undertakings and agreements incorporated and signed in the application form, please note the following:

- *The project leader (principle investigator) must report in the prescribed format to the NWU-EC:*
  - *annually (or as otherwise requested) on the progress of the project,*
  - *without any delay in case of any adverse event (or any matter that interrupts sound ethical principles) during the course of the project.*
- *The approval applies strictly to the protocol as stipulated in the application form. Would any changes to the protocol be deemed necessary during the course of the project, the project leader must apply for approval of these changes at the NWU-EC. Would there be deviated from the project protocol without the necessary approval of such changes, the ethics approval is immediately and automatically forfeited.*
- *The date of approval indicates the first date that the project may be started. Would the project have to continue after the expiry date, a new application must be made to the NWU-EC and new approval received before or on the expiry date.*
- *In the interest of ethical responsibility the NWU-EC retains the right to:*
  - *request access to any information or data at any time during the course or after completion of the project;*
  - *withdraw or postpone approval if:*
    - *any unethical principles or practices of the project are revealed or suspected,*
    - *it becomes apparent that any relevant information was withheld from the NWU-EC or that information has been false or misrepresented,*
    - *the required annual report and reporting of adverse events was not done timely and accurately,*
    - *new institutional rules, national legislation or international conventions deem it necessary.*

The Ethics Committee would like to remain at your service as scientist and researcher, and wishes you well with your project. Please do not hesitate to contact the Ethics Committee for any further enquiries or requests for assistance.

Yours sincerely

Prof MMJ Lowes
(chair NWU Ethics Committee)

Prof J Du Plessis
(Chairman: NWU Ethics Committee:Unit for Drug Research and Development))